USGS
science for a changing world

Geology of the Northern Part of the Harcuvar Complex, West-Central Arizona

Professional Paper 1752

U.S. Department of the Interior
U.S. Geological Survey

Geology of the Northern Part of the Harcuvar Complex, West-Central Arizona

By Bruce Bryant and J.L. Wooden

Professional Paper 1752

U.S. Department of the Interior
U.S. Geological Survey

U.S. Department of the Interior
DIRK KEMPTHORNE, Secretary

U.S. Geological Survey
Mark D. Myers, Director

U.S. Geological Survey, Reston, Virginia: 2008

For product and ordering information:
World Wide Web: http://www.usgs.gov/pubprod
Telephone: 1-888-ASK-USGS

For more information on the USGS—the Federal source for science about the Earth, its natural and living resources, natural hazards, and the environment:
World Wide Web: http://www.usgs.gov
Telephone: 1-888-ASK-USGS

Suggested citation:
Bryant, Bruce, and Wooden, J.L., 2008, Geology of the Northern Part of the Harcuvar Complex, West-Central Arizona: U.S. Geological Survey Professional Paper 1752, 52 p.

Contents

Figures

Tables

Geology of the Northern Part of the Harcuvar Complex, West-Central Arizona

By Bruce Bryant and J.L. Wooden

Abstract

In west-central Arizona near the northeast margin of the Basin and Range Province, the Rawhide detachment fault separates Tertiary and older rocks lacking significant effects of Tertiary metamorphism from Precambrian, Paleozoic, and Mesozoic rocks in the Harcuvar metamorphic core complex below. Much of the northern part of the Harcuvar complex in the Buckskin and eastern Harcuvar Mountains is layered granitic gneiss, biotite gneiss, amphibolite, and minor pelitic schist that was probably deformed and metamorphosed in Early Proterozoic time. In the eastern Buckskin Mountains, Early and Middle Proterozoic plutons having U-Pb zircon ages of 1,683±6.4 mega-annum (Ma) and 1,388±2.3 Ma, respectively, intruded the layered gneiss. Small plutons of alkaline gabbro and diorite intruded in Late Jurassic time. A sample of mylonitized diorite from this unit has a U-Pb zircon age of 149±2.8 Ma. In the Early Cretaceous, amphibolite facies regional metamorphism was accompanied by partial melting and formation of migmatite. Zircon from a granitic layer in migmatitic gneiss in the eastern Harcuvar Mountains has a U-Pb age of 110±3.7 Ma. In the Late Cretaceous, sills and plutons of the granite of Tank Pass were emplaced in both the Buckskin and eastern Harcuvar Mountains. In the Buckskin Mountains those intrusions are locally numerous enough to form an injection migmatite. A pluton of this granite crops out over almost half the area of the eastern Harcuvar Mountains.

Paleozoic and Mesozoic sedimentary rocks were caught as slices along south-vergent Cretaceous thrusts related to the Maria fold and thrust belt and were metamorphosed beneath a thick sheet of Proterozoic crustal rocks.

Inception of volcanism and basin formation in upper-plate rocks indicates that regional extension started at about 26 Ma, in late Oligocene. The Swansea Plutonic Suite, composed of rocks ranging from gabbro to granite, intruded the lower-plate rocks in the Miocene and Oligocene(?). Granite and a gabbro from the suite have a U-Pb zircon age of 21.86±0.60 Ma. Previously published $^{40}Ar/^{39}Ar$ ages of hornblende suggest that some of the Swansea Suite is Oligocene. The felsic rocks contain numerous inclusions ranging from porphyritic granite to porphyritic granodiorite. A sample from one inclusion has a U-Pb zircon age of 1,409±6.3 Ma. A discordia line for the U-Pb zircon data from the Swansea Plutonic Suite has an upper intercept at 1,408±3.4 Ma. The Swansea Plutonic Suite probably formed by interaction between mantle material and plutonic rocks at least as old as Middle Proterozoic. An irregular layer in the middle crust, which is thickest under and adjacent to the Buckskin Mountains, may be the level where that interaction took place.

During extensional deformation these rocks and all the older rocks were displaced southwest from beneath the rocks of the Colorado Plateau transition zone below an area extending 50–80 kilometers northeast of the Buckskin Mountains as far as Bagdad, Arizona, or beyond. At that time the rocks were variably mylonitized, and a northeast-trending lineation formed. Much of the evidence for the complex sequence of structural events preserved in these rocks in the western Harcuvar Mountains has been obliterated in the northern Harcuvar complex by Miocene deformation.

Introduction

A belt of metamorphic core complexes crops out in southeastern California and west-central Arizona in the Basin and Range Province southwest of the margin of the Colorado Plateau (fig. 1). The complexes consist of crystalline rock (commonly mylonitized) below a low-angle detachment fault. Overlying the detachment fault are unmetamorphosed Tertiary sedimentary and volcanic rocks, metamorphosed Mesozoic and Paleozoic sedimentary and volcanic rocks, and Proterozoic and younger plutonic and metamorphic rocks lacking pervasive mylonitic structures. Crystalline rocks below detachment faults in the Rawhide, Buckskin, Little Buckskin, Harcuvar, Harquahala, Little Harquahala, and Granite Wash Mountains have been informally named the Harcuvar metamorphic core complex (Rehrig and Reynolds, 1980), or simply Harcuvar complex, because in some areas it contains unmetamorphosed igneous rocks. The area described in this report, the northern part of the Harcuvar complex, includes the lower-plate rocks in the Buckskin, Little Buckskin, and eastern Harcuvar Mountains. This area is about 180 km northwest of Phoenix, Ariz., and 60 km southwest of Bagdad, Ariz. (fig. 1). Because only the valley of the Bill Williams River separates the Rawhide from the Buckskin Mountains and the Rawhide

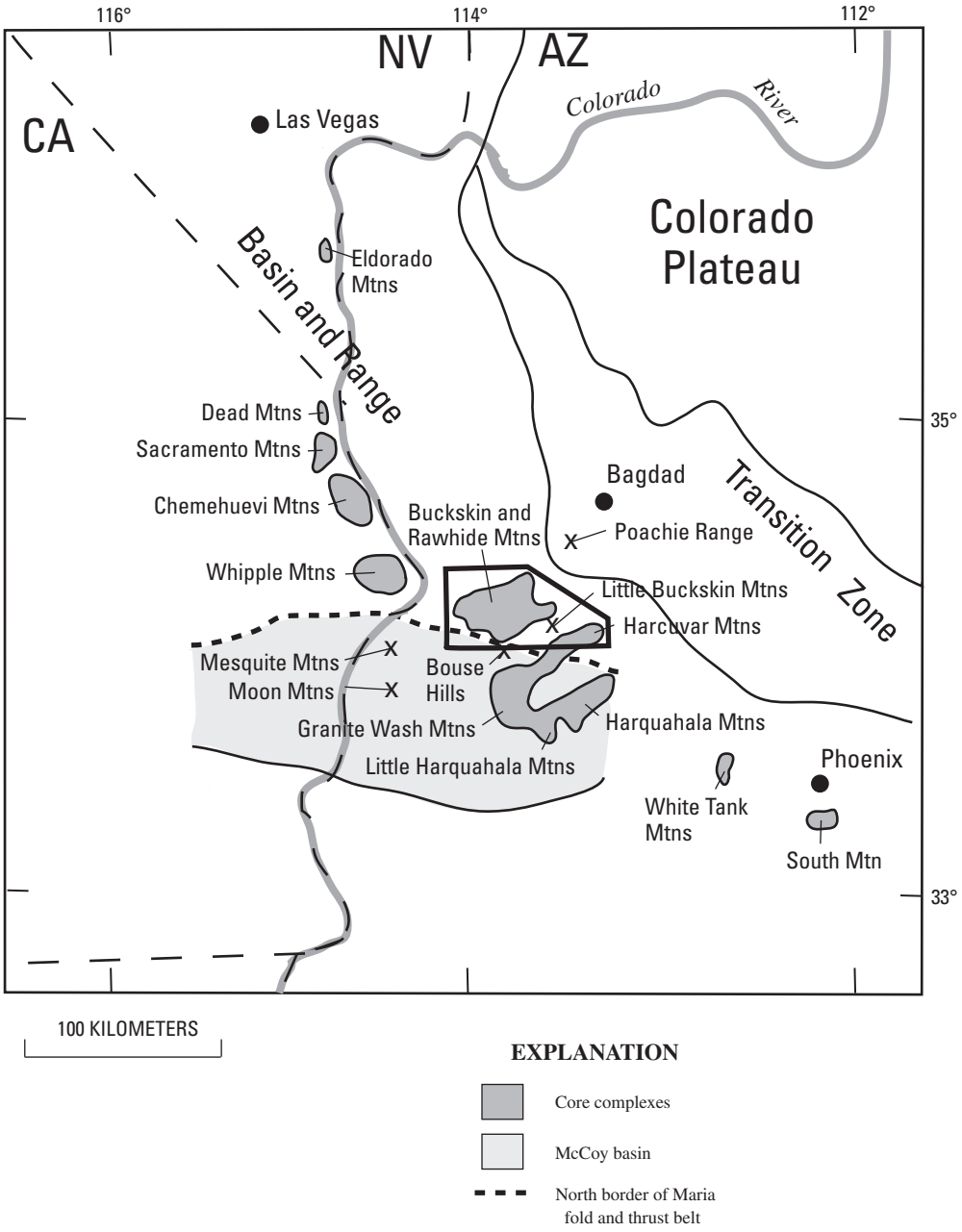

Figure 1. Location of northern Harcuvar complex and core complexes of west-central Arizona and adjacent part of California. Area of figure 2 outlined.

Mountains occupy only about 20 percent of the core complex in those two ranges, we here include the Rawhide Mountains with the Buckskin Mountains for the sake of brevity. The rocks below the surrounding detachment fault are part of the northern Harcuvar complex. In the Buckskin Mountains, that complex is about 40 km long in a northeast-southwest direction, and 20 km wide, and is exposed over about 800 km^2. Upper-plate rocks within the Buckskin Mountains occur in two synforms bounded by the Rawhide detachment fault that divide the complex into three antiforms, each cored by lower-plate metamorphic and igneous rocks. From northwest to southeast, they are called the Planet Peak, Clara Peak, and Ives Peak antiforms (fig. 2) (Rehrig and Reynolds, 1980; Spencer and Reynolds, 1989a). The folds and the detachment fault are cut by northwest-trending normal and reverse faults (Spencer and Reynolds, 1989a). Also included in this study are the rocks of the Harcuvar complex forming the eastern part of the Harcuvar Mountains. Southwest movement of the lower plate composed of the complex relative to the upper plate has been estimated as more than 50 km (Reynolds and Spencer, 1985), 75±20 km (Spencer and Reynolds, 1989b), and 66±8 km (Spencer and Reynolds, 1991). That distance and direction of separation places the rocks now exposed in the Buckskin Mountains beneath the Colorado Plateau transition zone in an area extending to 20 km northeast of Bagdad, Ariz. Seismic reflection data indicate that the detachment fault in the subsurface extends from its outcrop at the northeast margin of the Buckskin Mountains to the Colorado Plateau transition zone where it soles into a midcrustal reflection horizon at a depth of 18 km about 35 km northeast of the Buckskin Mountains (Clayton and Okaya, 1991), which is approximately below U.S. Highway 93. If this interpretation is correct, the rocks now exposed beneath the detachment fault in the eastern part of the Buckskin Mountains were at those depths when extension started.

The northern Harcuvar complex lies north of the Late Cretaceous Maria fold and thrust belt, an east-west-trending belt in which Proterozoic basement rocks moved southward over Paleozoic and Mesozoic rocks, including the Upper Jurassic to Upper Cretaceous (Barth and others, 2004) McCoy Mountains Formation (Reynolds and others, 1986; Spencer and Reynolds, 1990a). The Phanerozoic rocks were buried by the thrust sheet(s) deeply enough so that a greenschist facies regional metamorphic mineral assemblage formed in them during or after the thrusting.

Mylonitic lower-plate rocks similar to those in the Buckskin Mountains are exposed in the eastern part of the Harcuvar Mountains. These rocks are included in the northern Harcuvar complex. Rocks of the northern Harcuvar complex are also exposed in the Little Buckskin Mountain, a small antiform between the eastern parts of the Buckskin and Harcuvar Mountains.

Detachment faults bounding the lower-plate rocks in the Rawhide, Buckskin, and Harcuvar Mountains have been called the Rawhide, Buckskin, and Bullard faults, respectively. The Whipple Mountains detachment fault, which separates lower-plate rocks from upper-plate rocks in the Whipple Mountains 25 km west-northwest of the west end of the Buckskin Mountains, has been extended in cross sections to 8 km north-northwest of the detachment fault bounding the lower plate rocks in the Buckskin Mountains (Howard and others, 2000). Because the faults bounding these core complexes are parts of a single detachment, following the interpretations of Spencer and Reynolds (1991) and Reynolds and Spencer (1985), we apply the name Rawhide to this fault because it is better exposed in the Rawhide Mountains than in the other ranges in Arizona.

Previous Work

Lower-plate rocks in the northern Harcuvar complex have received little study. Brief descriptions were published of rocks from some mining districts (Bancroft, 1911). Reconnaissance geologic maps of Yuma and Mohave Counties show units of older Precambrian granite gneiss and schist and Mesozoic sedimentary rocks in the area of the northern Harcuvar complex. An area of Mesozoic sedimentary rock was mapped in the southwestern corner of the Buckskin Mountains. Overlying Paleozoic, Mesozoic, and Tertiary sedimentary rocks of the upper plate were mapped as partly in thrust fault contact and partly in depositional contact with the underlying rocks of the lower plate (Wilson, 1960; Wilson and Moore, 1959).

In a pioneering study of detachment faults, Shackelford (1976; 1989) mapped the lower-plate rocks in the Rawhide Mountains. He mapped most of the rocks as mylonitic gneiss, which he characterized as very homogeneous on a large scale and lacking any continuous marker horizons. He also mapped small areas of metasedimentary rock in the mylonitic gneiss. He favored a plutonic igneous protolith for the mylonitic gneiss and suggested that the enclosed small bodies of metasedimentary rock were pendants in the granitic terrane. At the southeast edge of the Rawhide Mountains a pluton of partly foliated quartz monzonite, intruded by small plugs of nonfoliated hornblende diorite along its south edge, intrudes the mylonitic gneiss. Shackelford inferred a Mesozoic or Tertiary age for these plutonic rocks. He recognized the parallelism between well-developed, pervasive mineral lineation in the mylonites below the detachment fault with slickenlines on and near the detachment fault.

In a reconnaissance study, Rehrig and Reynolds (1980) interpreted the layered gneisses in the Harcuvar complex to be, at least in part, of metasedimentary origin. In the Planet–Mineral Hill area in the western Buckskins, Spencer, Reynolds, and Lehman (1989a, b) mapped a sill-like body of intermediate to mafic dioritic(?) intrusive rock just below the detachment fault. In that publication and others on mining districts in the upper-plate rocks of the Buckskin Mountains, Spencer and Reynolds lumped the lower-plate rocks into a unit of mylonitic crystalline rocks of Proterozoic to Cenozoic age. Also, in the Reid Valley area they mapped a unit of metasedimentary rock composed of marble, siliceous marble, quartzite, calcareous quartzite, phyllite, and metasandstone. Spencer and Welty

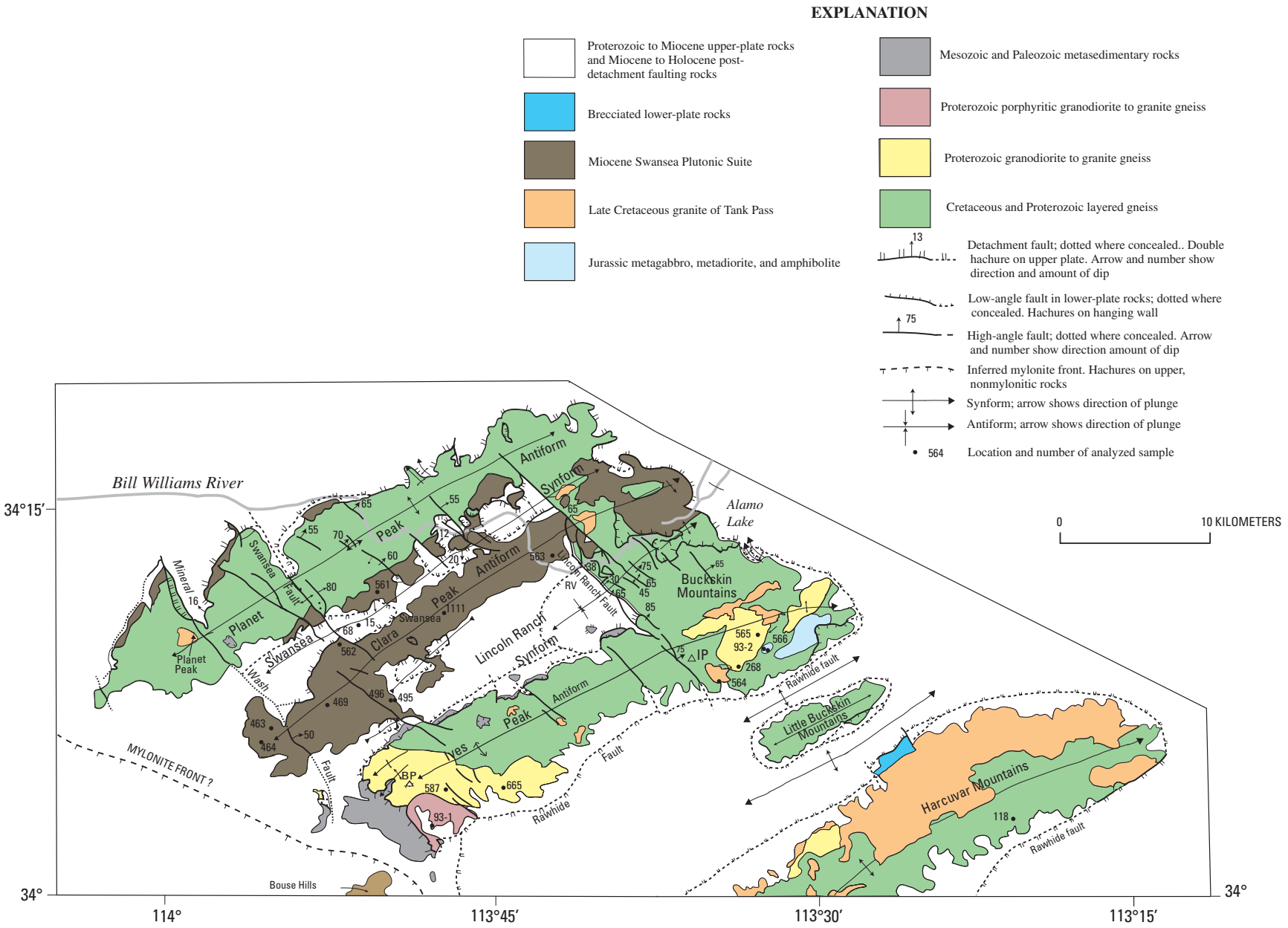

Figure 2. Geologic map of the northern Harcuvar complex showing locations of analyzed and(or) dated rocks. Letter prefixes of sample numbers not shown. Simplified from Bryant (1995). BP, Battleship Peak. IP, Ives Peak. RV, Reid Valley.

(1989) describe the mineral deposits in the Buckskin Mountains, some of which occur in the lower-plate rocks.

Osborne (1981) and Woodward (1981) conducted detailed mapping and structural studies of the upper-plate and lower-plate rocks near Swansea in the central and western Buckskin Mountains.

Marshak and Vander Meulen (1989) described the structure of metasedimentary and underlying basement rocks in the southwestern Buckskin Mountains and subdivided the metasedimentary rocks into map units based on detailed mapping of that area (Marshak and others, 1987).

Seismic studies through the Buckskin Mountains show a thickened middle crust and a thinned lower crust above a subhorizontal Moho at 26–28-km depth. No faults offsetting the seismically determined layers were detected (McCarthy and others, 1991; Clayton and Okaya, 1991).

K-Ar, $^{40}Ar/^{39}Ar$, and fission-track dating studies (Richard and others, 1990; Bryant and others, 1991) show that the lower-plate rocks in the northern Harcuvar complex cooled below about 500°C in Late Cretaceous to early Tertiary time after a Cretaceous metamorphic and plutonic event and cooled below about 280°C in middle Miocene time after undergoing mylonitization under upper greenschist facies conditions. At this time new biotite formed and older biotite was completely degassed, but hornblende was only locally partially degassed, as indicated by $^{40}Ar/^{39}Ar$ spectra. Foster and others (1993) showed that fission-track dates of apatite decrease from southwest to northeast in the Harcuvar and Buckskin Mountains from 21 to 14 Ma and 16 to 13 Ma, respectively. They interpreted these data as showing a slip rate on the Rawhide detachment fault of 7–8 mm/yr. Brady (2002), in a 15-km transect confined to the central part of the Buckskin Mountains, concluded on the basis of (U-Th)/He dating of apatite that part of the lower plate had a slip rate of 4.2 mm/yr over more than 3 my from about 14 to 11 Ma. Carter and others (2004) concluded, based on (U-Th)/He apatite dating, that slip rate along the Rawhide fault in the Harcuvar Mountains was 2.6 km/my (2.6 mm/yr) during the time interval 23–15 Ma but increased to 30 km/my (30 mm/yr) after 15 Ma.

Present Work

In 1986 and 1987, during mapping of the Alamo Lake 1:100,000 quadrangle, lower-plate rocks of the Buckskin and Little Buckskin Mountains were mapped in reconnaissance fashion. In 1987 Bryant helped with the reconnaissance mapping of the Harcuvar Wilderness Study Area (Drewes and others, 1990) and in 1988 completed reconnaissance mapping in the eastern Harcuvar Mountains.

Wooden, as part of his regional studies of crystalline rocks in the Southwestern United States, obtained the geochronologic and Pb isotope data from 1987 to 1993. Preliminary reports (Bryant and Wooden, 1989; Bryant, 1992b; Bryant, Wooden, and Nealey, 1993) on this work show the distribution of the rock types, briefly summarize their characteristics, and announce the discovery of a suite of Oligocene(?)–early Miocene plutonic rocks, which crop out over a significant part of the northern Harcuvar complex in the Buckskin Mountains. The results of mapping in the northern Harcuvar complex are shown on the Alamo Lake 1:100,000 quadrangle (Bryant, 1995). In addition, Bryant and others (1996) gave a summary of the geochronology and metamorphic history of the northern Harcuvar complex. Here we present our field, structural, chemical, and isotopic data and discuss the history and origin of the rock units in the northern part of the Harcuvar complex in the Buckskin and eastern Harcuvar Mountains.

In this report we refer to features that can be located on the 1:100,000-scale Alamo Lake quadrangle and to many detailed features that must be located on the 1:24,000 topographic quadrangle maps that are available throughout the area. The small scale of figure 2 allows only an overview of the entire northern Harcuvar complex.

Geology

Cretaceous–Early Proterozoic layered gneiss crops out over much of the Planet Peak and Ives Peak antiforms in the Buckskin Mountains (fig. 2). Early and Middle Proterozoic and Cretaceous granite, Jurassic diorite and gabbro, and Tertiary gabbro and granite intrude the gneiss (fig. 2). Paleozoic and Mesozoic metasedimentary rocks (not all between distinguished in fig. 2) occur as sheets below the detachment fault and as lenses in the layered gneiss. All of these rocks are mylonitized in various degrees. The mylonitic rocks generally have a well-developed, northeast-trending mineral lineation. About a quarter of the lower plate in the Buckskin Mountains is underlain by distinctive heterogeneous, variably mylonitized, plutonic rock we assign to the Swansea Plutonic Suite (Bryant and Wooden, 1989). This rock unit crops out over much of the Clara Peak antiform in the middle of the Buckskin Mountains; it extends on to the southern flank of the Planet Peak antiform and forms a sill just below the detachment fault on the northwestern flank of the Planet Peak antiform. In the southwestern part of the Buckskin Mountains, it locally extends south of the Lincoln Ranch synform.

In the Little Buckskin and eastern Harcuvar Mountains, rocks of the Swansea Plutonic Suite are absent except for very few microdiorite dikes. Cretaceous granite is much more extensively exposed in the eastern Harcuvar Mountains than in the Buckskin or Little Buckskin Mountains. Layered Early Proterozoic to Cretaceous gneiss is widespread in the northern Harcuvar complex.

Rock Units

Proterozoic and Cretaceous Layered Gneiss

Layered gneiss forms much of the northern Harcuvar complex. Some of the freshest and most extensive exposures are along the canyon of the Bill Williams River between Alamo Dam and Reid Valley. Many washes in the Buckskin and Rawhide Mountains have good exposures, and Ives Peak, the highest peak in the Buckskins (not named on the USGS topographic maps, but indicated by the 1,197-m spot elevation on the Alamo Lake 1:100,000 quadrangle), has cliffs of layered gneiss containing sills of Cretaceous granite.

The layered gneiss is a heterogeneous unit, but its variations are similar throughout the northern Harcuvar complex. It consists of layers of biotite-quartz-feldspar gneiss, granite gneiss, biotite-hornblende gneiss, hornblende-biotite gneiss, amphibolite, and minor amounts of biotite-muscovite schist (see figs. 3, 4, 24, 25, 29, 30). In many places the granite layers grade into the nongranitic layers, and the rock is a migmatite. Layers range from a centimeter to more than 10 meters thick. Foliation is everywhere well developed, and many of the rocks are mylonitized to various degrees. The mylonitic texture is best developed and most pervasive in the eastern Buckskin and Harcuvar Mountains and in the Little Buckskin Mountains. In the western Buckskins, in many outcrops, mylonitic texture is only locally developed, and then only in the granitic layers. Many of the felsic layers contain porphyroclasts of feldspar 0.5 to 2 cm in diameter. Much of the amphibolite is not mylonitized or is only weakly mylonitized. Layering ranges from very well defined to faint in the more granitic parts of the unit. Concordant and discordant pegmatite lenses, layers, and dikes are widespread. In some areas the lenses are the remains of stringers and dikes disrupted by ductile deformation during Tertiary mylonitization or some older episode of shearing. Where the characteristic effects of Tertiary mylonitization are lacking, the rocks are well foliated.

The layered gneiss locally contains numerous sills of leucocratic garnet-bearing biotite granite, especially near mapped bodies of that granite, which we correlate with the Late Cretaceous granite of Tank Pass of the Harcuvar and Granite Wash Mountains. In a few places the leucocratic granite cuts older granite layers in the layered gneiss. Here and there in the layered gneiss unit are pods and lenses of gabbro, metagabbro, and hornblendite as much as 4 m thick and 20 m long. Locally, the gabbro contains segregations of hornblende-plagioclase pegmatite as much as 10 cm in diameter and having a grain size of 2 cm. The mafic rocks range from unmetamorphosed to locally converted to amphibolite.

The layered gneiss unit contains rocks with a variety of textures and compositions. Some amphibolites, even in the eastern Buckskin Mountains, do not show the effects of Tertiary mylonitization. In hornblende and biotite-hornblende gneiss, the hornblende grains commonly form porphyroclasts. The effects of Tertiary mylonitization are much more pervasive in rocks containing quartz than in rocks that lack it. The diverse rocks of the layered gneiss unit have a variety of textures depending on their mineralogy and the severity of mylonitization they underwent. Although the effects of mylonitization are much more pervasive in the eastern than the central and western Buckskin Mountains, weakly mylonitized rocks can be found in the eastern Buckskin Mountains and strongly mylonitized rocks in the western Buckskin Mountains. No well-defined contact separates areas of more and less pervasive mylonitization.

In strongly mylonitized quartz-feldspar rocks, the feldspars commonly form porphyroclasts in a finer grained matrix of recrystallized, cataclastically broken down material. Quartz may form porphyroclasts, which tend to be ductilely elongated, but in many rocks it forms elongate lenses of recrystallized quartz. Biotite may form porphyroclasts that commonly show the effects of deformation. They are bent or, in some cases, folded. In many rocks the biotite was reconstituted during mylonitization and forms small synkinematic grains in the matrix.

In the least mylonitized quartz-feldspar rocks, those minerals are commonly about 0.5 mm in diameter, but some feldspar grains are several millimeters long. Quartz has a mosaic texture, either filling in around the feldspar grains or as aggregates as much as several millimeters long. Biotite is synkinematic to postkinematic. In parts of the rocks, finer grained feldspar (probably recrystallized mortar) rims the larger feldspar grains.

Mafic rocks range from metagabbro to amphibolite and hornblendite. Amphibolite occurs as layers or lenses (see fig. 25*C*) in the gneiss and as zones and margins on metagabbro bodies. Few amphibolites are mylonitized, but those that are, generally have actinolite formed at the expense of hornblende.

Muscovite-biotite schist commonly has large muscovite porphyroclasts that are deformed into lenticular “fish” that show sense of shearing. Biotite forms sparse smaller porphyroclasts and is commonly seen as grains inferred to be synkinematic with the mylonitization. One sample from NW corner sec. 19, T. 10 N., R. 12 W. contains porphyroclasts of sillimanite as much as 1 mm long in addition to muscovite as much as 2 mm long in a sericitic matrix.

The layered gneiss unit has not been directly dated and apparently has a long and complex history. It is intruded by plutons of granitic rock. In one small area, some samples of the plutonic rocks have been dated as Early Proterozoic and some as Middle Proterozoic (see “Proterozoic Granitic Rocks” in Geochronology section). The gneiss contains granitic layers that appear to be of two generations. One type of granitic layer has a range in texture and composition and in many places has gradational contacts with gneiss of various compositions. These granitic layers appear to have formed during an event involving migmatization and partial melting. The other type of granitic layer is composed of relatively homogeneous granite and leucogranite that we interpret to be intrusive and correlative with the granite of Tank Pass, which has a U-Pb zircon

Figure 3. Migmatitic layered gneiss and granite in the eastern Harcuvar Mountains. Granitic layer is similar to analyzed sample HA–118, which was collected within about 10 meters from this exposure. Smith Peak 7½-minute quadrangle, in bottom of canyon 500 meters from south line and 30 meters from east line of sec. 7, T. 8 N., R. 10 W. Hammer is 22 centimeters long.

Figure 4. Layered mylonite from layered gneiss in the eastern Buckskin Mountains. Derived from calc-silicate gneiss and biotite-quartz-feldspar gneiss containing lenses of pegmatite. Alamo Dam 7½-minute quadrangle, sec. 16, T. 10 N., R. 13 W. in wash 460 meters from south line and 200 meters from west line.

age of 78–80 Ma in the western Harcuvar Mountains (DeWitt and Reynolds, 1990).

The protolith of the layered gneiss unit is difficult to determine. Most of the rocks have igneous compositions ranging from granite to gabbro but locally are layers of biotite-muscovite schist that represent aluminous rocks that could have been shale in a section rich in tuffaceous sedimentary rock or a horizon of weathering on volcanic rock. Some pods of mafic and ultramafic rock retain igneous texture in whole or in part. Some of these bodies are of Jurassic age (see "Jurassic Plutonic Rocks" in Geochronology section), but perhaps some are of Proterozoic age.

Proterozoic Granodiorite to Granite Gneiss

Coarse- to fine-grained mylonitic and nonmylonitic biotite and hornblende-biotite granodiorite gneiss form several plutons in the Buckskin Mountains. In the northeastern Buckskin Mountains, this unit is generally coarse grained and contains porphyroclasts of feldspar as much as 7 cm long (fig. 5*A*). The rock is pervasively mylonitized and displays a well-developed northeast-trending lineation. Stringers and lenses of aplite and pegmatite as much as 7 m thick occur in the granite. The granite commonly contains amphibolite xenoliths. Locally, it has concordant streaks, inclusions, and layers of more biotitic biotite-quartz-feldspar and feldspar porphyroclast biotite-quartz-feldspar gneiss.

The contact with the layered gneiss unit is difficult to locate precisely. In places, the rock mapped in this unit is a medium-grained biotite granite (fig. 5*B*); in one place, that rock type cuts the coarse-grained granite. At the scale of the mapping, differentiating the two rock types was not feasible.

In the southern part of the central Buckskin Mountains, rocks of the unit are generally medium grained but contain zones of coarse-grained, porphyritic granite (fig. 6) like that of the porphyritic granite unit. Foliation is well developed, but the northeast-trending lineation is only locally present except in mylonite zones. The best developed mylonite is directly beneath a unit of metasedimentary rock that dips southwest off the southwestern end of the Ives Peak antiform (fig. 2). Stringers, lenses, and dikes of pegmatite as much as 2 m thick cut the granite. The granite contains xenoliths of amphibolite and layered gneiss.

In both the northeastern and south-central areas, sills of leucogranite and aplite, locally containing garnet, cut the plutonic rocks. These are interpreted to be of Cretaceous age (see "Late Cretaceous Granite of Tank Pass"). In the western Buckskin Mountains intrusions of fine- to medium-grained, mylonitized granitic rock in this unit are interpreted to be of Miocene age. Other aplitic and pegmatitic stringers and lenses are probably of Proterozoic age (fig. 5*A*)

The textures of the granitic gneisses in the two outcrop areas differ because of differences in degree of cataclasis and ductile deformation during Miocene time. Megascopically, the contrast is most obvious in the development of the northeast-trending mineral lineation. In the northeastern Buckskin Mountains that lineation is generally well developed throughout the rock; to the southwest it tends to be restricted to local zones.

In the northeastern Buckskin Mountains, quartz forms aggregates of 0.05–0.2-mm grains as much as 3 mm long and a few ductilely deformed porphyroclasts as much as 1.5 mm long. Plagioclase (oligoclase) occurs in porphyroclasts as much as 4 mm in diameter. Potassic feldspar forms anhedral porphyroclasts as much as 1 mm in diameter. Biotite as much

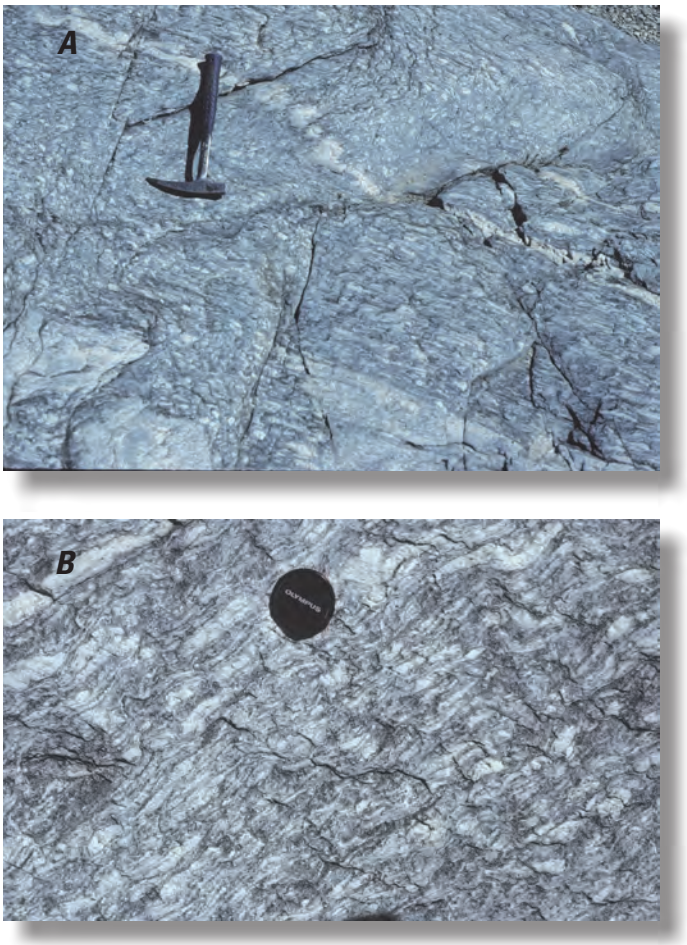

Figure 5. Mylonitic granodiorite gneiss from the eastern Buckskin Mountains. Alamo Dam 7½-minute quadrangle. In wash, SE¼SE¼ sec. 36, T. 10 N., R. 13 W. *A*, Fold in mylonitic foliation. Granitic rock contains aplite and pegmatite stringers. Hammer is 22 centimeters long. *B*, Elongate feldspar porphyroclasts. Lens cap is about 4 centimeters in diameter.

as 1 mm in diameter is synkinematic to locally postkinematic. The two feldspars, quartz, and biotite form a matrix to the larger grains.

In the south-central Buckskin Mountains, anhedral quartz is 0.3–1 mm in diameter and forms mosaic-textured aggregates. Locally. the quartz is strained and broken down into subindividuals. Plagioclase (oligoclase) forms anhedral porphyroclasts as much as 2 mm in diameter, which are locally bent. Potassic feldspar forms porphyroclasts as much as 5 mm in diameter. Synkinematic biotite is generally less than 1 mm in diameter but locally as much as 3 mm in diameter. The largest grains are locally bent. Quartz and feldspar with a grain size of 0.1–0.5 mm and a granoblastic texture form the matrix of the feldspar porphyroclasts. Mylonitic zones in the granite gneiss of the south-central Buckskin Mountains have textures similar to the mylonitic granitic rocks of the northeastern Buckskin Mountains.

Accessories in rocks of both areas are allanite, epidote, sphene, apatite, opaque mineral, zircon, and myrmekite. Secondary minerals are chlorite from biotite, epidote, sericite, and carbonate from plagioclase.

Proterozoic Porphyritic Granodiorite to Granite Gneiss

Well-foliated porphyritic granodiorite to granite gneiss underlies a small area east of Butler Pass in the southwestern part of the Buckskin Mountains, which is exposed beneath lower-plate metasedimentary rock in two places. In many places, feldspar porphyroclasts 2–3 cm long in a finer grained, well-foliated matrix form a flaser structure. The gneiss contains concordant to slightly discordant sills of pegmatite and aplite 0.1–0.3 m thick. A 2-m-diameter body of coarse-grained hornblendite is included in the porphyritic granite gneiss in one place. The porphyritic rock has a gradational contact with equigranular granite gneiss; zones of porphyritic rock occur in the equigranular rock near the contact.

The porphyritic granodiorite is apparently closely related to the adjacent equigranular granite. We have no geochronological data for that body, but we believe that it is Proterozoic. No intrusions resembling it were found in the slice of Paleozoic and Mesozoic metasedimentary rock overlying it along a ductile fault, but many intrusions in that slice appear to be related to the Swansea Plutonic Suite.

Paleozoic and Mesozoic Metasedimentary Rocks

At the southwesern margin of the Buckskin Mountains, Phanerozoic metasedimentary rocks form a gently southwest-dipping fault slice between mylonitic Proterozoic plutonic rocks below and nonmylonitic Early Proterozoic rocks and early Miocene granitic rocks above. The nonmylonitic rocks are exposed in the Bouse Hills (fig. 1), which are south of the western Buckskin Mountains. The slice of metasedimentary rocks crops out over about 16 km^2 on and southwest of Battleship Peak (fig. 2; Marshak and Vander Meulen, 1989). Elsewhere in the Buckskin Mountains, similar rocks form numerous smaller slices below the detachment fault above and within the mylonitized plutonic rocks. These rocks have not been found in the eastern Harcuvar Mountains.

The slice at Battleship Peak is approximately concordant with the foliation in the underlying metamorphosed plutonic rocks. However, as Marshak and Vander Meulen (1989) pointed out, it is discordant in detail. Near the base of the metasedimentary rocks, the augen gneiss, much of which does not have pervasive northeast-trending mylonitic lineation, is intensely mylonitized. In one place, the margin of a sill of biotite-quartz-feldspar porphyry is foliated. The porphyry is probably a part of the Miocene Swansea Plutonic Suite. On the east side of Battleship Peak, foliation in nonlineated augen gneiss below the metasedimentary rock dips gently north. The

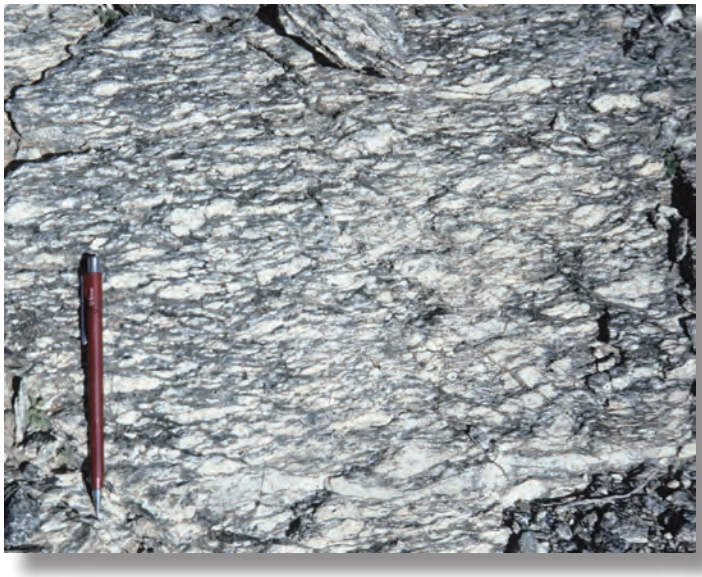

Figure 6. Mylonitic coarse-grained granite gneiss from the central Buckskin Mountains. Flattened feldspar mostly 1 to 2 centimeters long and 0.5 centimeter thick, but some are as much as 4 centimeters long. Butler Pass 7½-minute quadrangle. On ridge on west side of easternmost major wash in the east-central part of the quadrangle, 130 meters S. 24°E. from spot elevation 2,374, and 3,120 feet S. 80° E. from spot elevation 2,579 on Battleship Peak. Pencil is 12 centimeters long.

base of the metasedimentary rock dips very gently southwest. At the contact between metasedimentary and basement rock, the augen gneiss is intensely sheared along planes dipping parallel with the base of the metasedimentary rock and has a northeast-trending lineation. In one locality northeast-trending lineation occurs in the basement rocks only within 2 m of the contact with the metasedimentary rocks. In other places the lineated rock below the contact is as much as 5 m thick. At another locality the foliation in porphyritic granodiorite is concordant with the base of the metasedimentary rock only within about 4 m of the contact. A 1- to 1.5-m-thick sill of Oligocene(?)-Miocene Swansea Plutonic Suite rock is parallel with the mylonitic foliation in the porphyritic granite 2–3 m below the contact.

The metasedimentary rocks consist of marble, quartzite, sandy marble, calcareous quartzite, and calc-silicate schist and gneiss. The marble is white, light gray, pale yellowish gray, pale greenish gray, pale brownish gray, yellowish gray, or yellowish brown and stands out in the darker gray and brownish-gray-weathering layered gneiss. The yellowish brown and yellowish-gray marbles are generally dolomitic. Quartzite is white, pale gray, greenish gray, and, where calcareous, weathers brown. Calc-silicate gneiss and schist are pale green, greenish gray, or dark greenish gray and difficult to distinguish in outcrop from fine-grained biotite-quartz-feldspar mylonite or mylonitic fine-grained diorite or granodiorite of the Swansea Plutonic Suite.

Slices of metasedimentary rock are locally abundant. An almost continuous slice crops out along the northwestern flank of the Ives Peak antiform as far northeast as Reid Valley. About 4 km north of Battleship Peak, that slice is in fault contact with mylonitized Miocene plutonic rocks of the Swansea Plutonic Suite. A zone of moderately to very gently north-dipping slices of metasedimentary rock in the layered gneiss northeast of Reid Valley extends to the northeastern margin of the Buckskin Mountains near Alamo Dam (fig. 7). The slices in that zone are as much as 2 km long and 20 m thick, and three or more slices are 50–150 m thick, measured perpendicular to foliation and layering, but are too thin to show at 1:100,000 scale.

North of that zone, slices of similar rock occur scattered in the layered gneiss. Another concentration of slices as much as 500 m long is 3 km north of Swansea and extends about 3.5 km to the northeast. The slices are at the contact with and in the layered gneiss within 200 m of the contact of the Swansea Plutonic Suite. In that area the Swansea Plutonic Suite intrudes some of the slices of metasedimentary rock.

Slices of marble are as small as 0.5 m thick and 10 m long. They tend to pinch and swell due to the ductility contrast between the marble and the adjacent quartzo-feldspathic layered gneiss.

Sills and lenses of pegmatite and leucocratic granite, probably of Cretaceous age, are widespread throughout the slices of metasedimentary rock. They have been folded along with the metasedimentary rock and locally are very weakly foliated. Some of the layers thought to be part of the metasedimentary strata in the field are sills proved to be mylonitized fine-grained biotite or biotite-hornblende diorite, quartz diorite, or granodiorite when examined in thin section. In some, igneous texture is preserved. These are probably part of the Swansea Plutonic Suite. Others consist of mylonitized, coarser grained granitic rock and resemble many of the layers in the layered gneiss unit. They may represent tectonic intercalations.

In the Battleship Peak area the metasedimentary rocks can be divided into six map units that change thickness and character along strike, according to Marshak and others (1987) and Marshak and Vander Meulen (1989, who also suggest that metasedimentary rocks were derived from both Paleozoic and Mesozoic protoliths, but did not correlate them with specific formations. They felt that the top unit probably had a Paleozoic protolith, and the unit underlying it had a Mesozoic protolith, although facing criteria were not found in those metamorphic rocks. They interpret the sequence as overturned by folding or repeated along a thrust fault.

Thin sections show that the metasedimentary rocks are completely recrystallized and that no sedimentary textures and structures are preserved other than layering that probably represents transposed bedding. Calcite and dolomite are fine to medium grained. Quartz occurs in elongate, ductilely deformed grains and aggregates of grains that are as

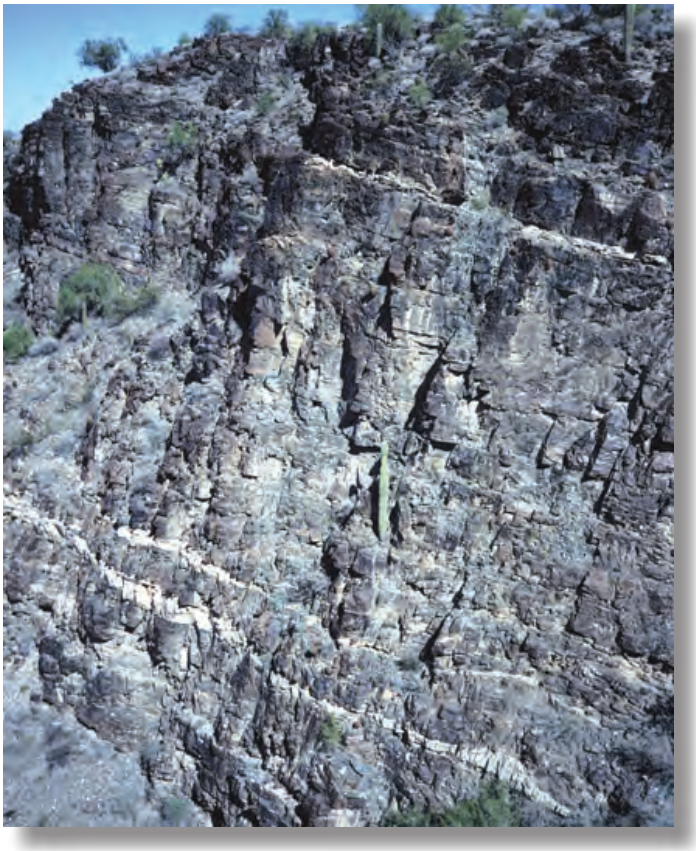

Figure 7. Thin layers of marble in migmatitic layered gneiss in the eastern Buckskin Mountains. Three light-colored, locally discontinuous marble layers as much as 3 meters thick pinch and swell. Alamo Dam 7½-minute quadrangle. Canyon wall on tributary to Ives Wash in SE¼SE¼ sec. 15, T. 10 N., R. 13 W.

much as 1 mm long. Common calc-silicate minerals in impure quartzites, marbles, and calc-silicate schist and gneiss are epidote and tremolite-actinolite. Amphibole is in grains as much as 1 mm long aligned with the northeast-trending lineation. Some of the amphibole is green to olive green and is probably actinolitic hornblende. In some samples the composition of the amphibole differs between layers of different compositions. Some of the larger amphibole grains have a lenticular outline and are probably porphyroclasts. In a thin section perpendicular to the axis of one tight fold, the amphibole forms polygonal arcs around the nose of the fold, which is cut by shears parallel with its axial plane. In an adjacent layer, quartz grains are ductilely elongated in a northeast trend on the axial plane of the fold. In this case deformation and recrystallization of the quartz continued along the axial plane of the fold after folding and amphibole crystallization.

About 20 percent of thin sections of this unit that we examined contain diopside. In some rocks it is in bent or broken grains as much as 3 mm in diameter, which are partly altered to calcite, actinolite, or a very fine "dust" within the grains. In other rocks the diopside appears to be in equilibrium with amphibole and(or) epidote. Many diopside grains in these rocks display well-developed polysynthetic twinning.

A few of the metasedimentary rocks contain euhedral to anhedral, pale yellowish brown garnet as much as 0.6 mm in diameter that is partly altered to calcite, epidote, and(or) chlorite. In one sample the garnet is apparently contemporaneous with epidote and amphibole in the main mineral assemblage.

Synkinematic to postkinematic biotite is as much as 0.3 mm long, and lenticular and bent porphyroclasts of biotite are as much as 1 mm long.

The textures and mineralogy of the metasedimentary rocks suggest that they may have been metamorphosed twice, once probably in the Cretaceous and again during the Miocene extensional deformation. The earlier mineral assemblage consists of epidote, amphibole, diopside, garnet, and biotite and formed under amphibolite facies conditions. During Miocene shearing, new biotite, quartz, epidote, carbonate, actinolite, and chlorite formed under greenschist facies conditions.

Jurassic Metagabbro, Metadiorite, and Amphibolite

Variously metamorphosed diorite and gabbro at the southern edge of the eastern Buckskin Mountains in the south-central part of T. 10 N., R. 12 W. were previously assigned a Proterozoic age (Bryant and Wooden, 1989). However, U-Pb dating of zircon from a metadiorite in that area indicates that the rocks are about 148 Ma or Late Jurassic, as described herein.

The metadiorite and metagabbro crop out in an area about 5 km long and 1 km wide and contain much layered gneiss. The area underlain by these rocks is mapped as one pluton but appears to consist of numerous intrusions of various dimensions in the layered gneiss or to contain many inclusions of gneiss. The mafic rocks range from metadiorite and metagabbro having some relict igneous texture to biotite-hornblende-plagioclase gneiss, hornblende-biotite schist, and amphibolite. The layered gneiss between the intrusions is commonly mylonitized. The mafic rocks are cut by sills of felsic rock and pegmatite.

One particularly good exposure of well-foliated, ductilely deformed gabbro is in the Alamo Dam 7½-minute quadrangle and in a wash 280 m N. 80 W. from hill 2461 in the southwest corner of sec. 31, T. 10 N., R. 12 W. There, the metagabbro is cut by two types of sills, both of which have been drawn out into distinctively shaped fragments ("fish") indicating that the lower rock moved southwest relative to the upper rock (fig. 8). Both sills are trondhjemite. One is gray and contains biotite and the other is white and contains muscovite. They differ from sills of leucocratic rock in the layered gneiss, which are granite where we have studied them.

Textures in the metadiorite and metagabbro range from granoblastic to cataclastic. One granoblastic-textured rock has anhedral plagioclase (An_{34-46}) showing normal and weak oscillatory zoning and forming a mosaic texture with a grain size of

0.5 mm. Anhedral to subhedral blue-green hornblende as much as 2 mm long is in elongate aggregates as much as 6 mm long. This texture probably is the result of Cretaceous metamorphism without any overprint by later events. A rock showing severe cataclastic deformation has anhedral, rounded, locally bent, porphyroclasts of plagioclase (An_{28}) as much as 1 mm in diameter and anhedral dark green porphyroclasts of hornblende as much as 1 mm long in a matrix of quartz, plagioclase, and hornblende with a grain size of 0.05–0.3 mm. Zones of microbreccia or ultramylonite containing rounded grains of plagioclase and hornblende in a cryptocrystalline to glassy matrix cut the rock.

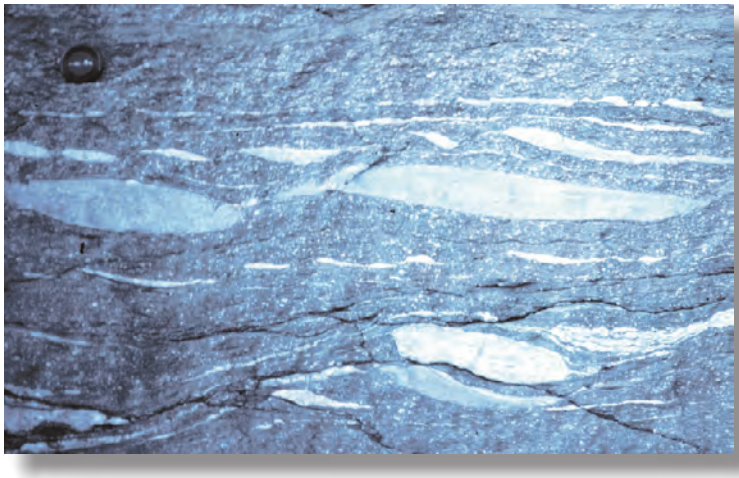

Figure 8. Mylonitic biotite hornblende gneiss derived from gabbro containing trondhjemite sills that have been deformed into "fish." Analyzed samples Appendix nos. 11, 13, and 14 are from this outcrop. Plane of photograph approximately parallel with northeast-trending lineation. Northeast is to the left. South side of wash, Alamo Dam 7½-minute quadrangle. Sec. 31, T. 10 N., R. 12 W., 140 meters from south line, 420 meters from east line. Lens cap is about 4 centimeters in diameter.

Some rocks of the unit contain subhedral plagioclase phenocrysts as much as 4 mm long. They contain secondary epidote, suggesting that during metamorphism the plagioclase was decalcified to its present andesine composition from labradorite, the composition typical of gabbros.

Biotite is a major constituent of many rocks of the unit. It occurs in synkinematic to postkinematic crystals as much as 1.5 mm long. In a few rocks the grains have been bent during younger deformation.

Accessory minerals include epidote that appears to be contemporaneous with metamorphic biotite and plagioclase, apatite, sphene, opaque minerals, zircon, and allanite. Chlorite and some of the epidote formed late in the history of the rock.

Late Cretaceous Granite of Tank Pass

Light-colored granite forms numerous sills and small plutons in the layered gneiss in the Buckskin and Little Buckskin Mountains and large sill-like bodies in the eastern Harcuvar Mountains. There the main body is at least 200 m thick. Its top is subconcordant with layering in the country rock, and no floor is exposed. Many sills of granite intrude the country rock overlying the main body. We correlate this granite with the granite of Tank Pass of the western part of the Harcuvar Mountains, which has a U-Pb zircon date of 78–80 Ma (DeWitt and Reynolds, 1990). A sample of a 5- to 30-cm-thick dike of leucocratic granite from the Harcuvar Mountains, about 2.5 km south of the area of this study, has a zircon age of 70±2 Ma, based on single-crystal determinations. Only one crystal gave a concordant analysis. Other grains analyzed are discordant due to inheritance from rocks of both Early and Middle Proterozoic age. Uncertainties in the lower intercepts of regressions based on the discordant grains overlap a 78–80-Ma zircon date on the granite of Tank Pass of the western Harcuvar Mountains (Isachsen and others, 1999). In the western Harcuvar Mountains, the granite of Tank Pass is cut by the granodiorite of Granite Wash, hornblende from which has a plateau age of 78.6±0.4 Ma (Richard and others, unpublished data cited in Isachsen and others, 1999). Since the granite of Tank Pass is foliated even where not mylonitized and the dike dated is not, the dike may be somewhat younger than the granite of Tank Pass.

In the Buckskin Mountains, sills of the granite of Tank Pass are especially numerous adjacent to mapped plutons, and the plutons have complex, discordant contacts where they pass into sills. In the Planet Peak area in the western part of the range, many intrusions of leucocratic granite were combined to form a map area of granite. In the Little Buckskin Mountains, where no plutons were mapped, sills probably related to the granite of Tank Pass are numerous, and other workers might map a body of granite on the crest of that range.

Concordant pegmatite lenses, stringers, and knots as much as 1 m thick cut the granite in places. These pegmatites are widespread in the layered gneiss country rock, and they cut the slices of metasedimentary rock. The granite locally contains inclusions of layered gneiss from the wallrock.

The granite of Tank Pass (fig. 9) is a mylonitic, leucocratic, medium- to coarse-grained biotite and muscovite-biotite granite containing sparse accessory garnet and having a color index of about 5. It has a well-developed mylonitic foliation parallel to the foliation in the layered gneiss country rock. Northeast-trending, stretched mineral lineation ranges from very well developed to absent.

Figure 9. Mylonitic biotite granite in the eastern Buckskin Mountains correlated with the Late Cretaceous granite of Tank Pass in the Harcuvar Mountains. Southwest part of Alamo Dam 7½-minute quadrangle about 200 meters from analyzed sample (Appendix no. 16; table 5). In wash S. 56° W. from spot elevation 3,110. Knife is 7 centimeters long.

Quartz is in aggregates of ductilely deformed grains as much as 3 mm long. Plagioclase, generally An_{12-22}, is in anhedral to subhedral porphyroclasts as much as 5 mm long. Potassic feldspar forms porphyroclasts as much as 4 mm long. Synkinematic and postkinematic biotite flakes are generally 0.5 mm, but locally as much as 1.5 mm, in diameter. In a few rocks, muscovite is intergrown with biotite. All these minerals also form a matrix of recrystallized cataclastic material. Myrmekite is widespread. Accessory pale red anhedral to subhedral garnet is as much as 2 mm in diameter. Other accessory minerals are apatite, sphene, zircon, opaque mineral, and allanite. Secondary minerals are chlorite from biotite, carbonate in late veinlets, and sericite.

Oligocene(?) and Miocene Swansea Plutonic Suite

In the Buckskin Mountains a distinctive group of plutonic rocks forms the Clara Peak antiform and extends across the Swansea synform to the southeastern flank of the Planet Peak antiform and locally to the northwestern flank of the Ives Peak antiform (fig. 2). These plutonic rocks underlie about 370 km^2 of the lower plate in the Buckskin and Rawhide Mountains but are partly covered by upper-plate and younger, postdetachment rocks. These rocks are mapped as the Swansea Plutonic Suite (Bryant and Wooden, 1989) and consist of a variety of rocks that are well mixed on a scale that precludes distinguishing the separate rock types at a scale of 1:100,000.

The rocks of the Swansea Plutonic Suite range from gabbro to granite. Gabbro and diorite are medium to coarse grained, locally porphyritic only locally mylonitized, and intruded by more felsic and intermediate rocks of the suite. The felsic and intermediate rocks are fine to medium grained and variously porphyritic and have a well-developed mylonitic texture and a northeast-trending mineral lineation formed by ductilely deformed quartz grains and aggregates (fig. 10). Aplite is a minor phase, which intrudes the other rocks sparsely and is mylonitized.

Another major component of the complex is porphyritic granite, which is found in the felsic phase as bodies a meter to tens of meters thick. The porphyritic granite is not found to be included in or cutting the mafic rocks. Fine- to medium-grained granites cut the porphyritic granite. Contacts between the porphyritic granite and the felsic phase are generally sharp but locally gradational. The porphyritic granite has well-developed foliation and lineation and contains K-feldspar phenocrysts (now porphyroclasts) as much as 3 cm in diameter (fig. 11). The porphyritic granite does not resemble the wallrock exposed in the Buckskin Mountains, nor are bodies of porphyritic granite concentrated in any particular area in the felsic phase of the Swansea Plutonic Suite in the Buckskin Mountains.

Approximate modes of Swansea Plutonic Suite rocks show that they range from gabbro to leucomonzogranite according to the IUGS classification (Streckeisen, 1973). Fifteen to 20 percent of the samples studied are either diorite or granodiorite. Color index ranges from 2 to 62. About 15 percent of the rocks examined have a microcrystalline matrix composing 25 percent or more of the rock and consisting of feldspar and probably quartz and, locally, some very fine grained biotite. Another 7 percent of the rocks have a similar matrix that forms less than 25 percent of the rock.

The mafic rocks contain euhedral to subhedral plagioclase 0.5–5 mm long, which is generally calcic andesine and displays normal and, less commonly, oscillatory zoning. Locally, the crystals are strained and bent. Anhedral to subhedral hornblende as much as 3 mm long fills in around the plagioclase grains. Some mafic rocks contain a minor amount of biotite in primary grains as much as 1 mm in diameter and as secondary grains 0.1 mm in diameter. Accessory minerals are sphene, apatite, and opaque minerals. Secondary minerals are chlorite, actinolite, and epidote. Because these rocks contain andesine and have a color index of less than 50, they are diorites according to the IUGS classification (Streckeisen, 1973), but a few have a color index of greater than 50, indicative of gabbro in that classification. Geochemical composition of two samples of mafic rock indicates that they are gabbros when compared with a compilation of chemical compositions of rocks called gabbro from the literature by Le Maitre (1976). (See section “Geochemistry” herein.)

Figure 10. Mylonitic biotite granodiorite from the felsic phase of the Swansea Plutonic Suite. Texture and composition similar to analyzed and dated sample (Appendix no. 25, tables 2 and 5). Swansea 7½-minute quadrangle. Sec. 19, T. 10 N., R. 15 W., 430 meters from east line, 30 meters from south line. Face of outcrop parallel northeast-trending mineral lineation. Knife is 7 centimeters long.

Figure 11. Mylonitic porphyritic granite or monzogranite from inclusion in felsic phase of the Swansea Plutonic Suite. Reid Valley 7½-minute quadrangle. Section 8 or 9, T. 10 N., R. 14 W. U-Pb zircon age indicates that these inclusions are derived from Middle Proterozoic basement rock (tables 1 and 2; fig. 16). Pencil is 7 centimeters long.

Most of the rocks that contain any quartz have a mylonitic foliation because the quartz deformed ductilely under the conditions of metamorphism during extensional deformation. The quartz is interstitial to feldspars, and it forms aggregates as long as 3 mm composed of 0.05- to 0.2-mm-diameter grains. The individual grains in the aggregates have strain shadows in most rocks, but in a few they are in mosaic-textured aggregates, suggesting that in those rocks recrystallization of the quartz lasted longer than deformation of the rock. In a few rocks the quartz crystals as much as 1 mm in diameter have not been broken into smaller grains. Plagioclase ranges from euhedral phenocrysts to anhedral porphyroclasts 1–4 mm long, is calcic oligoclase to sodic andesine, and displays normal and oscillatory zoning. Locally, the plagioclase grains are bent and broken. Potassic feldspar is in anhedral to subhedral porphyroclasts 1–7 mm long, some of which are strained, bent, and broken. Some potassic feldspar is weakly perthitic, and some has poorly developed microcline twinning. Brown biotite forms bent porphyroclasts 0.5–2.5 mm in diameter. Brownish-green, new biotite 0.05–0.2 mm in diameter occurs in the matrix of recrystallized cataclastic material. Green to dark green, anhedral to subhedral hornblende forms grains as much as 1.3 mm long, some of which have rounded edges and are probably porphyroclasts. Accessory epidote, allanite, sphene, apatite, zircon, and opaque minerals complete the main mineral assemblage. Allanite is commonly rimmed by epidote. Secondary minerals are epidote, chlorite, actinolite, and carbonate and locally are a major component where all the biotite and hornblende have been altered. Many rocks have such a fine-grained matrix that it is difficult to tell whether it represents results of cataclastic breakdown of larger grains or a matrix of a porphyritic rock.

Because the inclusions of porphyritic granodiorite to granite are a component of the Swansea Plutonic Suite but are in areas too small to map at 1:100,000, we describe them here. The rocks contain aggregates of quartz with a grain size of 0.05–0.3 mm as much as 2 mm long. The quartz grains are usually strained but locally recrystallized into mosaic-textured areas. Anhedral porphyroclasts of plagioclase are locally bent and broken. Potassic feldspar forms porphyroclasts as much as 1.2 cm long, which are fractured, strained, and broken. The potassic feldspar is locally perthitic and shows microcline twinning. Biotite occurs as locally bent porphyroclasts as much as 0.5 mm in diameter and as new, very small grains 0.1 mm and less in diameter. Green to dark green hornblende is in porphyroclasts as much as 1 mm long. Accessory minerals are allanite commonly rimmed by epidote, sphene, apatite, epidote, opaque mineral, and zircon. Epidote and chlorite are secondary minerals from alteration of plagioclase and biotite.

The various rocks have sharp and gradational contacts with each other and with their country rocks. Diffuse contacts with country rock are formed by numerous small intrusions of

Swansea rocks near the contact. Inclusions of country rock are numerous in some areas and range from a meter to hundreds of meters in length. Pegmatites are rare in the suite except locally near contacts with country rock. Most of the area mapped as the Swansea Plutonic Suite is underlain by mixed felsic, intermediate, and mafic rocks with felsic and intermediate rocks dominant. An area about 2 km in diameter and two smaller areas north of Reid Valley in the central Buckskin Mountains are underlain predominantly by mafic rocks. An area more than 2 km long and offset by a northwest-trending fault with apparent left-lateral displacement was mapped south of Swansea in the western Buckskin Mountains (Bryant, 1995). Except for a few dikes, no rocks of this suite were identified in the eastern Harcuvar Mountains.

The map relations of the Swansea Plutonic Suite indicate that it lies above layered gneiss in the eastern Buckskin Mountains. At least locally, such as 2–4 km downstream from the Alamo Dam, the contact is a brittle fault. However, in some places of relatively good exposures, such as the west part of sec. 29, T. 11 N., R. 14 W., the Swansea rocks are above the layered gneiss along a contact dipping gently in about the same direction as the overlying detachment fault, and no significant faulting is apparent along that contact. One exposure in that area shows that the Swansea plutonic rock cuts the layering of the layered gneiss. The rocks are mylonitized, but the low-dipping contact apparently does not represent a major ductile fault zone. Another exposure in the same area shows Swansea rocks interlayered in the layered gneiss unit. In secs. 19 and 20, T. 10 N., R. 15 W., on the southeastern flank of the Planet Peak antiform, the low-angle contact of the Swansea with overlying layered gneiss above cuts lenses of metasedimentary rock in the layered gneiss unit. The complex intrusive relations between the Swansea rocks and the layered gneiss wallrock are exposed locally along this part of the contact. On the northwestern flank of the Ives Peak antiform in secs. 21 and 22, T. 9 N., R. 15 W., the contact of Swansea rocks is along a gently dipping brittle fault subparallel with the overlying detachment fault. It is above a slice of metasedimentary rock that is in ductile fault contact with layered gneiss below. The Swansea contact may be steep for 2 km southwest of Alamo Dam, but the dip of the contact is not well constrained due in part to poor exposures and in part to lack of detailed mapping. The same applies to the contact 5 km west of Alamo Dam. Probably the overall shape of the Swansea Plutonic Suite mass is that of a northeast-southwest-trending lens parallel to the regional Tertiary extension and mineral lineation. Although the contacts are brecciated in many localities, in other localities they are not. Apparently the contact is not primarily a fault but was a favorable horizon for late brittle fault movements associated with the overlying detachment fault.

In the eastern Buckskin Mountains an area of layered gneiss 2 km long probably represents the floor of the Swansea rocks, and the contact may be a low-angle brittle fault like that exposed on the north side of the canyon of the Bill Williams River 2–4 km downvalley from Alamo Dam. The contact of the body of layered gneiss surrounded by Swansea rocks in the Rawhide Mountains is poorly exposed. Breccia is found in many areas near the contact but seems to be lacking in others. Consequently, that contact is not shown as a fault on the Alamo Lake 1:100,000 geologic map (Bryant, 1995).

Sparse small intrusions of Swansea plutonic rocks (fig. 12) are found in the layered gneiss away from the contact. The slices of metamorphosed sedimentary rock contain sills of variously mylonitized igneous rocks that are probably part of the Swansea Plutonic Suite. Sparse northwest-trending dikes of unmetamorphosed diabase and hornblende diorite and variably foliated medium-grained granodiorite cut the layered gneisses and are probably related to the Swansea Plutonic Suite. The granodiorite dikes contain phenocrysts of quartz, biotite, plagioclase, and hornblende as much as 5 mm in diameter. The dikes are most numerous in the southeastern part of T. 9 N., R. 15 W. and the northeastern part of T. 8 N., R. 15 W. These dikes resemble those in the Harcuvar and Harquahala Mountains (Drewes and others, 1990; DeWitt and others, 1988; Richard and others, 1990). One such dike from the Harquahala Mountains has a 22.3-Ma $^{40}Ar/^{39}Ar$ total gas age on hornblende (Richard and others, 1990). K-Ar ages of hornblende and biotite from another northwest-trending dike of diorite in the Harquahala Mountains are 28.6±1.9 Ma and 22.1±1.3 Ma, respectively (Shafiqullah and others, 1980). Hornblende from an undeformed diorite sill in the Harcuvar Mountains has a K-Ar date of 25.7 Ma (Rehrig, 1982). In the Harquahala Mountains, dikes of this age are predominantly gabbro but include some rhyolite and dacite (DeWitt and others, 1988).

Figure 12. Small intrusion of granodiorite of the felsic phase of the Swansea Plutonic Suite into layered migmatitic gneiss. Both rocks were mylonitized during the Miocene. Alamo Dam 7½-minute quadrangle at north end of spillway of Alamo dam.

Rocks Probably Correlative with the Swansea Plutonic Suite

In the eastern Bouse Hills, south of the southwestern part of the Buckskin Mountains, a pluton of granodiorite to granite lacks mylonitic textures and has a biotite K-Ar date of 20.5±1.1 Ma (Spencer and Reynolds, 1990b). The granite intrudes Proterozoic crystalline rocks, which are overlain by 24.0- to 19.5-Ma volcanic rocks of various compositions. An upper felsic volcanic unit unconformably overlies tilted older volcanic rocks and has a biotite K-Ar date of 20.5 Ma, the same age as the pluton (Spencer and Reynolds, 1990b). No chemical data are available for that pluton. The older volcanic sequence contains extrusive rocks that are the same age as the Swansea Plutonic Suite and may be extrusive equivalents. The Bouse Hills are interpreted to be a continuation of the lower-plate rocks of the Buckskin Mountains (Spencer and Reynolds, 1991). If so, they are above the mylonitized metasedimentary rocks of the Battleship Mountain slice at the southwestern part of the Buckskin Mountains. A southwest-dipping mylonite front must separate the granite of the eastern Bouse Hills from metasedimentary rocks in the Buckskin Mountains (sec. C–C', Bryant, 1995). Although mapped separately from the Swansea Plutonic Suite (Bryant, 1995), the granitic rock in the Bouse Hills is probably correlative with the Swansea Plutonic Suite.

In the northeastern part of the Bouse hills, medium-grained hornblende-biotite granodiorite and hornblende diorite intergrade. Clots of mafic minerals define a foliation, and the rocks contain a few cognate inclusions of diorite.

The granitic rocks in the northeastern Bouse Hills consist of euhedral to subhedral plagioclase An_{35-22} with normal and oscillatory zoning in grains as much as 3 mm long, subhedral to anhedral hornblende as much as 2 mm long, interstitial anhedral quartz as much as 3 mm in diameter, and anhedral to subhedral biotite as much as 2 mm in diameter. Accessory minerals are sphene, zircon, apatite, and opaque mineral. Secondary minerals are chlorite from biotite and sericite from plagioclase.

Geochronology

U-Pb zircon dating of rocks in the northern Harcuvar complex (tables 1 and 2) in the Buckskin Mountains shows that Early Proterozoic and Middle Proterozoic plutonic rocks cut the layered gneisses, which must be Early Proterozoic or older. A pluton of diorite and gabbro in the eastern Buckskin Mountains is of Late Jurassic age. A granitic layer in the migmatitic layered gneisses in the eastern Harcuvar Mountains is of Early Cretaceous age, showing that at least part of the migmatization is of that age. The Swansea Plutonic Suite, which is widespread in the Buckskin Mountains, is of Oligocene(?) and early Miocene age, similar to that of widespread volcanic rocks above the Rawhide detachment fault and of plutonic rocks in other core complexes of the region.

Proterozoic Granitic Rocks

Sample B–565A (Appendix sample 6) is- fine to medium-grained mylonitic granite, and sample B–565 (Appendix 7) is mylonitic porphyritic granite. These samples were taken about 25 m apart at a locality in the eastern Buckskin Mountains in sec. 31, T. 10 N., R. 12 W. Sample B–562 (Appendix sample 9) is mylonitic porphyritic granite from an inclusion 0.8 m thick concordant with the mylonitic foliation in the felsic phase of the Swansea Plutonic Suite west of Swansea. Four zircon fractions from B–565 define a chord with an upper intercept at 1,638.2±6.4 Ma. Four zircons each from B–565 and B–562 define chords with upper intercepts of 1,388.5±2.3 and 1,408±1.5 Ma, respectively (fig. 13). Note that the lower intercepts of all three discordia lines are at about 22 Ma. Since the granitic rocks that intrude the layered gneiss in the lower-plate rocks are of both Early and Middle Proterozoic ages, we designate all the mapped metaplutonic rocks as either Early or Middle Proterozoic, pending more detailed information that would allow us to differentiate them in the field. Elsewhere in the Harcuvar complex, U-Pb geochronologic studies of Proterozoic plutonic rocks are at present (2006) unavailable.

Jurassic Plutonic Rocks

Sample B–566 (Appendix sample 12) represents a mylonitized hornblende diorite in a gabbro and diorite body forming a pluton on the south side of the east end of the Buckskin Mountains. Five zircon fractions define a discordia line with a lower intercept at 149±2.8 Ma and an upper intercept at 1,653±150 Ma (fig. 14). The value of the upper intercept suggests that Early Proterozoic crust contributed to the origin of the rock. A sixth fraction of zircon is substantially off that chord and was not used in calculating the regression.

This Late Jurassic pluton is north and northeast of any known igneous rocks of that age in the region. The closest known Jurassic igneous rocks of an age similar to the pluton in the eastern Buckskin Mountains are in the Granite Wash Mountains about 45 km to the south-southwest. There, sills and probable flows of basalt to trachyandesite (Gleason and others, 1999) are in sedimentary rocks of the McCoy Mountains Formation (Laubach and others, 1987). Ages of detrital zircon from that formation in western Arizona are all Jurassic or older (Spencer and others, 2005). In the New Water Mountains about 30 km southwest of the Granite Wash Mountains, an andesitic lava flow in the McCoy Mountains Formation has a U-Pb zircon age of 154±2.1 Ma (Spencer and others, 2005). Initial Σ_{Nd} isotopic values of about +5 from two of the most mafic igneous rocks in the McCoy Mountains Formation in the Granite Wash Mountains suggest that those rocks were derived from depleted mantle sources. Rocks having a variety of smaller to negative Σ_{Nd} values may be due to variable interaction with those magmas with crustal rocks or mantle-source heterogeneity (Gleason and others, 1999). The basin in which the McCoy Mountains Formation was deposited has been interpreted to be an extension of the Bisbee basin of

Table 1. U-Pb ages of rocks in the northern Harcuvar complex.

Appendix sample no.	Unit	Field sample no.	Age (Ma)	Comment
7	Mylonitic fine- to medium-grained granodiorite to granite gneiss	B–565	1,388.4±2.3	Early Miocene Pb loss
6	Mylonitic porphyritic granite gneiss	B–565A	1,638.2±6.4	Early Miocene Pb loss
9	Mylonitic porphyritic granite inclusion in Swansea Plutonic Suite	B–562	1,408±1.5	Early Miocene Pb loss
12	Mylonitic hornblende diorite	B–566	149±2.8	Early Proterozoic inheritance
15	Mylonitic granite layer in migmatitic gneiss	HA–118	110±3.7	Early Proterozoic inheritance
18 25	Hornblende gabbro Mylonitic granite	B–563 B–561	21.86±0.60	Middle Proterozoic inheritance

southeastern Arizona and adjacent parts of Mexico and New Mexico; the basin was formed by passive continental rifting when Jurassic arc magmatism retreated due to foundering of the subducted slab (Lawton and McMillan, 1999).

Late Jurassic dikes of the Independence dike swarm and related small intrusions are found in eastern California from the central Sierra Nevada on the north to the southern Mojave Desert on the south. The rocks are predominantly mafic but range to silicic and alkalic. Numerous interpretations of their tectonic significance have been made, and none has been established as the one preferred to date (Carl and Glanzer, 2002).

In the Granite Wash Mountains, the McCoy Mountains Formation overlies Jurassic volcanic rocks correlated with Planet Volcanics of Reynolds and Spencer (1989). This unit consists of felsic metavolcanic rocks and is mapped in the hanging wall of the Rawhide detachment fault at the west end of the Buckskin Mountains. The Planet Volcanics are about 160–155 Ma based on isotopic analysis of zircon (Reynolds and others, 1987) and are the most northerly dated Jurassic volcanic rocks of a regional blanket of felsic metavolcanic rock in southwestern Arizona. Probably correlative metavolcanic rock is found in the hanging wall of the Rawhide detachment on the north side of the eastern Buckskin Mountains (Shackelford, 1976; Lucchitta and Suneson, 1994b).

The presence of a Jurassic plutonic rock in the eastern Buckskin Mountains certainly indicates that either magmatic effects of the extension that formed the McCoy basin continued a considerable distance north of where its deposits are preserved or the processes responsible for the Independence dike swarm extended much farther east than presently known. If we move the Harcuvar complex 60 km northeast relative to the upper plate, that rock should have originated close to lat. 34°30' and long. 113°, the northeast corner of the Alamo Lake 30'× 60' quadrangle and at a depth of 10 km or more beneath the present land surface. No Jurassic plutonic rocks are known at the surface in that area.

Rocks Migmatized in the Cretaceous

Sample HA–118 (Appendix sample 15) from the eastern Harcuvar Mountains is from a layer of granite gneiss like that shown in figure 3 in a well-layered sequence of biotite-quartz-feldspar gneiss, biotite plagioclase porphyroclast gneiss, granite gneiss, and pegmatite. These rocks, which are variously mylonitic, are typical of much of the northern Harcuvar complex and are shown as an Early Proterozoic and Cretaceous layered migmatitic gneiss unit on the Alamo Lake 1:100,000-scale geologic map (Bryant, 1995). Three fractions of zircon from the granite gneiss layer define a discordia line with a lower intercept at 110±3.7 Ma and an upper intercept at 1,669±21 Ma (fig. 15). This indicates that at least some, and perhaps all, of the migmatization in the Early Proterozoic layered gneisses occurred in Cretaceous time. Without more data we hesitate to conclude that no migmatization occurred in Proterozoic time. The only comparable data from similar rocks in the region are from Mesquite Mountain about 45 km west-southwest of the southwest margin of the Harcuvar complex in the Buckskin Mountains. There, a sill of biotite granite in a migmatitic complex has a U-Pb zircon date of 67.2±1.4 Ma, which is interpreted to be the time of injection and migmatization in response to thickening of the crust in the Maria fold and thrust belt (Knapp and Walker, 1989). This date is younger than the 78–80 Ma date on the granite of Tank Pass (DeWitt and Reynolds, 1990), to which we relate the numerous sills and small intrusions in the Buckskin Mountains and the larger plutons in the eastern Harcuvar Mountains. It is similar to the 70±2 Ma age of zircon based on only one concordant analysis (Isachsen and others, 1999) from a dike in the Harcuvar Mountains 2.5 km south of the area of this study. Garnet-bearing granite pegmatite, syn- to late kinematic in relation to latest movement of a thrust fault in the Moon Mountains 50 km southwest of the Buckskin Mountains, has a similar U-Pb zircon age of 71.1±6.7 Ma (Knapp and Walker, 1989).

Table 2. Analytical data and ages of zircons from the northern part of the Harcuvar complex in the lower plate of the Rawhide detachment fault in the Buckskin and eastern Harcuvar Mountains.

[App. no., Appendix number; Field sam. no., field sample number; wt., weight; ppm, parts per million; ±%, plus or minus percent; Ma, mega-annum; mg, milligrams]

						Measured ratios		Corrected ratios						Age (Ma)		
App. no.	Field sam. no.	Fraction	Sam. wt. (mg)	U (ppm)	Pb (ppm)	$^{206}Pb/^{204}Pb$	$^{208}Pb/^{206}Pb$	$^{206}Pb/^{238}U$	±%	$^{207}Pb/^{235}U$	±%	$^{207}Pb/^{208}Pb$	±%	$^{206}Pb/^{238}U$	$^{207}Pb/^{238}U$	$^{207}Pb/^{208}Pb$
							Proterozoic rocks									
6	B-565A	Mylonitic porphyritic granite (granodiorite to granite gneiss)														
		NM102-163	12.5	895	203	336	0.082	0.22091	0	3.056	0.2	0.10034	0.1	1,287	142	1,630
		NM-63	12	104	230	11,100	0.082	0.21685	0	2.993	0.3	0.10013	0.2	1,265	140	1,626
		M63-102	4.6	84.1	18	764	0.080908	0.2046	0.07	2.920	0.12	0.10065	0.09	1,231	138	1,636
		M102-163	6.2	629	137.8	421	0.081419	0.21396	0.18	2.965	0.19	0.10051	0.04	1,250	139	1,634
7	B-565	Mylonitic granite (granodiorite to granite gneiss)														
		NM+102	19.2	198	323	491	0.126	0.15479	0	1.880	0.4	0.08809	0.1	928	107	1,384
		NM-63	15.4	208	375	17,190	0.13	0.17118	0	2.085	0.4	0.08836	0.1	1,019	114	1,390
		NM63-102		223	375	478	0.132777	0.158834	0.06	1.926	0.06	0.08795	0.02	950	109	1,381
		M-63		181	321	604	0.137069	0.16658	0.08	2.022	0.09	0.08805	0.03	993	112	1,383
		M63-102	6.8	189	316	340	0.139948	0.15683	0.14	1.900	0.15	0.08788	0.03	939	108	1,380
9	B-562	Mylonitic porphyritic granite (inclusion in Swansea Plutonic Suite)														
		NM+163	11.9	425	107.3	31.250	0.168	0.23294	0	2.864	0.23	0.0089	0.1	1,350	137	1,408
		NM-100	10.5	423	101.4	23,810	0.173	0.22059	0.11	2.709	0.13	0.08909	0.07	1,285	133	1,406
		M+163	9.2	533	132	25,000	0.156	0.2298	0.07	2.825	0.16	0.08919	0.13	1,333	136	1,408
		M-100	11.2	414	97.2	24,100	0.170	0.2164	0.12	2.660	0.19	0.08917	0.14	1,263	131	1,408
							Jurassic rocks									
12	B-566	Mylonitized hornblende diorite (metagabbro and amphibolite)														
		NM+163	7.4	518	9.6	266	0.090	0.01882	0.08	0.12671	0.56	0.04884	0.54	120.2	121.1	140
		NM100-130	8.6	445	10.4	270	0.084	0.02469	0.07	0.17496	0.36	0.05139	0.34	157.2	163.7	258.5
		NM-100	13.6	422	11.1	487	0.085	0.02664	0.09	0.20501	0.6	0.05582	0.56	169.5	189.4	445
		M+163	6.5	506	11.7	285	0.066	0.02387	0.08	0.16555	0.8	0.05029	0.78	152.1	155.5	208.5
		M100-130	8.5	431	11.2	110	0.106	0.02539	0.05	0.18796	0.17	0.05368	0.16	161.6	174.9	357.8
		M-100	8.7	42.8	11.9	408	0.085	0.02828	0	0.22932	0.67	0.05882	0.62	179.8	209.6	560.3
							Cretaceous rocks									
15	Ha-1118	Granite mylonite layer in layered migmatitic gneiss.														
		NM+130	7.1	573	21	543	0.08	0.03671	0.44	0.39703	0.58	0.07844	0.34	232.4	339.5	1,158
		NM-100	6.4	679	26	526	0.084	0.03748	0.35	0.40969	0.36	0.07928	0.05	237.2	348.6	1,179
		M-All		721	36	684	0.084	0.04947	0.23	0.584	0.27	0.08563	0.14	311.3	467.1	1,330
							Tertiary rocks									
25	B-561	Granite mylonite (Swansea Plutonic Suite)														
		NM-63	5.6	177	9.4	133	0.156	0.005	0.16	0.04234	0.6	0.06141	0.55	32.15	42.1	653.7
		NM102-163	11.3	144	11	116	0.161	0.00705	0.16	0.06723	0.28	0.06919	0.22	45.3	66.1	904.3
		M-63	9.8	230	11.5	109	0.183	0.00455	0.16	0.03617	0.54	0.05759	0.49	29.3	36.1	514.2
		M102-163		155	17.1	105	0.154	0.01014	0.15	0.10604	0.28	0.07584	0.22	65	102.3	1,091
18	B-563	Hornblende gabbro (Swansea Plutonic Suite)														
		NM+130	11.4	261	1.64	145	0.526	0.00385	0.32	0.027	2.7	0.05176	2.5	24.8	27.5	274.8
		M-100	10.8	306	2.5	76.5	0.770	0.00365	0.41	0.02454	5.7	0.04881	5.4	23.5	24.6	138.9

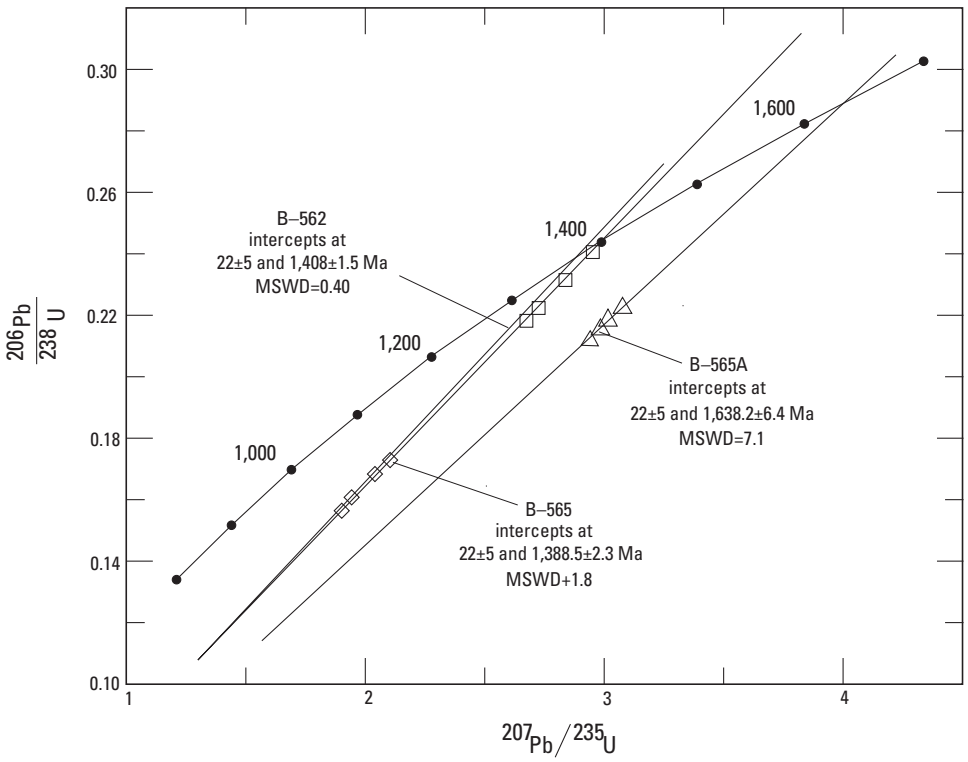

Figure 13. U-Pb zircon concordia diagram for mylonitic granitic gneiss and mylonitic porphyritic granite and porphyritic granodiorite inclusion in felsic rocks of the Swansea Plutonic Suite. Sample B–565, mylonitic granitic gneiss and sample B–565A mylonitic porphyritic granite from the eastern Buckskin Mountains; sample B–562, inclusion near Swansea in the central Buckskin Mountains. MSWD, mean standard weighted deviation.

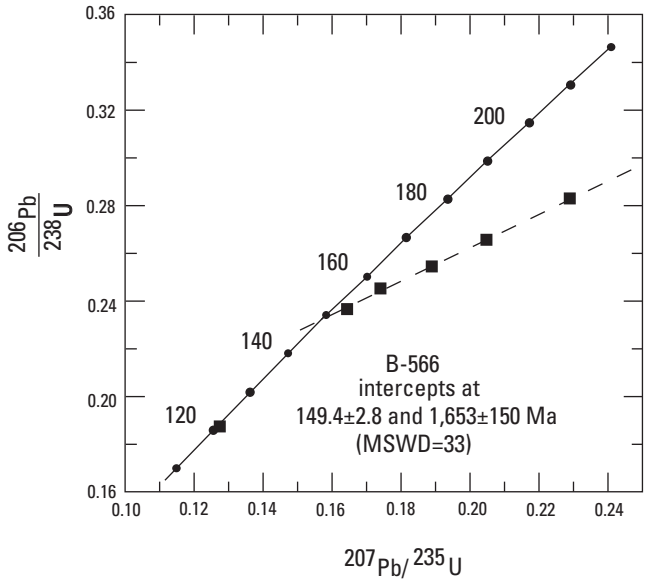

Figure 14. U-Pb zircon concordia diagram for sample B–566 of mylonitic horblende diorite from the eastern Buckskin Mountains. MSWD, mean standard weighted deviation.

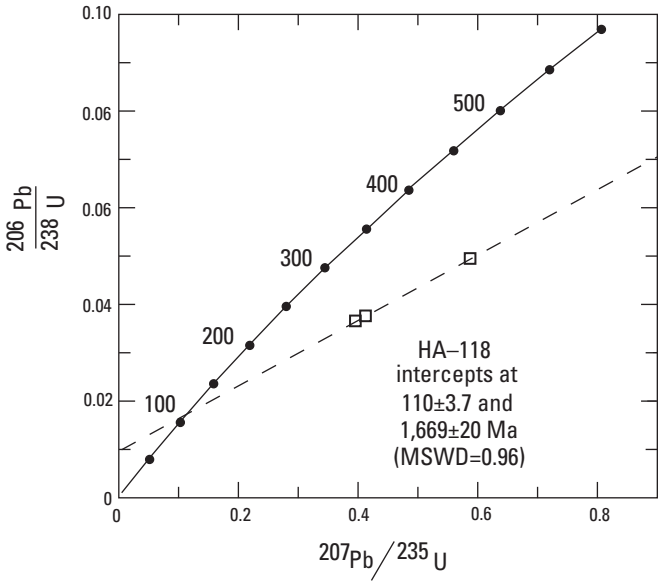

Figure 15. U-Pb zircon concordia diagram for sample HA–118 from a migmatitic-looking granite layer in layered gneiss in the eastern Harcuvar Mountains. MSWD, mean standard weighted deviation.

Swansea Plutonic Suite

Sample B–561 (Appendix sample 25) of mylonitic granite from the felsic phase of the Swansea Plutonic Suite north-northeast of Swansea and sample B–563 (Appendix sample 18) of hornblende gabbro from the pluton mapped in the Alamo Lake 1:100,000 quadrangle and crossed by the Bill Williams River. U-Pb isotopic analyses of four zircon fractions from the felsic phase and two fractions from a sample of the mafic phase fall on a chord with a lower intercept of 21.86±0.60 Ma and an upper intercept of 1,427±26 Ma (fig.16*A*). The value of the upper intercept suggests that the felsic rocks were derived in part from crust containing Middle Proterozoic rock. Analyses of four zircon splits from sample B–562 of porphyritic granite, which forms numerous inclusions in the felsic phase of the Swansea Plutonic Suite, fall on a chord with an upper intercept at 1,409±6.3 Ma and a lower intercept at 31±110 Ma (fig.16*B*). Thus the porphyritic granite has an age similar to the upper intercept for the felsic phase of the Swansea Plutonic Suite. When all the zircon data, except the two points from the gabbro, are plotted together, they form a chord with an upper intercept of 1,408.5±3.4 Ma and a lower intercept of 21.49±0.34 Ma (fig.16*C*).

$^{40}Ar/^{39}Ar$ plateau ages by Joan Fryxell (Richard and others, 1990) of hornblende from the mafic rocks of the Swansea Plutonic Suite range from 29.9 to 26.2 Ma. We assume that the hornblende samples came from gabbro and diorite occurring as small bodies not mappable at 1:100,000. The youngest of the hornblende ages is based on a better plateau than the older ages. This suggests that the discrepancies with the U-Pb zircon isotopic age are due to excess ^{40}Ar or contamination with xenocrysts, as Nelson and others (1992) have demonstrated for laccoliths in the Henry and La Sal Mountains of Utah. The published age spectra of hornblendes from the Swansea Plutonic Suite, however, lack the obvious features of those of the hornblendes that gave mixed older ages for the Utah plutons. Unfortunately, the zircons we analyzed and the hornblende Fryxell analyzed are not from the same samples. The field relations, in our opinion, favor a close time relationship between the felsic and mafic members of the suite.

Whole-Rock and Feldspar Pb-Isotopic Compositions

Whole-rock and feldspar Pb-isotopic analyses (table 3) of rocks from the northern Harcuvar complex fit the regional relations between Proterozoic Pb-isotopic crustal provinces as described by Wooden and Miller (1990), Wooden and Dewitt (1991), and Bryant and others (2001). There are relatively few analyses from Proterozoic rocks in the northern Harcuvar complex compared to the nearby Colorado Plateau transition, and most of those in the northern Harcuvar complex are from Mesozoic and Tertiary igneous rocks.

On a greatly enlarged part of a Pb^{207}/Pb^{204} vs. Pb^{206}/Pb^{204} diagram (fig.17*A*), lead isotope ratios cluster in tight groups between reference lines for the Mojave and central Arizona provinces from Wooden and DeWitt (1991). Only a few of the Pb isotope ratios in rocks of the Poachie region could be shown here because of their wide range. We show them here because the Poachie region, according to our favored tectonic interpretation, was about 15 km above the rocks of the northern Harcuvar complex before regional extension. The range of Pb-isotope ratios in the rocks analyzed in the northern Harcuvar complex resembles that of rocks in the Poachie region (Bryant and others, 2001). Most of the northern Harcuvar samples are from Phanerozoic igneous rocks rather than from Proterozoic rocks, which were used to determine the reference lines. The Poachie region is near the eastern margin of the Mojave Pb-isotope province and has a larger range of Pb-isotopic ratios than the Mojave province to the west. The Pb isotopic ratios in the Poachie region differ significantly from those in the central Arizona province to the east (Bryant and others, 2001). Tight clustering of the lead-isotope contents of the various rock types in the Swansea Plutonic Suite indicates that the lead-isotope content of the magma was very homogeneous despite the heterogeneous aspect of the rocks. Feldspar from the inclusion of Proterozoic granitic rock in the Swansea Plutonic Suite is less radiogenic than feldspars from other Proterozoic rocks analyzed in the northern Harcuvar complex. The inclusion is interpreted as residuum from partial melting of the Proterozoic crust leading to reduction of the U/Pb ratio in the incompletely melted rock, which was incorporated in the magma.

None of the suites of Cretaceous or Tertiary plutons in the Whipple Mountains have as uniform Pb isotopic composition as the Swansea Plutonic Suite, although most of them form fairly well defined groups on the diagrams. These groups fall between the Mojave and central Arizona reference lines on the $^{207}Pb/^{204}Pb$ vs. $^{206}Pb/^{204}Pb$ diagram (fig. 17*A*). The members of the 89-Ma suite have a greater spread in their Pb isotopic composition than the other Tertiary igneous rock suites analyzed (fig. 17*A*,*B*). This may be due to the effects of Late Cretaceous regional metamorphism or to difficulty in accurately identifying rocks belonging to that suite.

Geochemistry

Analytical Methods

Ten major elements were determined by wavelength dispersive X-ray fluorescence spectrometry (Taggart and others, 1990). In most samples, Rb, Sr, Y, Zr, and Nb and in some samples, Cr, Ni, Cu, Zn, Ba, La, and Ce were determined by energy-dispersive XRF by using a Kevex 7000 EDXRF analyzer (King and Lindsay, 1990). Rare-earth elements were determined by inductively coupled plasma-mass spectrometry by using an internal standard for drift correction, matrix effects, and oxide formation calculation (Lichte and others,

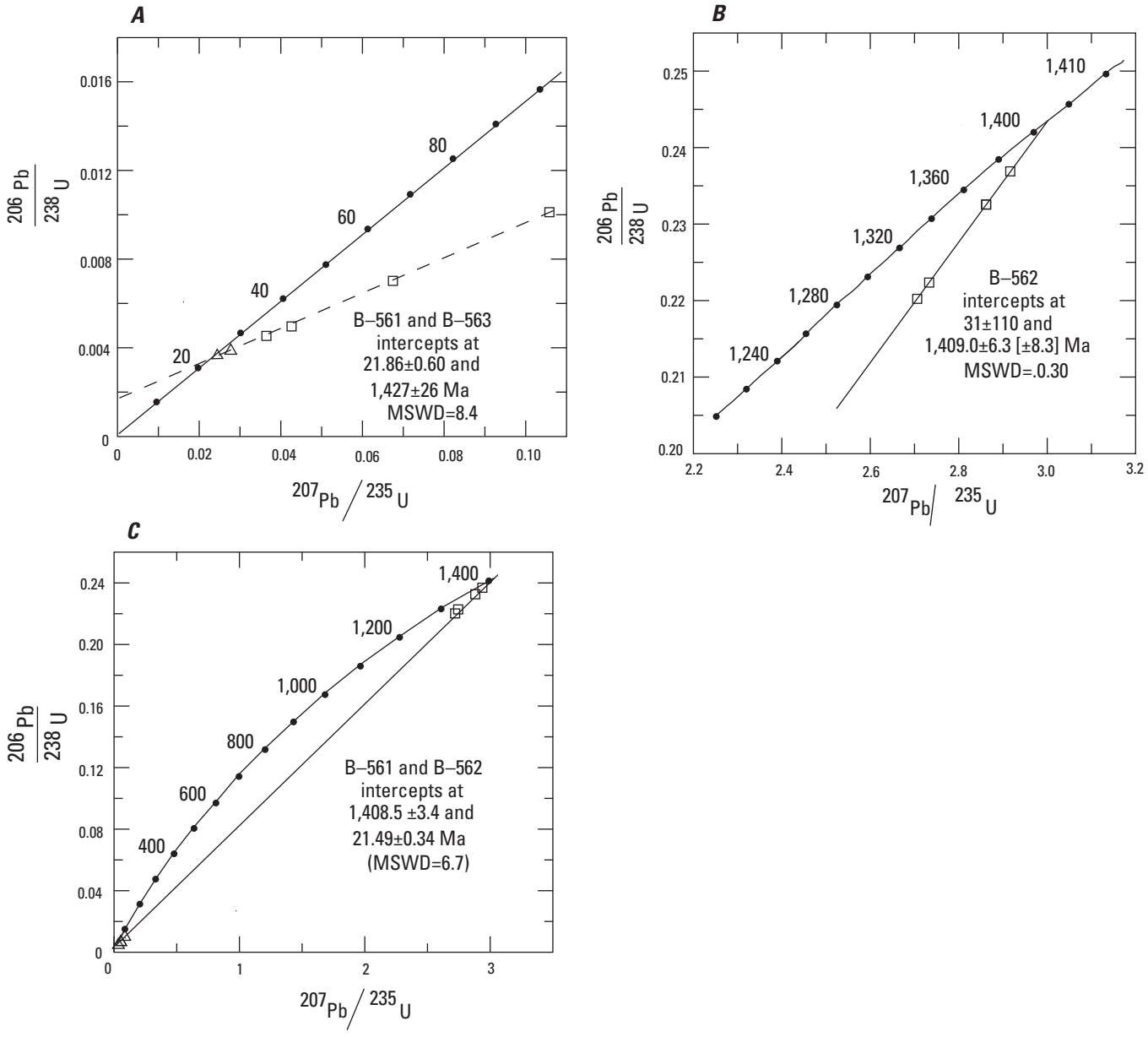

Figure 16. U-Pb concordia diagrams for gabbro and granite of the Swansea Plutonic Suite and combined with inclusions in the suite. *A*, Sample B–561 (open squares) and sample B–563 (open triangles) represent a mylonitic granite from north-northeast of Swansea and a hornblende gabbro from a pluton cut by the Bill Williams River northwest of Reid Valley, respectively (Appendix samples 25 and 18). *B*, Sample B–562 from an inclusion of mylonitic porphyritic granodiorite in mylonitic granite west of Swansea (Appendix sample 9). *C*, Sample B–561 (open triangles) and sample B–562 (open squares) plotted together showing isotopic relations between the Swansea Plutonic Suite and its inclusions. MSWD, mean standard weighted deviation.

Table 3. Whole-rock and feldspar (F) Pb-isotopic compositions of rocks from the northern Harcuvar complex and from Cretaceous and Tertiary plutonic rocks from the Whipple Mountains. Ages in the Whipple Mountains based on Wright and others (1986).

[no., number]

			Measured			Calculated				Δ
Appendix sample no.	Age (Ma)	Field sample no.	$^{206}Pb/^{204}Pb$	$^{207}Pb/^{204}Pb$	$^{208}Pb/^{204}Pb$	$^{238}U/^{204}Pb$	$^{235}U/^{204}Pb$	$^{232}Th/^{204}Pb$	Th/U	$^{207}Pb/^{204}Pb$
6	1,640	B-565AF	19.163	15.668	38.971	10.1	8.7	36.8	3.7	3.9
7	1,400	B56AF	19.409	15.676	41.782	10.9	9.0	58.7	6.3	2.1
9	1,400	B-562	17.155	15.494	37.192	3.5	3.3	16.7	4.8	7.5
12	149	B-566F	17.871	15.526	37.663	5.8	4.3	22.0	3.8	3.2
15	110	HA-118F	18.965	15.573	38.919	9.4	5.8	36.2	3.8	-3.6
16	70	B-564	19.201	15.665	39.512	10.2	8.6	43.0	4.2	3.1
17	22	B-469	18.831	15.631	39.070	9.0	7.6	37.9	4.2	3.7
18	22	B-563	18.856	15.636	39.156	9.1	7.7	38.9	4.3	3.9
22	22	B-495C	18.865	15.635	39.172	9.1	7.7	39.1	4.3	3.7
25	22	B-561	18.879	15.638	39.188	9.1	7.8	39.3	4.3	3.9
25	22	B-561F	18.862	15.636	39.127	9.1	7.7	38.5	4.2	3.8
Whipple Mountains										
	89	NP-3	18.258	15.582	38.574	7.1	6.5	32.3	4.6	6.3
	89	89WP-12	18.508	15.617	38.900	7.9	7.1	36.0	4.5	5.6
	89	89WP-32	18.509	15.618	39.096	7.9	7.2	38.2	4.8	5.7
	89	89WP-6	18.139	15.585	38.329	6.7	6.1	29.6	4.4	6.3
	89	89WP-5	18.123	15.582	38.431	6.7	6.0	30.7	4.6	6.1
	89	89WP-23	17.912	15.560	38.152	6.0	5.3	27.5	4.6	6.1
	89	89WP-9	17.876	15.536	37.872	5.8	4.6	24.4	4.2	4.1
	89	89WP-3	19.071	15.673	39.106	9.8	8.9	38.4	3.9	5.3
	89	MR-194	17.871	15.553	38.206	5.8	5.1	28.2	4.8	5.9
	89	MR-162	18.149	15.542	38.330	6.7	4.8	29.6	4.4	1.2
	73	MR-322C	18.309	15.605	39.016	7.3	6.8	37.3	5.1	6.5
	73	MR-292	18.947	15.676	39.074	9.4	9.0	38.0	4.1	6.9
	73	Mr-322	18.280	15.579	38.761	7.2	5.9	34.4	4.8	4.2
	73	Mr-302	18.252	15.572	38.826	7.1	5.7	35.2	5.0	3.8
	26	WT-1	19.120	15.622	39.080	9.9	7.3	38.1	3.8	-0.3
	26	89WP-4	19.101	15.542	38.949	9.9	7.9	36.6	3.7	1.9
	26	89WP-13	19.024	15.648	38.954	9.6	8.1	36.6	3.8	3.3
	26	89WP-31	19.037	15.563	39.006	9.7	8.3	37.2	3.8	3.7
	26	89WP-16	19.098	15.647	38.896	9.9	8.1	36.0	3.6	2.5
	19	WE-38	18.556	15.587	39.053	8.1	6.2	37.8	4.7	2.1
	19	WE-7	18.294	15.592	39.077	7.2	6.4	38.0	5.3	5.4
	19	WE-93A	18.504	15.612	39.104	7.9	7.0	38.3	4.8	5.2
	19	WSW-166	18.216	15.577	38.976	7.0	5.9	36.9	5.3	4.7

1987). Uranium and thorium were determined by delayed neutron counting following neutron irradiation of the sample (McKown and Knight, 1990). Fluorine and FeO were determined by ion-selective electrode potentiometry (Pribble, 1990) and potentiometric titration (Papp and others, 1990), respectively. In some samples some rare earths and other minor elements were determined by instrumental neutron activation analysis (Baedecker and McKown, 1987). Rare-earth elements shown in diagrams are normalized to chondrite values from Hanson (1980).

Proterozoic Granitic Rocks

Isotopic dating shows that Early and Middle Proterozoic granitic rocks form part of the northern Harcuvar metamorphic complex. Overprints by both Mesozoic and Tertiary structural and metamorphic events make it difficult to separate rocks of the two ages in the field without more detailed study than presented here. The distinctively coarse-grained, porphyritic, granitic inclusions in felsic rocks of the Swansea Plutonic Suite are probably all of Middle Proterozoic age, and one of the other six samples of Proterozoic granitic rock analyzed has been dated as Middle Proterozoic. Unfortunately we have no analysis of the one granitic rock dated as Early Proterozoic.

The Proterozoic granitic rocks are generally alkali-calcic (fig. 18*A*; table 4) and average in alkali content (fig. 18*B*). The inclusions of Middle Proterozoic granitic rocks in the Swansea Plutonic Suite are more potassic than the other analyzed Proterozoic granitic rocks. The inclusions are Fe-rich whereas the other granitic rocks are Mg-rich to average (fig. 18*C*).

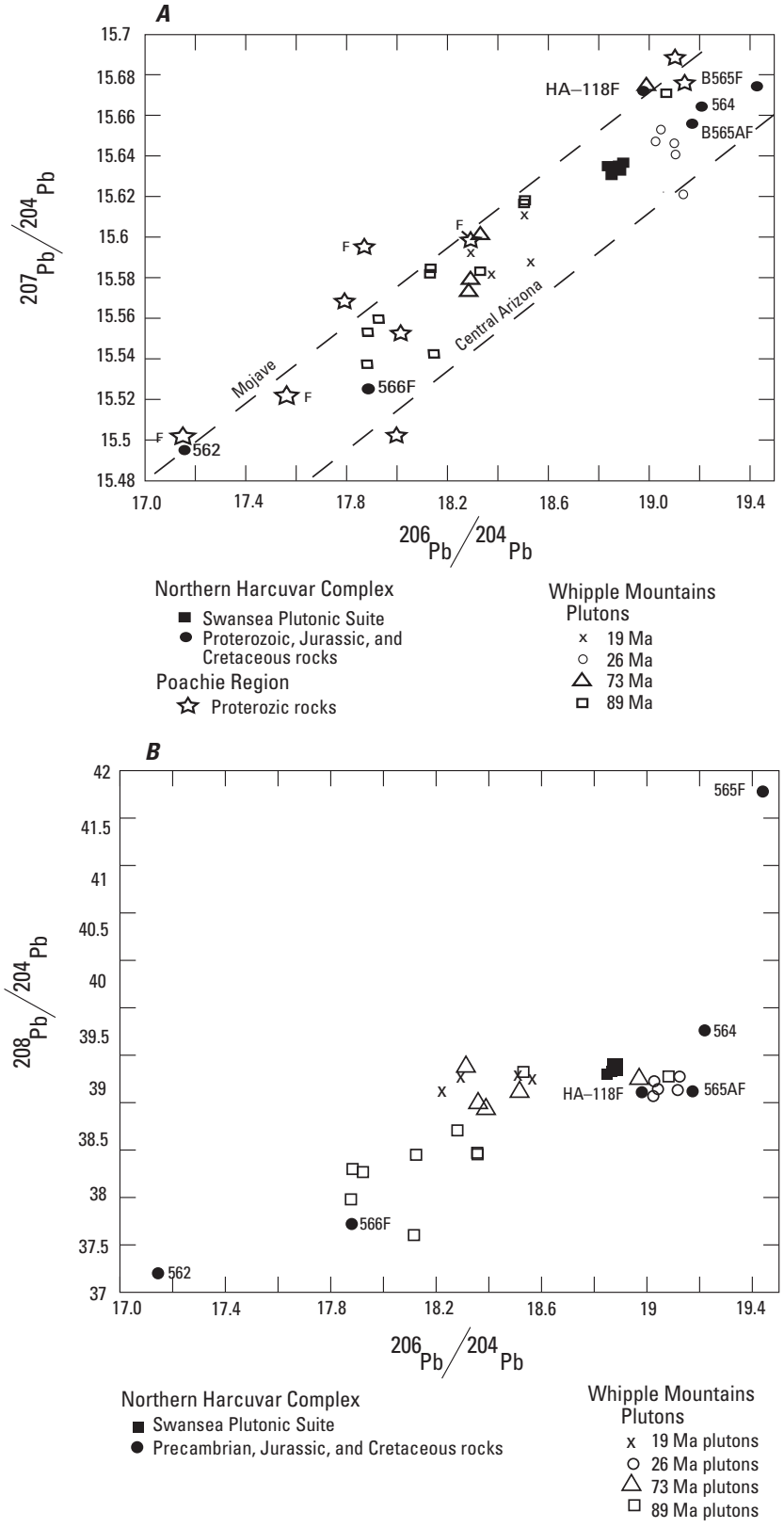

Figure 17. Whole-rock and feldspar lead (Pb) isotopic compositions of some rocks from the northern Harcuvar complex and Mesozoic and Tertiary plutonic rocks in the Whipple Mountains (Wright and others, 1986). F indicates determination on feldspar. *A*, $^{207}Pb/^{204}Pb$ vs. $^{206}Pb/^{204}Pb$. Dashed lines are 1.7–giga-annum (Ga) reference isochrons from Wooden and DeWitt (1991). Proterozoic rocks from the Poachie region from table 8, Bryant and others (2001). *B*, $^{208}Pb/^{204}Pb$ vs. $^{206}Pb/^{204}Pb$.

In the Poachie region to the northeast, which once may have overlain some of the rocks that now form the northern Harcuvar complex, Early Proterozoic plutonic rocks are both Mg- and Fe-rich. In that region the Middle Proterozoic Signal Granite is Fe-rich, whereas other Middle Proterozoic rocks studied are Mg-rich (Bryant and others, 2001). The Proterozoic granitic rocks of the northern Harcuvar complex in the Buckskin Mountains are metaluminous to weakly peraluminous (fig. 18*D*), although the four samples we know to be Middle Proterozoic are peraluminous, as is the Signal Granite of the Poachie region.

Uranium/Thorium (U/Th) ratios and U and Th contents are highly variable except that the U and Th contents of the inclusions in the felsic rocks of the Swansea Plutonic Suite are lower than that of the other Proterozoic granitic rocks (fig. 19*A*). Zirconium contents are 58–259 ppm except in the inclusions where they are 344–550 ppm (fig. 19*B*). Cerium (Ce) contents range from 51 to 198 ppm, and the Ce contents of the inclusions are in the higher part of that range (fig. 19*D*). Strontium (Sr) contents of the Proterozoic granitic rocks range from 207 to 959 ppm whereas contents of the inclusions in the felsic phase of the Swansea Plutonic Suite are relatively uniform at 350–408 ppm (fig. 19*C*). Rubidium/Strontium (Rb/Sr) ratios range widely compared to the younger igneous rocks in the northern Harcuvar complex and are similar to those in the Proterozoic rocks of the Poachie region (Bryant and others, 2001).

Total rare-earth elements in rocks we analyzed range from 350 to 437 ppm. The range is similar to that of the Proterozoic rocks of the Poachie region, except for the Signal Granite, which has a higher rare-earth content (Bryant and others, 2001). Chondrite normalized (CN) light-rare-earth-element vs. heavy-rare-earth-element (LREE/HREE) enrichment [(La/Yb)CN] ranges from 8.5 to 11. Chondrite normalized rare-earth element diagrams (fig. 20*A*) show higher total REE content compared to the younger rocks, a moderate slope in the LREEs and a gentle slope in the HREEs. The diagrams for both the dated Middle Proterozoic rocks and an undated rock for which we have REE analytical data have small europium anomalies (fig. 20*A*; sample B–93–1, fig. 20*E*). In the Poachie region, REEs in most of the Middle Proterozoic plutonic rocks have Eu anomalies, whereas those anomalies are much less common among the Early Proterzoic rocks (Bryant and others, 2001).

Jurassic Plutonic Rocks

The Jurassic rocks (table 5), which were identified in a single pluton in the southern part of the eastern end of the Buckskin Mountains (fig. 2), have a distinctive geochemical signature in relation to other units for which we have data in the northern Harcuvar complex. We have not dated any of the more felsic varieties, which probably were emplaced as sills or dikes of related magma in the diorite and gabbro during the Jurassic igneous event. The felsic material could be of Tertiary or Cretaceous age, but the geochemistry of the felsic rocks in the mafic rock seems to fit that of the enclosing rock rather than the Tertiary or Cretaceous igneous rocks (figs. 18,19). Also, textures of the felsic rocks do not resemble those of the Tertiary Swansea Plutonic Suite.

The most mafic rock analyzed is alkalic, and the other rocks from the pluton analyzed form trends from alkalic to calcic, very potassic to very sodic, metaluminous to peraluminous, and very Fe-rich to Mg-rich to average with increasing SiO_2 content (table 5; figs. 18*A*,*B*,*C*,*D*). The most silicic rock in the pluton has a high U and Th content (fig. 19*A*), whereas the other rock types have low U and Th contents. Zirconium contents are 60–146 ppm (fig. 19*B*). Strontium contents are high (820–1,300 ppm) except for the most silicic rock, which has 440 ppm (fig. 19*C*). Cerium contents are 41–54 ppm except in the gabbro, which contains 101 ppm (fig. 19*D*). In contrast to the Proterozoic igneous rocks, the Jurassic suite, except for its most siliceous member, has lower Th, U, Zr, and Ce contents (fig. 19*A*,*B*,*D*).

Total REE content decreases from 222 in the most mafic rock to 106 ppm in the most felsic rock. Light-rare-earth vs. heavy rare-earth element (LREE/HREE) enrichment ranges widely [(La/Yb)CN=6.9–35.9], and the enrichment values are not systematic with SiO_2 content. The most silicic rock (sample B–93–2b, fig. 20*B*) has the lowest enrichment value, a flat REE pattern, and a prominent negative europium anomaly. No similar rocks are known nearby.

Cretaceous Plutonic Rocks

The two Cretaceous rocks analyzed (table 5) apparently each have different origins. One (HA–118) is a granite layer in migmatitic gneiss and has a U-Pb zircon age of 110 Ma. This rock may represent a locally derived partial melt formed during a Cretaceous metamorphic event. The other (B–564) is a granite intrusion correlated with younger Cretaceous granitic rocks in the Harcuvar Mountains.

Both rocks are alkali-calcic, sodic, and weakly peraluminous (fig. 18*A*,*B*,*C*,*D*), but B–564 is Mg-rich whereas HA–118 is average. HA–118 shows a very strong LREE enrichment [(La/Yb)CN=47.7], whereas B–564 is only weakly enriched in LREE [La/Yb)CN=4.2] (fig. 20*C*). Total REE content of the granitic layer is 131 ppm compared to 52 ppm for the intrusion.

Swansea Plutonic Suite

Rocks of the Swansea Plutonic Suite (table 6) range from 60 to 72 percent SiO_2 for the felsic types, and typical mafic rocks have about 50 percent SiO_2. Petrographic studies indicate that some rocks of the suite probably would fill the 50 to 60 percent SiO_2 gap in the rocks analyzed. Rocks of the suite are alkali-calcic, Mg-rich, average to sodic, and mildly metaluminous to mildly peraluminous, except for the gabbro, which is strongly metaluminous (fig. 18).

Thorium contents (fig. 19*A*) are relatively uniform except that the most felsic rocks (>65% SiO_2) have higher

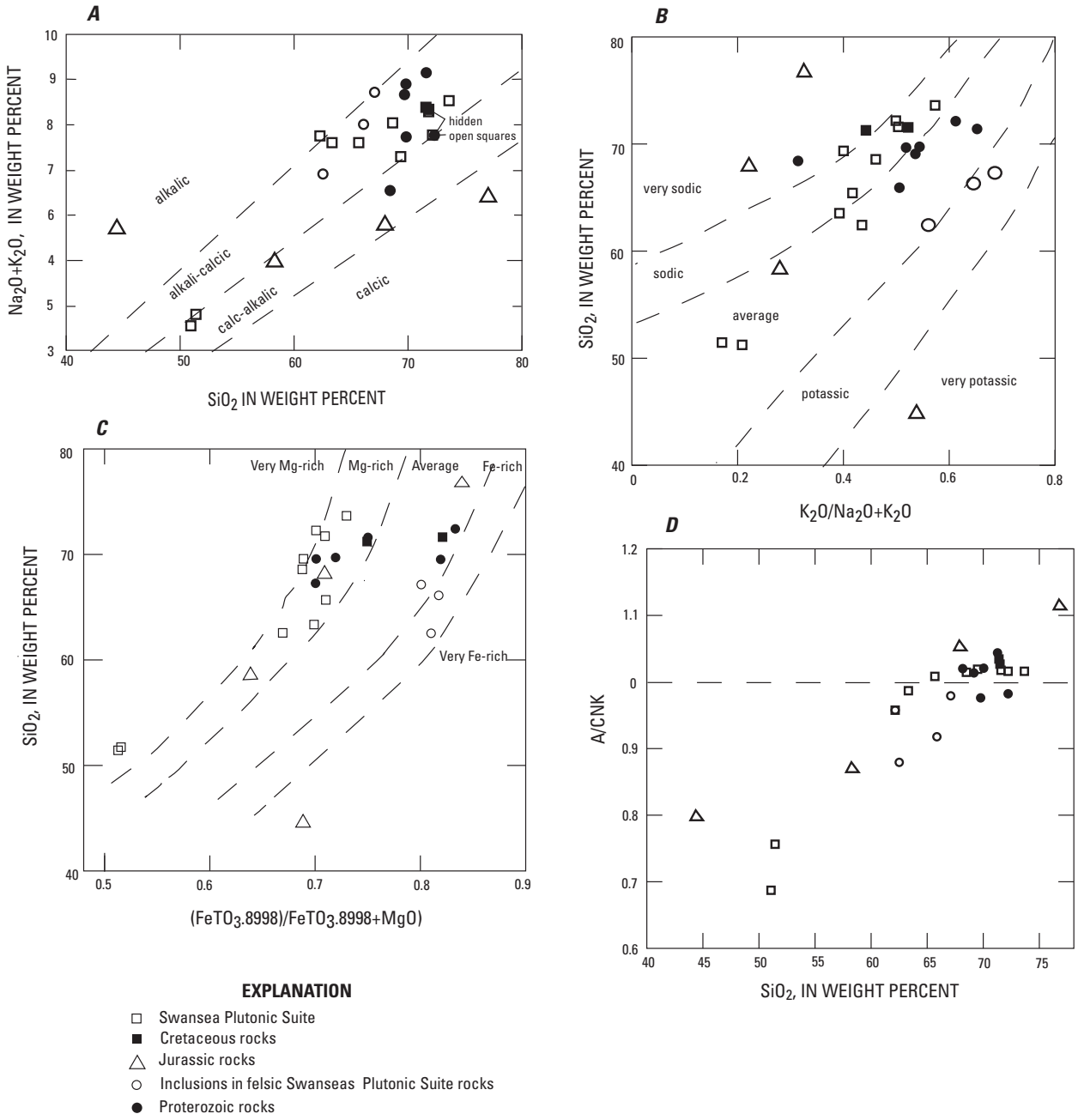

Figure 18. Chemical diagrams for rocks of the northern Harcuvar complex. *A*, SiO_2 vs. Na_2O+K_2O. Fields of alkalinity from Anderson (1983) and DeWitt (1989). *B*, SiO_2 vs. K_2O/Na_2O+K_2O. Fields from Fridrich and others (1998). *C*, SiO_2 vs. Fe/Fe+Mg. Fields from Fridrich and others (1998). *D*, SiO_2 vs. A/CNK.

Table 4. Major-oxide and trace-element concentrations in some Proterozoic granitic rocks and inclusions in the Swansea Plutonic Suite (Tsp), northern Harcuvar metamorphic complex.

[nd, not determined; LOI, loss on ignition; $FeTO_3$, total Fe as Fe_2O_3; <, less than]

	Proterozoic granitic rocks						Inclusions in Tsp		
Appendix no.	1	2	3	4	5	6	8	9	10
Field no.	B-268A	B-93-1	B-587	B-665	B-653	B-565A	B-495-92	B-562	B-1111
Lab no.	D-363785	D-363786	D-363787	D-363787	D-363788	D-288864	D-5254487	D-288864	D-525489
Job no.	UD76	VK74	UD76	UD76	UD76	SL11	VH78	SL11	VH78
Major-oxide concentration, in weight percent[1]									
SiO_2	67.1	68.4	68.5	68.6	70.6	71.7	60.9	65.2	65.5
Al_2O_3	16.9	14.0	15.3	16.3	14.8	13.1	14.9	15.5	14.7
$FeTO_3$	2.58	4.10	2.72	1.48	1.94	3.82	7.84	5.02	4.84
MgO	1.01	0.82	1.05	0.50	0.57	0.68	1.66	1.01	1.09
CaO	3.91	2.47	2.01	2.37	1.51	1.87	4.38	3.49	2.35
Na_2O	4.46	2.98	3.99	4..24	3.18	3.07	3.00	2.84	2.77
K_2O	1.95	4.59	4.54	4..47	5.82	4.64	3.76	5.06	5.71
TiO_2	0.27	0.70	0.39	0.36	0.26	0.54	1.35	0.85	0.83
P_2O_5	0.21	0.26	0.13	0.13	0.08	0.23	0.52	0.29	0.31
MnO	0.06	0.09	0.03	<0.02	0.04	0.07	0.11	0.05	0.06
LOI	1.14	0.57	0.77	0.54	0.47	0.41	0.71	0.61	1.00
Total	98.45	98.41	98.66	98.67	98.8	99.72	99.13	99.92	99.16
[2]FeO						1.65		1.99	
[2]F						0.03		0.02	
Trace-element concentration, in parts per million[3]									
Nb	<10	21	8	8	15	20	24	13	15
Rb	71	180	183	141	243	157	98	95	100
Sr	856	235	503	959	260	206	380	359	405
Zr	.58	250	140	162	139	259	560	344	380
Y	11	64	10	5	21	51	59	45	45
Ba	1,190	1,150	1,140	1,670	1,070	750	1,700	1,800	2,150
Ce	122	168	69	58	51	nd	198	nd	146
La	54	82	26	10	16	nd	70	nd	63
Cu	6	<10	<5	6	<5	5	18	29	25
Ni	<5	<10	24	5	7	<4	10	7	10
Zn	56	70	52	45	63	72	89	59	30
Trace-element concentration, in parts per million[4,5]									
Cs	nd	3.3	nd	nd	nd	nd	nd	nd	nd
Hf	nd	8.37	nd	nd	nd	nd	nd	nd	nd
Ta	nd	2.8	nd	nd	nd	nd	nd	nd	nd
La	nd	88.5	nd	nd	nd	76.4	nd	81.6	nd
Sc	nd	11.3	nd	nd	nd	nd	nd	nd	nd
Ce	nd	177	nd	nd	nd	151	nd	177	nd
Pr	nd	nd	nd	nd	nd	17.6	nd	23.3	nd
Nd	nd	76	nd	nd	nd	60.0	nd	89.3	nd
Sm	nd	15.7	nd	nd	nd	11.4	nd	18.0	nd
Eu	nd	2.3	nd	nd	nd	2.17	nd	3.69	nd
Gd	nd	nd	nd	nd	nd	9.22	nd	14.1	nd
Tb	nd	2	nd	nd	nd	1.46	nd	2.24	nd
Dy	nd	nd	nd	nd	nd	9.06	nd	12.7	nd
Ho	nd	nd	nd	nd	nd	1.79	nd	2.42	nd
Er	nd	nd	nd	nd	nd	4.90	nd	6.43	nd
Tm	nd	nd	nd	nd	nd	0.75	nd	0.91	nd
Yb	nd	6.97	nd	nd	nd	4.54	nd	5.10	nd
Lu	nd	0.89	nd	nd	nd	0.65	nd	0.66	nd
[6]U	1.41	7.4	5.5	3.77	3.89	3.86	1.32	0.981	0.899
[6]Th	8.02	44.3	11.8	5.6	4.8	22.8	9.09	2.2	5.6

[1]Major oxides determined by wavelength dispersive X-ray fluorescence: J.R. Evans, J. Taggart, A. Bartel, D.F. Siems, and J.S. Mee, analysts.

[2]FeO determined by potientiometric titration and F by ion-selective electrode potentiometry: J. Sharkey and E. Brandt, analysts.

[3]Trace elements determined by energy-dispersive X-ray fluorescence: J. Kent, D.F. Siems, J.E. Taggart, and J.S. Mee, analysts.

[4]Rare earth and trace elements determined by neutron activation analysis in No. 2: G.A. Wandless, analyst.

[5]Rare earths determined by inductively coupled plasma-mass spectrometry in Nos. 6, 8: R. Moore analyst.

[6]Th and U determined by delayed neutron activation analysis except for No. 2: E.J. Knight, R.B. Vaughn, D. McKown, and R.E. McGregor, analysts.

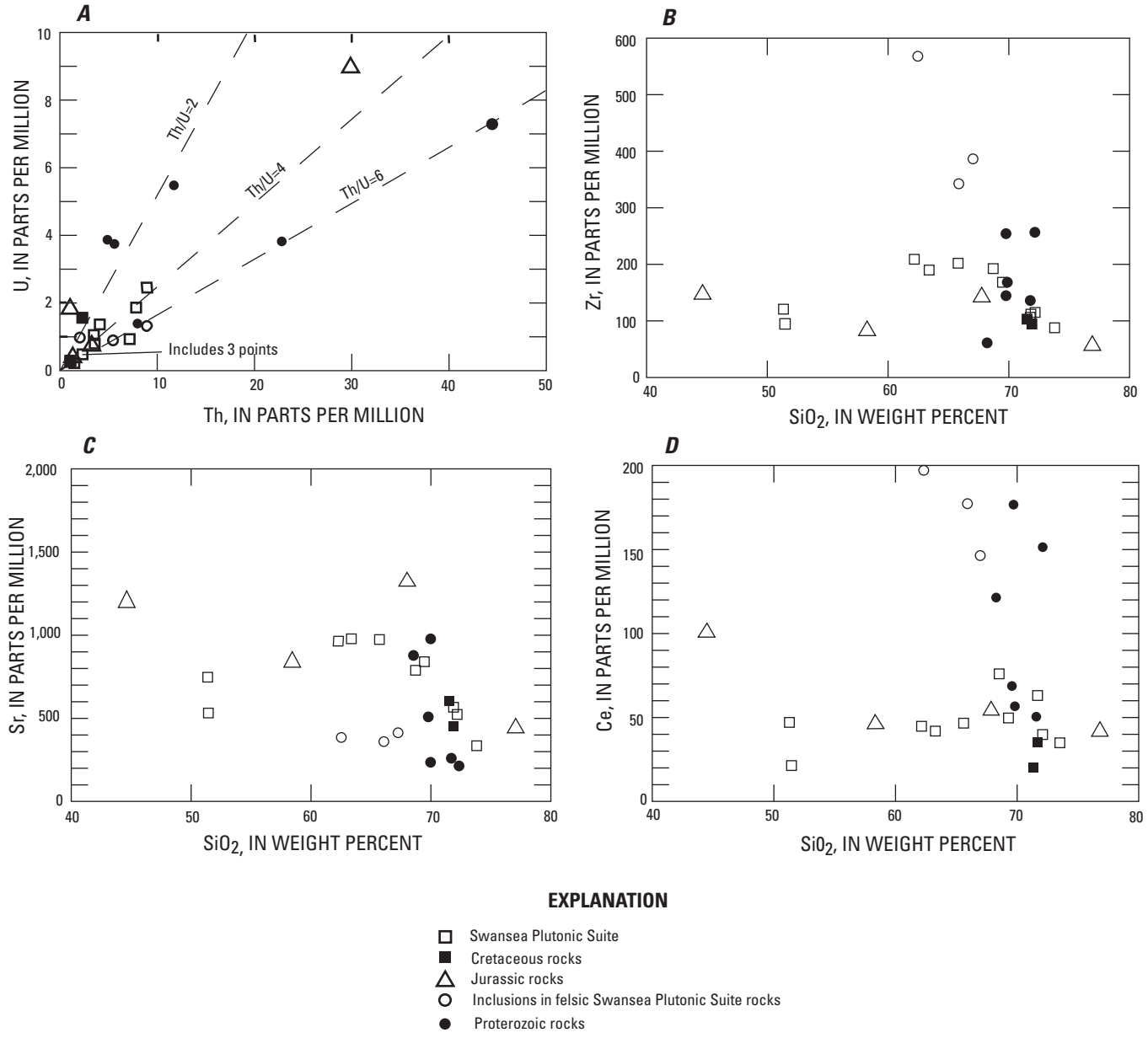

Figure 19. More chemical diagrams for rocks of the northern Harcuvar complex. *A*, U vs. Th; *B*, SiO_2 vs. Zr; *C*, SiO_2 vs. Sr; *D*, SiO_2 vs. Ce.

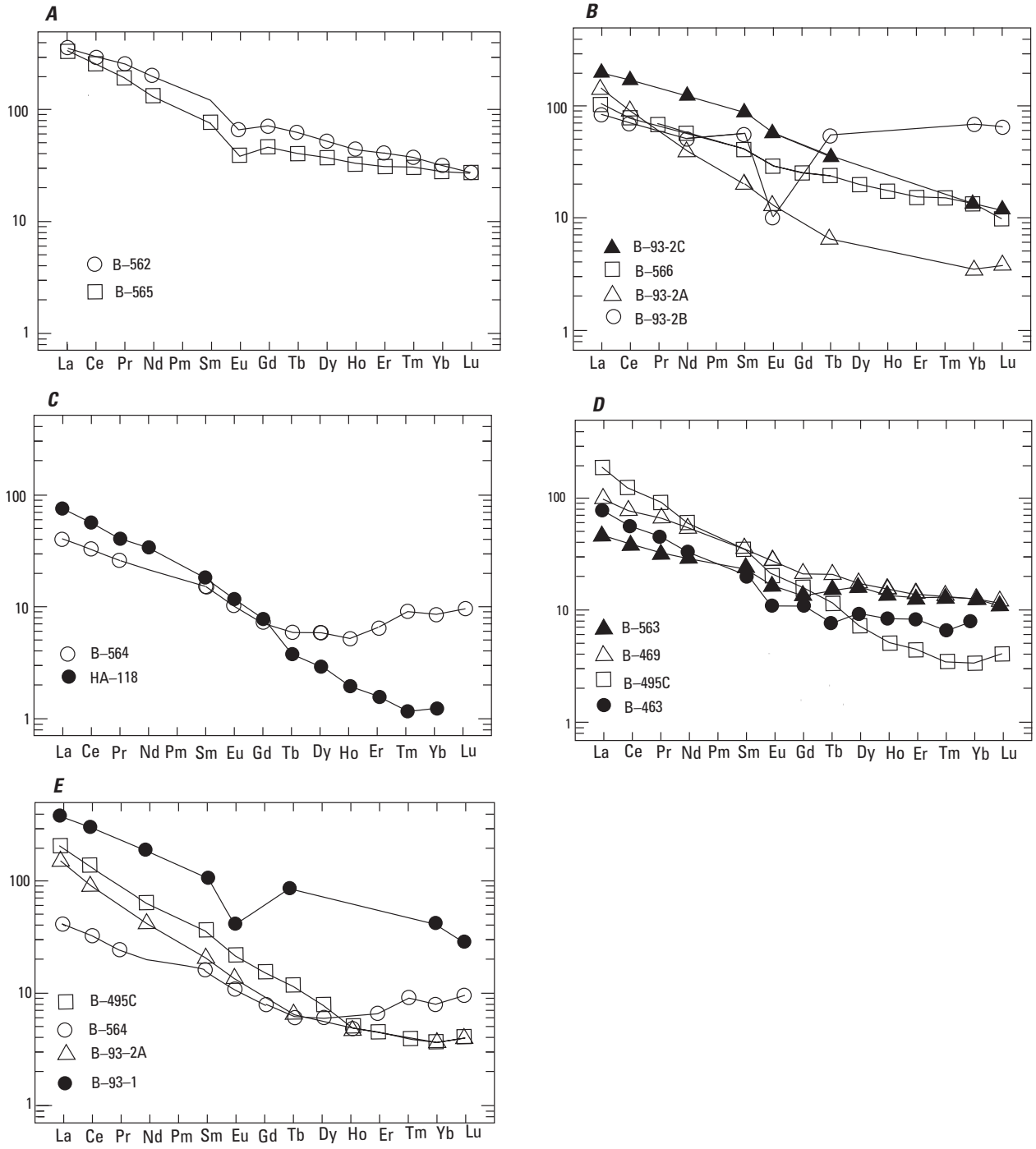

Figure 20. Chrondite-normalized rare-earth element contents of igneous rocks in the northern Harcuvar complex. *A*, Middle Proterozoic granite (B–565) and inclusion of porphyritic granite in felsic rock of the Swansea Plutonic Suite (B–562). *B*, Jurassic plutonic rocks. Mylonitic biotite-hornblende gneiss (B–93–2C) and mylonitized diorite (B–566) from main body of pluton and well-foliated biotite trondhjemite and mylonitic muscovite trondhjemite from disrupted late-phase dikes in pluton. *C*, Cretaceous rocks. Mylonitic biotite granite from pluton (B–564) and mylonitic granitic layer in layered migmatitic gneiss (HA–118). *D*, Swansea Plutonic Suite. Gabbros (B–563 and B–469), aplite sill in felsic rocks (B–495C), and mylonitic granite, the most siliceous of the samples analyzed from the suite (B–463). The latter two samples define the range of REE contents of the eight samples analyzed of the felsic unit in the suite. *E*, Samples of igneous rocks of four ages having SiO_2 contents of about 68 percent. Proterozoic (B–93–1), Jurassic (B–93–2A), Cretaceous (B–564), and Miocene (B–495C).

Table 5. Major- and trace-element concentrations in some Jurassic and Cretaceous plutonic rocks from the northern part of the Harcuvar complex.

[nd, not determined; <, less than]

	Jurassic rocks				Cretaceous rocks	
Appendix no.	11	12	13	14	15	16
Field no.	B-93-2C	B-566	B-93-2A	B-93-2B	HA-118	B-564
Lab no.	D-529418	D-288868	D-529416	D-529417	D-363380	D-288866
Job number	VK74	SL11	VK74	VK74	UD58	SL11
Major oxide concentration, in weight percent[1]						
SiO_2	42.9	57.3	66.7	75.9	70.6	71.1
Al_2O_3	18.3	17.5	17.1	13.9	14.9	15.9
$FeTO_3$	14.0	7.74	3.26	0.86	2.16	1.6
MgO	5.61	3.53	1.19	0.15	0.44	0.48
CaO	8.57	7.04	4.18	1.50	1.93	2.04
Na_2O	2.56	3.52	4.44	4.44	3.98	4.73
K_2O	2.95	1.37	1.22	1.87	4.19	3.61
TiO_2	1.84	0.65	0.34	0.1	0.24	0.25
P_2O_5	1.18	0.30	0.13	0.05	0.13	0.08
MnO	0.17	0.09	0.03	0.01	0.03	<0.02
LOI	0.91	1.29	0.41	0.45	0.22	0.44
Total	98.08	99.06	98.59	98.78	98.6	99.81
[2]FeO	nd	4.29	nd	nd	0.99	0.73
[2]F	nd	0.02	nd	nd	0.01	0.01
Trace-element concentration in parts per million[3]						
Nb	<10	<10	<10	76	<10	12
Rb	87	47	36	28	83	113
Sr	1,150	820	1,300	440	445	605
Zr	142	83	146	60	90	100
Y	30	21	10	86	4	14
Trace-element concentration in parts per million[3,4]						
Ba	2,350	800	1.250	1,150	1,630	960
Cu	38	67	37	11	7	5
Ni	34	49	<10	<10	<2	<4
Zn	140	52	32	<10	58	38
Co	35.8	29	7.8	0.96	4	5
Cr	46	550	<20	<20	<1	<2

Table 5. Major- and trace-element concentrations in some Jurassic and Cretaceous plutonic rocks from the northern part of the Harcuvar complex.—Continued

[nd, not determined; <; less than]

	Jurassic rocks				Cretaceous rocks	
	Trace-element concentration in parts per million[5,6]					
Cs	1.6	nd	0.49	0.15	nd	nd
Hf	2.7	nd	3	3.9	nd	nd
Ta	0.40	nd	0.14	8	nd	nd
Sc	25.2	nd	4.65	6.93	nd	nd
La	45.1	23.7	32.5	19	18	9.7
Ce	101	46.4	54.1	41.4	35	20.2
Pr	nd	6.3	nd	nd	3.9	2.5
Nd	56	26.2	18	23	16	10.1
Sm	13.3	6.16	3.05	8.49	2.8	2.37
Eu	3.27	1.64	0.76	0.59	0.68	0.59
Gd	nd	5.14	nd	nd	1.6	1.48
Tb	1.3	0.87	0.24	2.02	0.14	0.22
Dy	nd	5.01	nd	nd	0.74	1.48
Ho	nd	0.98	nd	nd	0.11	0.29
Er	nd	2.42	nd	nd	0.26	1.08
Tm	nd	0.38	nd	nd	0.03	0.23
Yb	2.3	2.31	0.59	11.7	0.21	1.44
Lu	0.3	0.25	0.096	1.64	nd	0.24
[7]Th	1.1	<1.5	3.34	29.8	1.3	2.4
[7]U	1.81	<0.4	0.73	9	0.29	1.56

[1]Major oxides determined by wavelength dispersive X-ray fluorescence: D.F. Siems, J.S. Mee, J.E. Taggart, A.J. Bartel, and K. Stewart, analysts.

[2]FeO determined by potentiometric titration and F by ion-selective electrode potentiometry: C.S. Papp, E.Brandt, and J. Sharkey, analysts.

[3]Trace elements determined by energy-dispersive X-ray fluorescence: J.R. Evans, J. Kent, and R.R. Larson analysts.

[4]Trace elements determined by X-ray spectroscopy: P.H. Briggs, and D.C. Fey, analysts. Trace elements in Nos. 10, 12, 13 determined by energy-dispersive X-ray fluorescence except for Co determined by inductively coupled plasma-mass spectrometry.

[5]Trace elements and rare earths in Nos. 10, 12, 13 determined by instrumental neutron activation analysis: G.A. Wandless, analyst.

[6]Rare earths determined by inductively coupled plasma-mass spectrometry: R. Moore, and G.O. Riddle, analysts.

[7]Th and U determined by delayed neutron counting: R.B. Vaughn, D.M. McKown, and R.E. McGregor, analysts. Th and U determined by instrumental neutron activation analysis in Nos. 10, 12, 13.

Table 6. Major-oxide and trace-element concentrations in rocks of the Swansea Plutonic Suite.

[nd, not determined; <, less than; >, greater than]

Appendix No.	17	18	19	20	21	22	23	24	25	26
Field no.	B-469	B-563	B-458A	B-495B	B-562-92	B-495C	B-464	B-496	B-561	B-463
Lab no.	D-288861	D-28288863	D-363374	D-363371	D-525488	D-288860	D-288865	D-363373	D-288862	D-363372
Job no.	SL11	SL11	UD58	UD58	VH78	SL11	SL11	UD58	SL11	UD58
Major-oxide concentration, in weight percent[1]										
SiO_2	50	50.4	60.6	61.6	64.4	67.8	68.7	70.9	71.2	72.2
Al_2O_3	16.5	17.9	18.0	18.0	17.3	16.3	16.3	14.7	15.1	14.0
$FeTO_3$	9.26	8.54	4.57	4.06	3.61	2.70	2.52	1.93	2.03	1.45
MgO	7.80	7.45	1.98	1.66	1.31	1.13	1.03	0.73	0.74	0.47
CaO	10.2	9.95	4.47	4.32	3.67	2.76	3.14	2.22	1.94	1.49
Na_2O	2.82	3.09	4.32	4.49	4.49	4.33	4.34	3.88	4.12	3.65
K_2O	0.73	0.64	3.22	2.89	2.93	3.63	2.86	3.74	4.06	4.69
TiO_2	1.0	0.84	0.55	0.55	0.53	0.38	0.39	0.25	0.25	0.18
P_2O_5	0.26	0.09	0.21	0.21	0.20	0.13	0.11	0.1	0.08	0.06
MnO	0.15	0.15	0.06	0.05	0.03	0.03	0.03	0.03	0.02	<0.02
LOI	1.55	1.45	0.69	0.61	0.56	0.39	0.57	0.37	0.48	0.36
Total	100.28	100.05	97.98	97.83	99.03	99.19	99.99	100.02	99.57	99.03
[2]FeO	5.99	5.76	2.62	2.27	nd	1.40	1.40	0.89	0.92	0.60
F	0.01	>0.01	0.04	0.03	nd	0.02	0.01	0.02	<0.01	0.01
Trace-element concentration in parts per million[3]										
Nb	<10	<10	<10	<10	<10	<10	<10	11	13	15
Rb	27	18	84	87	82	92	75	103	107	115
Sr	726	524	939	951	960	786	836	524	552	334
Zr	116	94	202	187	200	194	168	110	110	86
Y	18	16	7	7	12	7	10	9	14	11
Trace-element concentration, in parts per million[4]										
Ba	360	300	2,080	1,580	1,850	1,500	1,600	1,090	1,300	976
Co	35	41	13	12	41	9	7	5	6	4
Cr	370	240	22	24	nd	18	7	7	8	5
Cu	<2	100	32	178	<10	32	4	34	4	3
Ni	130	110	21	19	<10	15	5	3	9	5
Zn	63	43	52	48	20	45	45	38	20	23
Trace-element concentration, in parts per million[5]										
La	23.6	10.6	23	22	nd	43.6	27.3	22	35.2	19
Ce	47.2	22.0	45	42	nd	75.6	50.1	40	63.2	35
Pr	6.3	3.0	5.3	4.8	nd	8.4	6.0	4.3	7.1	3.8
Nd	24.9	12.4	22	20	nd	27.9	21.9	16	23.3	14
Sm	5.47	3.20	3.5	3.3	nd	4.96	4.56	2.5	4.16	2.6
Eu	1.63	1.01	0.94	0.90	nd	1.15	1.14	0.61	0.86	0.60
Gd	4.36	2.91	3.2	2.7	nd	3.28	3.26	1.6	3.23	2.1
Tb	0.78	0.58	0.41	0.38	nd	0.40	0.49	0.23	0.44	0.26
Dy	4.50	4.08	2.7	2.3	nd	1.81	2.66	1.6	2.58	2.2
Ho	0.88	0.77	0.52	0.43	nd	0.28	0.46	0.30	0.48	0.44
Er	2.41	2.10	1.3	1.1	nd	0.72	1.10	0.82	1.47	1.3
Tm	0.34	0.33	0.18	0.15	nd	0.089	0.17	0.10	0.22	0.17
Yb	2.24	2.14	1.1	0.93	nd	0.55	0.89	0.87	1.33	1.3
Lu	0.32	0.29	nd	nd	nd	0.10	0.12	nd	0.20	nd
[6]Th	2.4	1.6	2.4	2.3	3.60	7.22	3.5	4.1	7.91	9.07
[6]U	0.479	0.16	0.546	0.485	0.816	0.936	1.07	1.37	1.88	2.44

[1]Major oxides determined by wavelength-dispersive X-ray fluorescence: J.E. Taggart, A. Bartel, D.F. Siems, and J.S. Mee, analysts.

[2]FeO determined by potentiometric titration and F by ion-selective electrode potentiometry: E. Brandt and C.S. Papp, analysts.

[3]Trace elements determined by energy-dispersive X-ray fluorescence: J.R. Evans, and J. Kent, analysts.

[4]Trace elements determined by X-ray spectroscopy: D.L. Fey and P.H. Briggs, analysts. No. 26 determined by energy-dispersive X-ray fluorescence: J. Kent, analyst.

[5]Rare earths determined by inductively coupled plasma-mass spectrometry: G.O. Riddle and R. Moore, analysts.

[6]Th and U determined by delayed neutron activation analysis: R.E. McGregor, R.B. Waughn, and D. M. McKown, analysts.

Th contents (as much as 9 ppm). Th/U ranges from 2.6 to 6.7 in the felsic members of the suite and averages 4.1. Th/U for the two mafic members analyzed is 5.0 and 10.0. On a Th/U plot, a best fit line is Th/U~5.

Barium (Ba) contents are highest (1,500–2,000 ppm) in intermediate rocks (60–65 percent SiO_2) and fall to 1,000 ppm in the most felsic (70 percent or greater SiO_2). The mafic rocks (50 percent SiO_2) have Ba contents of 300–360 ppm. Cerium contents are relatively uniform at about 50 ppm but range from 30 to 70 ppm (fig. 19*D*). Zirconium ranges from about 100 ppm in the mafic rocks, is as much as 200 ppm in the intermediate rocks, and drops to 100 ppm in the most felsic rocks (fig. 19*B*). Strontium contents are 500–700 ppm in the mafic rocks, 900 ppm in the intermediate rocks, and as low as 300 ppm in the most felsic members of the suit (fig. 19*C*). Rubidium contents are 18–37 ppm in the mafic rocks, about 90 ppm in the intermediate rocks, and as much as 115 ppm in the most felsic rocks.

Rare earth abundances in the Swansea Plutonic Suite range from 83 to 169 ppm, light to heavy REE enrichment chrondite normalized [CN] La/Yb=3–53, and heavy REE enrichment [CN] Yb=2.6–10.8. Felsic rocks in the suite are depleted in HREE compared to the mafic rocks (fig. 20*D*), indicating possible removal of the HREE by pyroxene with or without amphibole or garnet during evolution of the magma. A fine-grained aplite sill (sample B–495*C*) intruded along the mylonitic foliation in the felsic phase of the suite has the greatest light to heavy rare earth enrichment and appears to be the end product of the process.

Comparison with Poachie Crust and Possible Origin

If we assume that the northern Harcuvar complex rocks were drawn out from beneath the Colorado Plateau from the vicinity of the Poachie region and areas to the northeast, it might be instructive to compare data on the two sets of rocks. Seismic data indicate that the northern Harcuvar complex came from depths of about 18 km (Clayton and Okaya, 1991). In the Poachie region, 25 kilometers from the northeastern edge of the exposures of the northern Harcuvar complex, felsic volcanic rocks of the same age as the Swansea Plutonic Suite form exogenous domes indicating that little denudation of the crust has occurred there since the early Miocene (Bryant, 1995; Bryant and others, 1991). The rocks of the Swansea Plutonic Suite differ in chemistry from the granitic rocks at the surface in the Poachie region and from their Proterozoic wallrock in the Buckskin Mountains. The upper intercept of the line in the U-Pb concordia diagram of samples from the Swansea Plutonic Suite and the Middle Proterozoic U-Pb age of zircons from inclusions of granitic rock indicate that Middle Proterozoic crust was involved in the generation of the magmas that formed the suite (fig. 16*C*). The uniform Pb isotopic composition of the Swansea rocks suggests that the melt was well mixed. The contrast of the Pb isotopic composition between the rocks of the Swansea Plutonic Suite and one such determination on an inclusion of Middle Proterozoic granitic rock suggest that the melt was not primarily derived from material like that in the inclusion but that the Middle Proterozoic granitic rock and any other crustal rocks that contributed to the magma were completely homogenized, except for some parts of the zircons contributed by those rocks, with melts from the lower crust and(or) upper mantle.

Much more thorough studies of the 16.4-Ma Searchlight (Bachl and others, 2001) and 15.7-Ma Aztec Wash (Falkner and others, 1995) plutons in the Colorado River extensional corridor in the Eldorado Mountains about 200 km north-northwest of the Buckskin Mountains influence our interpretations of the Swansea Plutonic Suite. The Aztec Wash pluton most resembles the Swansea Plutonic Suite, although it lacks the well-developed mylonitic foliation of the felsic and intermediate rocks of the Swansea Plutonic Suite because of its position in an accommodation zone in the extended terrane (Faulds and others, 1988). The Aztec Wash pluton is composed of granite and diorite and minor amounts of intermediate, more mafic, and more silicic rocks. The mafic and felsic rocks mingled extensively. The pluton was emplaced at levels of 5 km or less, and it is inferred on the basis of Pb, Sr, and Nd isotopic compositions to have formed from old enriched lithospheric mantle that underwent limited contamination from the crustal rocks it passed through on its way to the upper crust. A concordia plot of U-Pb zircon analyses has an upper intercept indicating contribution by Early Proterozoic crust or Cretaceous rocks derived from that crust.

The chemistry of the Aztec Wash pluton contrasts to some degree with that of the Swansea Plutonic Suite. Mafic rocks of that pluton have high incompatible element concentrations: K_2O is about 3 weight percent; Ba, 1,600 ppm; and LREE, 350 times chondrite, in contrast to the mafic rocks in the Swansea Plutonic Suite, for which K_2O is about 0.7 weight percent, Ba, about 330 ppm, and LREE is 75 times chondrite. Total REE abundances in the Aztec Wash pluton range from 94 to 570 ppm, much higher than the 65–169 ppm range in rocks analyzed in the Swansea Plutonic Suite. However, if we do not count the rare earth contents of the rocks in the Aztec Wash pluton that have SiO_2 contents of 52–57 percent, a range of silica content lacking in the analyzed samples from the Swansea Plutonic Suite, the range for the Aztec Wash pluton is reduced to 94–334 ppm compared to 83–169 ppm for rocks in the 60–75 percent SiO_2 range for the Swansea Plutonic Suite. The Aztec Wash pluton is richer in Th and U than the Swansea Plutonic Suite. Thorium ranges from 1.7 to 52 ppm, compared to 1.6–9.1 ppm for the Swansea rocks, and uranium from 0.6 to 11.7 ppm in the Aztec Wash pluton compared to 0.48 to 2.44 ppm in the Swansea Plutonic Suite. Th/U ratios of the Aztec Wash pluton and the Swansea Plutonic Suite are similar.

A possible interpretation of the origin of the Swansea Plutonic Suite is that it was derived from lithospheric mantle less enriched than that giving rise to the Aztec Wash pluton or from asthenospheric mantle. The magma homogenized its crustal component either by being hotter or by spending more

time in the lower crust than the material that formed the Aztec Wash pluton.

The Swansea Plutonic Suite crops out over a much larger area than the Aztec Wash pluton. Is its present configuration due to large-scale ductile deformation during and(or) after emplacement? Is it all of the same age, or was it emplaced as the lower plate was drawn southwestward? Interpretation of seismic data shows a bulbous layer having middle crustal velocities and as much as 15 km thick beneath the Buckskin Mountains (fig. 21). The 6.35–6.5 km/sec velocities in this layer could represent diorite or a mixture of mafic and silicic rocks (McCarthy and others, 1991). The layer pinches out near Bagdad in the transition zone northeast of the Buckskin Mountains and thins to the southwest in the Basin and Range away from the Buckskin Mountains. This layer might be a source for the Swansea Plutonic Suite now forming part of the upper crust exposed in the Buckskin Mountains. Limited data show that it is thicker along the belt of Miocene intrusions in the lower Colorado River extensional corridor than to the southeast or northwest. The layer thickens to 10 km beneath the Whipple Mountains, in which Miocene intrusive rocks also are exposed (McCarthy and others, 1991). McCarthy and Parsons (1994) speculate that the bulge in the midcrustal layer beneath the Buckskin Mountains is caused by addition of mantle-derived mafic magma and crustal flow of silicic rocks into a zone of large extension.

Relation Between Magmatism, Extension, and Core Complex Formation.

The Buckskin Mountains comprise the only large core complex in the region where a significant area of Miocene plutonic rocks is exposed. The only Tertiary igneous rocks exposed in the Harcuvar and Harquahala Mountains are early Miocene microdiorite dikes. Lister and Baldwin (1993) relate pulses of ductile deformation in core complexes to intrusion of igneous material and attribute differential uplift of the bounding detachment fault to those intrusions. On the other hand, Spencer and others (1996) favor the hypothesis that the large magnitude extension apparent in west-central Arizona adjacent to the Colorado Plateau transition zone was caused by a crust thickened during Cretaceous structural and igneous events that produced an elevated land mass and crustal root in that region. Variations in the few K-Ar and $^{40}Ar/^{39}Ar$ dates available are related to position along the northeast-southwest direction of extension and denudation of the core complex rather than to proximity to the outcrop area of the Swansea Plutonic Suite. Biotite was completely reequilibrated in Miocene time throughout the Buckskin Mountains. Biotite from an inclusion in Miocene plutonic rock has the same cooling age as biotite from many kilometers away. In the Harcuvar Mountains, the effects of Tertiary ductile deformation diminish in the middle of the range and in the Harquahala Mountains are confined to the northeastern end of the range (Rehrig and Reynolds, 1980). Miocene igneous rocks in these ranges are only in dikes, and those ranges apparently are composed of rock that came from a shallower depth than that in the lower plate exposed in the Buckskin Mountains (Richard and others, 1990).

Structure

Structures in the lower-plate rocks in the Buckskin Mountains and the eastern Harcuvar Mountains are high-angle reverse and normal faults, low-angle normal faults, mylonitic foliation and lineation, nonmylonitic foliation and lineation, and folds. We will discuss them from youngest to oldest in the order from relatively well dated structures to less well dated ones.

For the purposes of structural analysis the Buckskin Mountains have been divided into three parts: the eastern Buckskin Mountains east of the Lincoln Ranch fault zone, the central Buckskin Mountains between the Lincoln Ranch fault zone and the Swansea fault and a line projected along strike to the southeast, and the western Buckskin Mountains west of the Swansea fault and that line (fig. 22). Structures in the Little Buckskin Mountains are treated separately. In order to clarify the ages of the structures, the foliation and lineation in the Oligocene(?) and Miocene Swansea Plutonic Suite are compiled separately from structures in the older rocks. In the eastern Harcuvar Mountains, structures in the Alamo Dam SE and ECP 7½-minute quadrangles west of longitude 113º22'30"are compiled separately from those in the Smith Peak and Date Creek SW 7½-minute quadrangles east of longitude 113º22'30". Within each of these areas, structures in the Cretaceous granite of Tank Pass are compiled separately from those in the older rocks in order to determine whether any pre-Late Cretaceous structures could be detected in the older rocks. Except for the rocks containing northwest-trending mineral lineation, we used only the data we collected rather than all the data shown on the Harcuvar wilderness study area map (Drewes and others, 1990) so that any bias in the observations would be as uniform as possible.

Faults

The youngest structures are northwest-trending, high-angle reverse and normal faults, which offset the Rawhide detachment fault. They may be as young or younger than the youngest movement on the Sandtrap Wash fault, a northwest-trending fault just northeast of the Rawhide Mountains, which displaces 9.2-Ma basalt flows (Lucchitta and Suneson, 1994a; Bryant, 1995).

The Lincoln Ranch fault zone, first mapped by Wilson (1960), is an en echelon series of faults that extends from about the crest of the Planet Peak antiform to the southern edge of the Buckskin Mountains. Strands of the fault zone generally dip moderately to steeply northeast but locally dip steeply southwest. The Rawhide detachment fault and

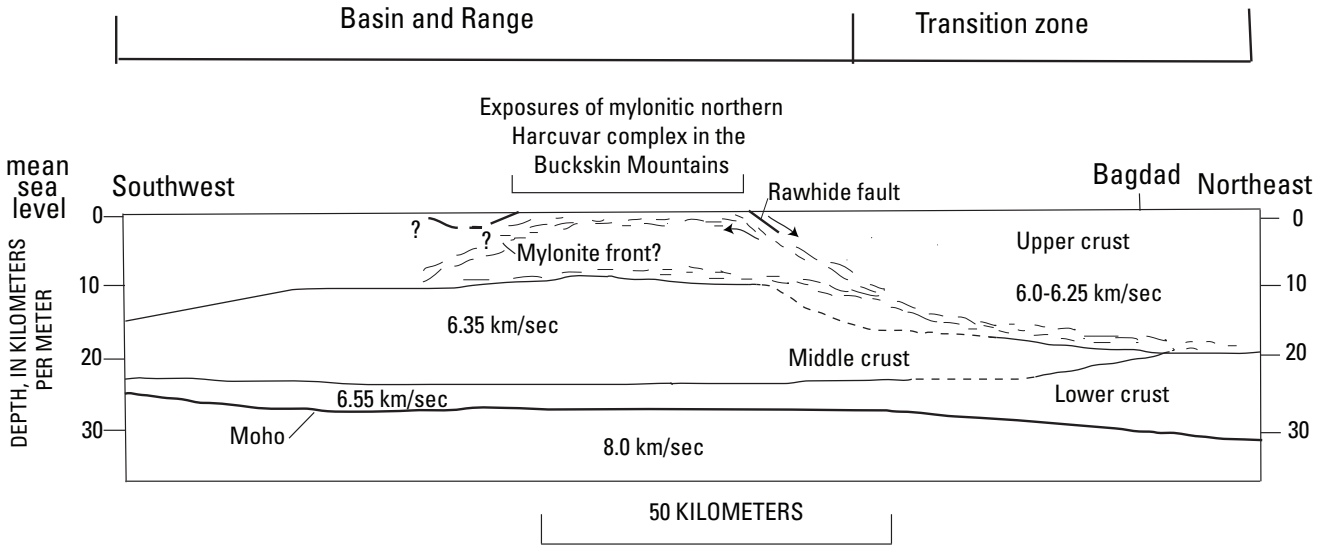

Figure 21. Northeast-southwest crustal section through the Buckskin Mountains based on geophysical and geologic data. Modified from McCarthy and others (1991) with added data based on Clayton and Okaya (1991) and McCarthy and Parsons (1994). Details in seismic velocity variations at near the top of the upper crust not shown. Dotted lines indicate inferred velocity discontinuities. Irregular discontinuous lines indicate reflective horizons. These lines are shown where the northern Harcuvar complex is exposed in the Buckskin Mountains because the rock is mylonitized. The northeastern-dipping reflective horizon projects to the Rawhide fault on the northeastern side of the Buckskin Mountains. At the southern end of the Buckskin Mountains a mylonitic front is interpreted to be above the thick, southwest-dipping slice of Paleozoic and Mesozoic metasedimentary rocks so that nonmylonitic Miocene granitic rock in the Bouse Hills is in the lower plate of the Rawhide fault as interpreted by Spencer and Reynolds (1991). km/sec, kilometers per second; Moho, Mohorovičic' discontinuity.

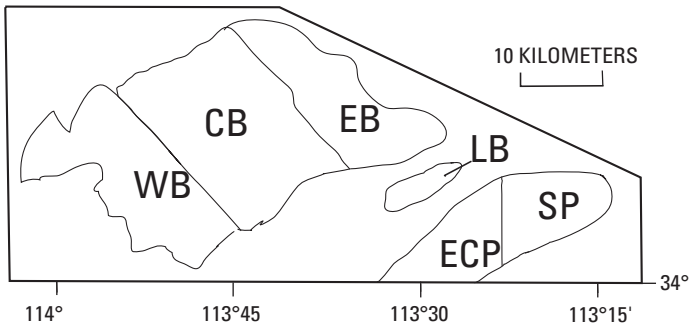

Figure 22. Areas of structural analyses in the northern Harcuvar complex. EB, eastern Buckskin Mountains; CB, central Buckskin Mountains; WB, western Buckskin Mountains. In the Harcuvar Mountains: SP, Smith Peak 7½-minute quadrangle and part of the Date Creek Ranch SW 7½-minute quadrangle; ECP, ECP 7½-minute quadrangle and part of the Alamo Dam SE 7½-minute quadrangle. LB, Little Buckskin Mountains.

overlying upper-plate rocks are displaced down to the southwest so that upper-plate rocks of the Swansea and Lincoln Ranch synforms are bounded on the northeast by the Lincoln Ranch fault. The net displacement on much of the fault is reverse. Slickenlines in a few exposures of the fault zone are subhorizontal (Spencer and Reynolds, 1989b; one additional locality found in this study) indicating that the most recent movement was dominantly strike slip. The map pattern suggests displacement dominantly in a vertical sense and a minimum displacement of 400 m in the Lincoln Ranch synform.

Southeast of the stepover in major displacement along the Lincoln Ranch fault zone are numerous shear zones having northwest trends and generally steep to moderate southwest dips. These zones consist of 1–2 m of brecciated or highly fractured rock and locally contain quartz and quartz-carbonate veins, fluorite, and secondary copper minerals. Specular hematite and secondary copper minerals also occur along fractures in rock of the shear zones. These shear zones have been prospected and locally mined for copper, lead, silver, and gold in the Bluebird subdistrict of the Alamo mining district (Spencer and Welty, 1989).

The Swansea fault cuts the Swansea synform, extends northwest beyond the Buckskin Mountains beneath younger rocks, and apparently dies out about 2 km southeast of the Swansea synform. Northwest of Swansea, rocks on the southwest side of the fault are displaced about 200 m up in relation to those on the northeast (Spencer and Reynolds, 1989b).

East of Battleship Peak, northwest-trending shear zones generally dip steeply to moderately northeast and locally contain quartz veins. Both the veins and the adjacent fractured rock locally contain specular hematite and chrysocolla in the Green Streak subdistrict of the Midway district (Spencer and Welty, 1989).

The Mineral Wash fault in the western Buckskin Mountains cuts through the entire width of the exposed lower-plate rocks and extends to the northwest through upper-plate rocks. At Planet Peak the southwest side is displaced upward at least 400 m. Dips of the Mineral Wash fault range from 50° southwest to 80° northeast along the northern part to 50° northeast near the crest of the Clara Peak antiform (Spencer, Reynolds, and Lehman, 1989b; Spencer and Reynolds, 1989b).

The northwest-trending faults are perpendicular to the trend of the antiforms and synforms in the Buckskin Mountains and a regional stretched mineral lineation in the mylonitic rocks of the lower plate.

Statistical analyses of observed brittle faults show mean trends of N. 42° W. and N. 45° W. and 60° northeast dips in the central and eastern Buckskin Mountains and N. 57° W. and 76° northeast dip in the western Buckskin Mountains (fig. 23*D*, *H*, *K*). In the eastern and western Buckskin Mountains some of the northwest-trending faults dip steeply southwest, and some steep faults have northerly or northeasterly trends.

Scattered, gently dipping faults are probably related to the Rawhide detachment fault. These faults are mappable below the Rawhide detachment fault in the southeastern part of the eastern end of the Buckskin Mountains, on the southern side of the eastern end of the Little Buckskin Mountains, and on the northern side of the Harcuvar Mountains southeast of the Little Buckskin Mountains. The latter two might be parts of one slice that extends beneath the valley separating the Harcuvar Mountains from the Little Buckskin Mountains. These faults have zones of brecciated mylonite along them as much as 100 m thick. One extensive such fault in the Lincoln Ranch synform in the eastern Buckskin Mountains is mapped in the valley of the Bill Williams River southwest of Alamo Lake (fig. 24*A*). This fault could not be followed north of the Clara Peak antiform and probably dies out in that area. Breccia along it has a sharp lower contact mapped as the fault and a gradational upper contact with nonbrecciated mylonite. Displacements of these faults seem to be minor, but lack of piercing points makes precise determinations impossible.

Other low-angle faults probably associated with late movements on the Rawhide detachment are best exposed in canyons and are best identified where the mylonitic foliation is discontinuous across them (fig. 24*B*).

Major Folds

Northwest-trending folds locally deform the detachment fault bounding the lower-plate rocks in the Centennial Wash quadrangle on the northern side of the Rawhide Mountains (Lucchitta and Suneson, 1994b) and on the northern side of the eastern Buckskin Mountains south of Alamo Lake (Bryant, 1995).

The next youngest structural features are the major northeast-trending antiforms and synforms in the detachment fault. The antiforms bring up the detachment fault and the underlying lower-plate rocks, which form the Buckskin, Little Buckskin, and Harcuvar Mountains (fig. 2). Measured dips of the detachment fault adjacent to the mountains range from less than 5° to 70° (Lucchitta and Suneson, 1994b; Spencer and Reynolds, 1989b; Reynolds and Spencer, 1984). The structural relief of these northeast-trending folds in the Buckskin Mountains is a few hundred meters (Spencer and Reynolds, 1989b). The structural relief of the synform between the Buckskin and Harcuvar Mountains is probably as much as 1,000 m (Spencer and Reynolds, 1989b; Bryant, 1995).

Dikes

The next youngest structural feature is a set of northwest-trending dikes of diabase, gabbro, and diorite. Some are undeformed, and others are at least locally foliated. Although these dikes have the same trend as the faults that offset the Rawhide detachment fault, they must be significantly older, for similar dikes are not found in nearby upper-plate rocks. None of the dikes in the Buckskin Mountains have been dated, but one from a well-developed swarm of similar dikes in the Harquahala Mountains has an $^{40}Ar/^{39}Ar$ total gas age on hornblende of 22.3 Ma (Richard and others, 1990). Similar

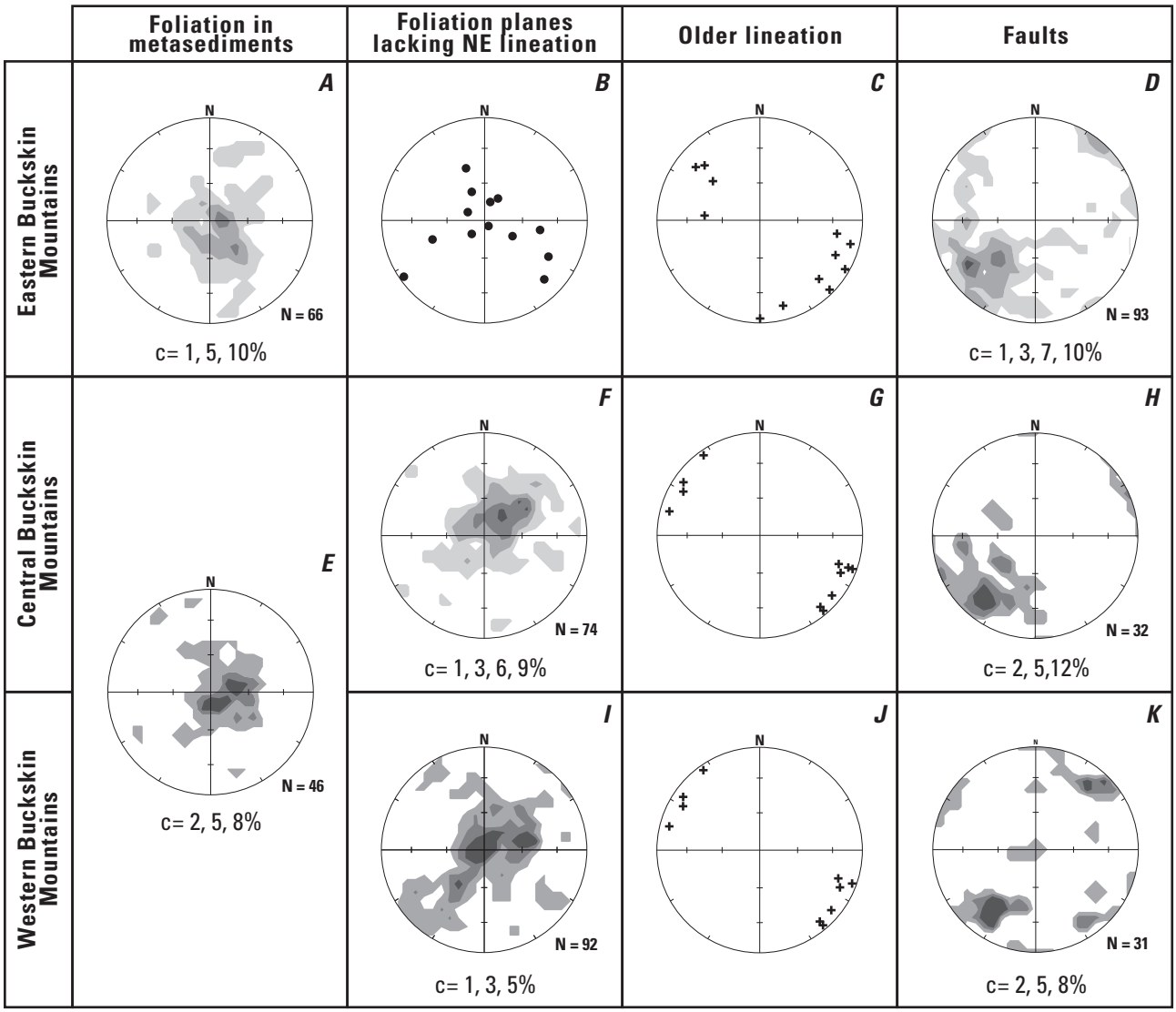

Figure 23. Structures in the Buckskin Mountains formed before, during, and after mylonitization in the Miocene. This and other structural diagrams are equal-area projections in the lower hemisphere with planes of projection horizontal and north at the top. Contours show percentage (%) of points falling within 1 percent of the area of the diagram. N, number of points; C, contours.

A

B

Figure 24. Low-angle brittle faults in the eastern Buckskin Mountains. *A*, Zone of breccia in layered gneiss along the canyon of the Bill Williams River about 4 kilometers northeast of Reid Valley. Breccia separates layered mylonitic gneiss below with regular structure from brittlely deformed mylonite with less regular structure above. View towards northeast from 1,200-foot knoll west of the Bill Williams River 170 meters east of the center of the east line of sec. 7, T. 10 N., R. 13 W., Reid Valley 7½-minute quadrangle. *B*, Low-angle brittle fault puts mylonitic layered gneiss with west dips above mylonitic layered gneiss with north dips. Alamo Dam 7½-minute quadrangle. Section 11, T. 10 N., R. 13 W., 300 meters from south line and 510 meters from east line. About 1,500 meters horizontally from detachment fault and probably less than 500 meters and possibly as little as 200 meters vertically below it.

dikes in the Harcuvar Mountains have mainly northwest trends, but a few have northeast trends (Drewes and others, 1990), and in the western Harcuvar Mountains the dikes trend northwest (Reynolds and Spencer, 1993).

Lineation

The next youngest structures are mylonitic foliation and lineation found in all the rock types in the northern Harcuvar complex. Most, and perhaps all, of the mylonitization is younger than the 22-Ma rocks of the Swansea Plutonic Suite. Mylonitic textures are lacking in the rocks of the Bouse Hills, which are interpreted to be in the lower plate (Spencer and Reynolds, 1991) but above a southwest-dipping mylonitic front that lies concealed beneath younger Tertiary and Quaternary rocks between the Buckskin Mountains and the Bouse Hills (Bryant, 1995, sec. C–C'). Most of the foliation is mylonitic and is formed by aligned biotite and, locally, by flattened feldspar and(or) quartz grains. The rocks have mesoscopic and microscopic features indicative of cataclastic breakdown of larger minerals, recrystallization, and ductile deformation of some minerals at conditions where some biotite was not recrystallized, although it completely lost argon in the samples dated (Rehrig, 1982; Spencer, Shafiqullah, and others, 1989). Published K-Ar ages of biotite in the Buckskin Mountains range from 17 to 13 Ma, suggesting that these micas became closed systems during and after the formation of mylonitic foliation and lineation.

The lineation is formed by ductilely streaked-out grains of quartz, biotite, or amphibole (fig. 25*A*). Rehrig and Reynolds (1980) first suggested that the mylonitic foliation and lineation in the Buckskin and Harcuvar Mountains were related to northeasterly extension during late Tertiary time. Now that we know that a substantial area of 20-Ma rock in the Buckskin Mountains has mylonitic foliation and lineation similar to that in the older rocks, there is no doubt that the mylonitic foliation and lineation are of Miocene age. Megascopic textures, such as the shape and orientation of porphyroclasts of mica or feldspar and of components of differing ductility in the layered gneisses, indicate that rock lower in the crust flowed southwest in relation to overlying rock (figs. 8, 25*B*; Spencer and Reynolds, 1989b).

Differential ductility of layers in the mylonite is especially well displayed where some layers are composed of marble (fig. 7). Another marked ductility contrast is between layered felsic gneiss and mafic rock (fig. 25*C*).

The lineation trends northeast, parallel with the direction of regional extensional deformation, and is about parallel with the axes of the large folds in the detachment fault that caused the northeast-trending ranges composed of lower-plate rocks. The mylonitic foliation and lineation become less pervasive toward the southwest in the Buckskin and Harcuvar Mountains, yet the statistical pattern of the foliation changes little.

The change in the degree of development of the northeast-trending lineation is best illustrated by dividing the number of readings of foliation in the pre-Miocene rocks containing northeast-trending lineation by the number of readings on foliation in those rocks lacking that lineation. The results are the following: eastern Buckskins, 50; central Buckskins, 3.6; and western Buckskins, 2.4. In the Harcuvar Mountains no foliation lacking northeast-trending lineation was recorded in the Smith Peak and Date Creek Ranch SW quadrangles at the eastern end of the range, but in the ECP Peak and Alamo Dam SW quadrangles to the west, the ratio is 8.4.

The statistical means of mylonitic lineation in the Buckskin Mountains are similar throughout the range and in both Miocene and older rocks. The mean lineations among the three geographical areas and the Miocene and pre-Miocene rocks are N. 43° W. to N. 49° W. (fig. 26*C, D, I, J, O, P*). Mean plunge of lineation in the pre-Miocene rocks range from 2° southwest in the eastern Buckskin Mountains to 11° southwest in the western Buckskin Mountains. In the Swansea Plutonic Suite of the eastern Buckskin Mountains (fig. 26*D*), mean plunge is notably steeper than in the older rocks and ranges from 13° to 33° because of a statistical difference in dip of the foliation in that area (fig. 26*B*). The Little Buckskin Mountains have a mean lineation of N. 42° E. plunging 3.5° northeast, similar to that in the Buckskin Mountains but with a different direction of plunge (fig. 27*B*). These directions are more northerly than the N. 60° E. trend of the Buckskin and Little Buckskin antiforms.

In the Harcuvar Mountains, the mean trends of the mylonitic lineation are the same in the Late Cretaceous granite and the older rocks (fig. 28*C*, *D*, *G*, *H*). They differ, however, from those in the ranges to the north. In the ECP and Alamo Dam SW 7½-minute quadrangles, the mean is about N. 55° E. (fig. 28*G*, *H*), whereas to the northeast it is N. 63° E. (fig. 28*C*, *D*, *L*). The northeastern end of the Harcuvar antiform is bent to the south, and the more easterly trend of the mean lineation azimuth is probably related to that bend.

Foliation

Foliation generally has gentle dips, except for the foliation in the Swansea Plutonic Suite in the eastern Buckskin Mountains (fig. 26*B*). In some areas, poles to foliation form a well-developed girdle around a northeast-trending axis. This is best shown in the Little Buckskin Mountains where the axis of the girdle is N. 55° E., almost the same as the N. 60° E. trend of that range (fig. 27*A*).

In the Buckskin Mountains, poles to foliation in pre-Miocene rocks form poorly developed girdles around gently plunging N. 70º E. axes in the eastern and central areas (fig. 26*A,G*) and N. 58° E. in the western area (fig. 26*M*). The N. 58° E. axis for the western Buckskin Mountains is parallel with the trend of the range and the folds in the detachment fault within the range. In the central Buckskin Mountains, the trend of these folds is about N. 60° E., whereas in the eastern Buckskin Mountains the trend of axis of the Ives Peak

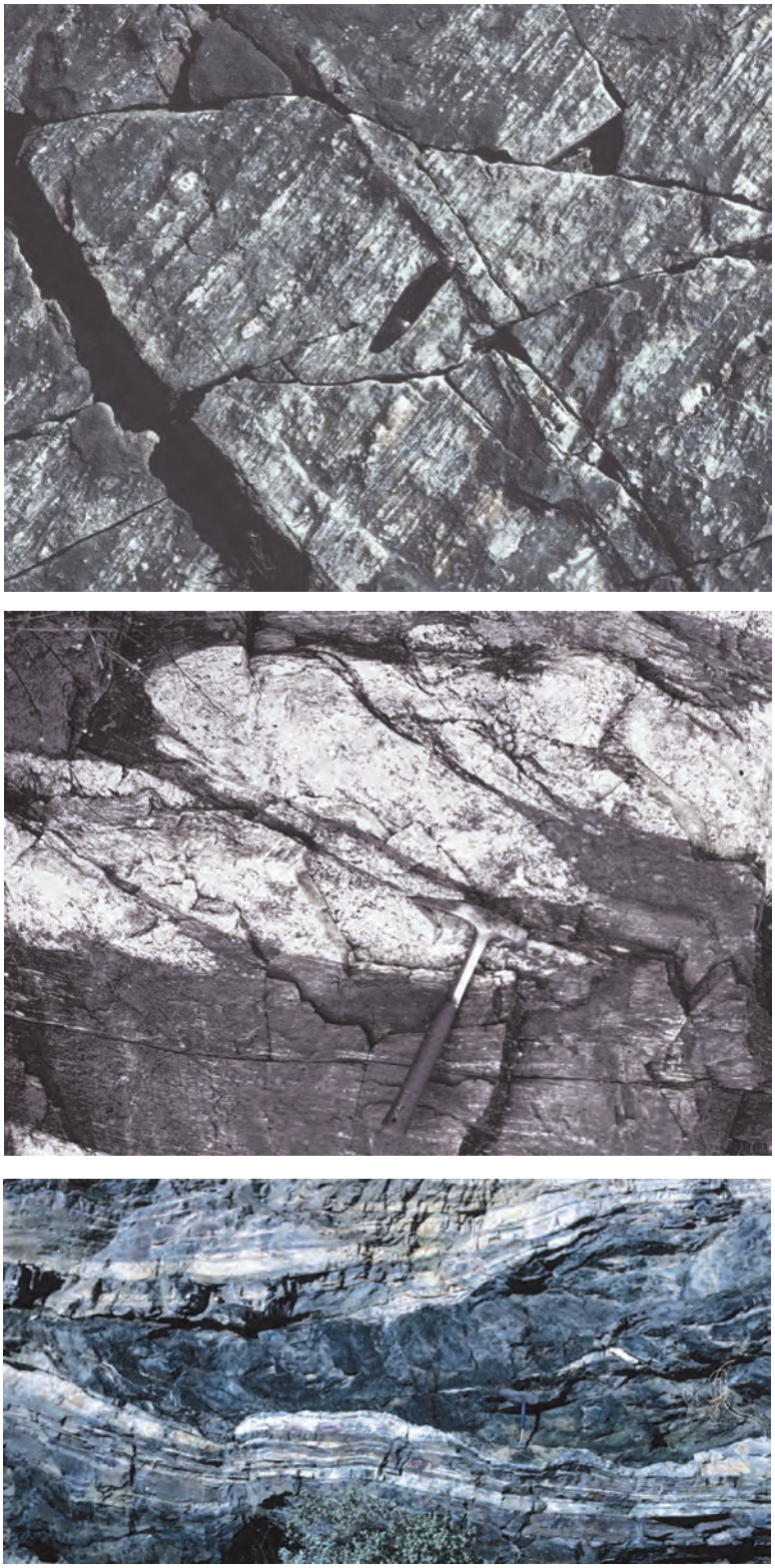

Figure 25. Features in mylonitized rock. *A*, Typical northeast-trending mineral lineation on mylonitic foliation plane in mylonitic biotite-quartz-feldspar gneiss. Alamo Dam 7½-minute quadrangle. In wash, sec. 32, T. 10 N., R. 12 W., 380 meters from north line and 770 meters from west line. Knife is 8 centimeters long. *B*, Imbricated pegmatite in mylonitized granitic rock, North is to the left. Alamo Dam 7½-minute quadrangle. On south side of wash in sec. 6, T. 9 N., R. 12 W., 540 meters from north line and 230 meters from west line. Hammer is 32 centimeters long. *C*, End of lens of less ductile rock ranging in texture from amphibolite to metagabbro in more ductile, mylonitic, layered migmatitic gneiss. Mafic rock forms lens as much as 4 meters thick and more than 20 meters long. Alamo Dam 7½-minute quadrangle. In wash sec. 15, T. 10 N., R. 13 W., 330 meters from south line and 330 meters from east line. Hammer is 32 centimeters long.

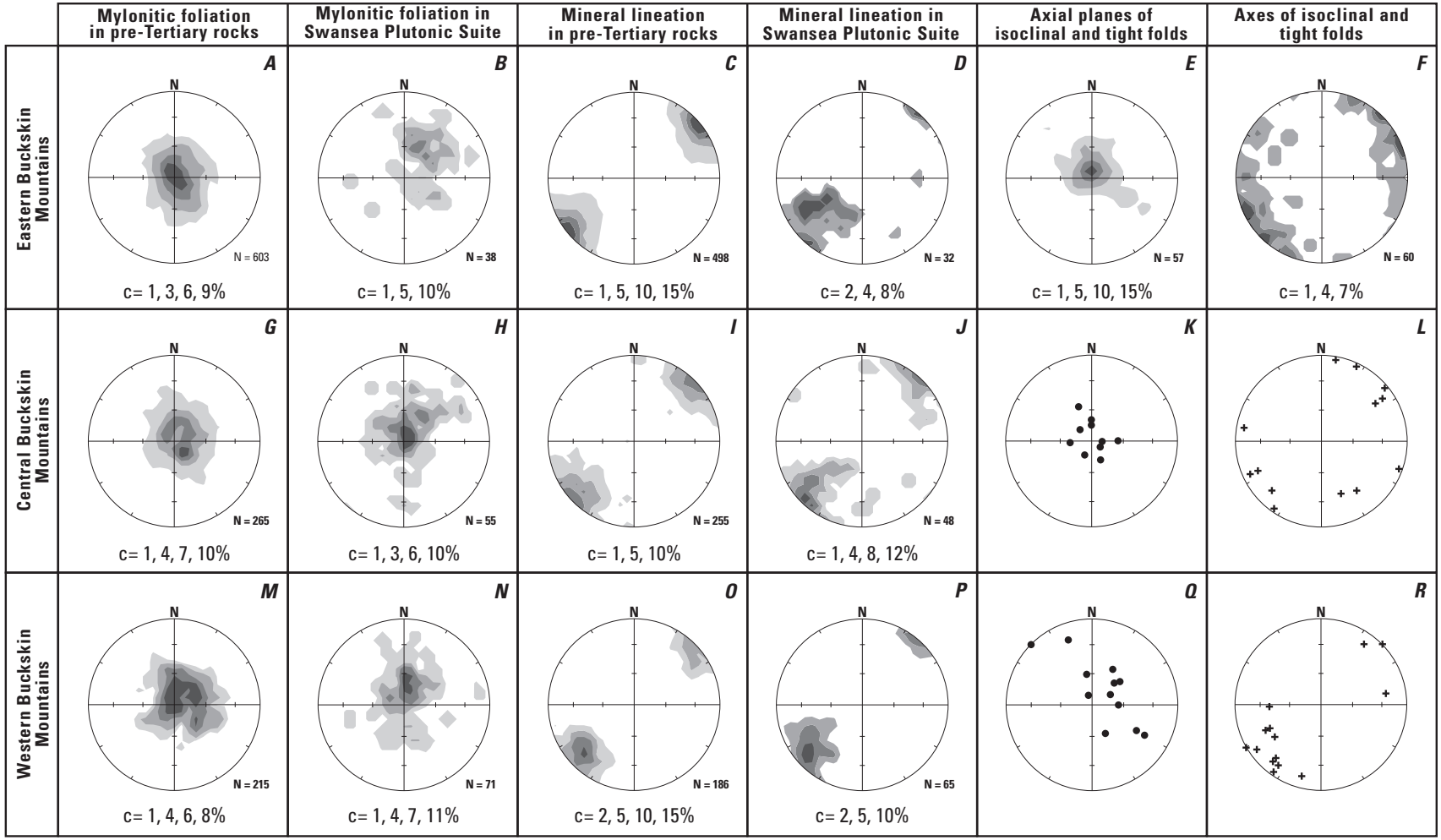

Figure 26. Structures in the Buckskin Mountains synchronous with mylonitization during the Miocene.

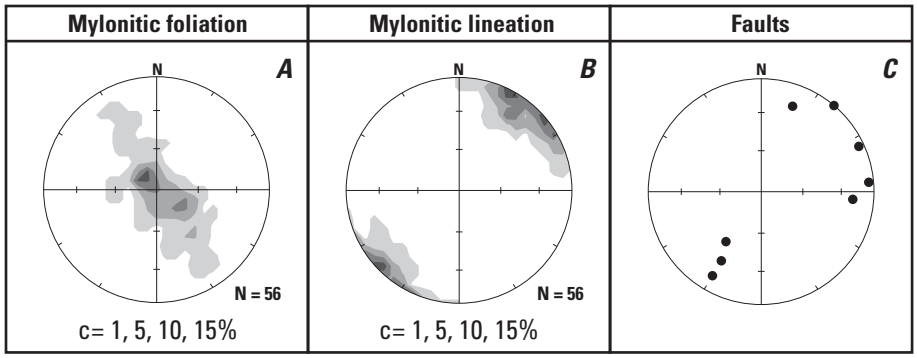

Figure 27. Structures in the Little Buckskin Mountains formed during and after mylonitization.

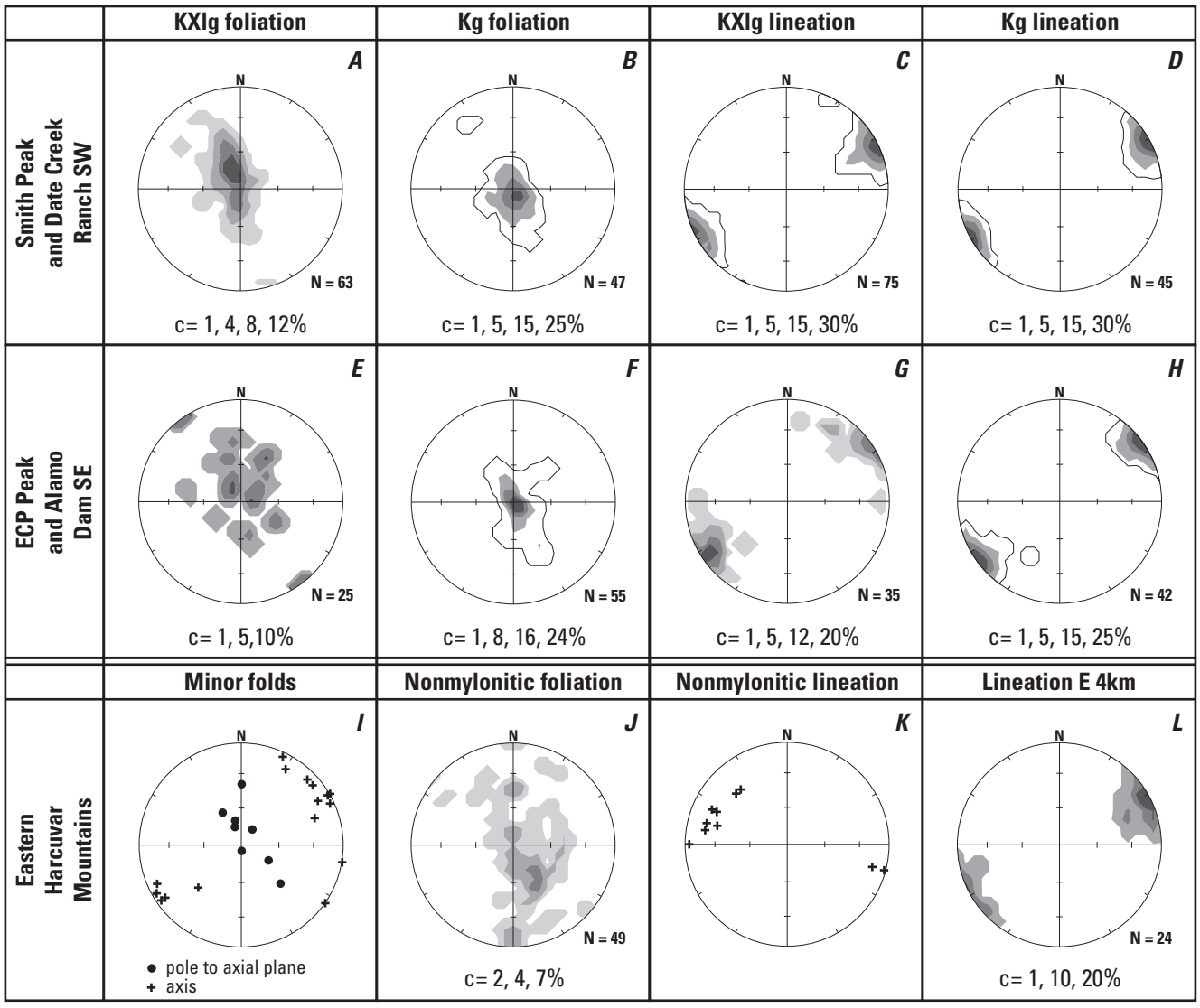

Figure 28. Structures in the eastern Harcuvar Mountains formed before and during mylonitization. Kg, granite of Tank Pass; KXlg, Proterozoic and Cretaceous layered gneiss.

antiform curves to a N. 80° E. trend. Thus, the N. 70° E. trend of the axes of the girdle formed by poles to foliation in the eastern Buckskin Mountains is approximately parallel with average trend of the larger structure.

The mylonitic foliation in the Swansea Plutonic Suite forms a different pattern. Poles to foliation form poorly developed girdles around northwest-trending axes ranging from N. 47° W. in the eastern Buckskin Mountains (fig. 26*B*) to N. 8° W. in the western Buckskin Mountains (fig. 2*6N*). The axes to the girdle are horizontal in the western and central Buckskin Mountains and plunge 15° northwest in the eastern Buckskin Mountains. The Swansea Plutonic Suite underlies the Clara Peak antiform and the Swansea synform, two of the major northeast-trending folds in the Buckskin Mountains. One might assume that the pattern of foliation reflects those structures, as the pattern of foliation in the pre-Miocene rocks does. Northwest-trending folds in the Swansea area are documented by Osborne (1981) and Woodward (1981). Those folds do not deform the detachment fault nearby, but since they deform mylonitic foliation in Miocene rocks, they must be of Miocene age. Detailed structural studies in the Battleship Peak area show that poles to foliation in the Precambrian rocks form a well-developed girdle around a horizontal northwest-trending axis, and poles to foliation in metasedimentary cover rocks form a poorly developed girdle of similar orientation (Marshak and Vander Meulen, 1989).

The difference in the statistical pattern of the foliation in the western Buckskin Mountains obtained by Woodward (1981), Osborne (1981), and Marshak and Vander Meulen (1989) compared to the one described here is probably due to the small size of the areas they studied compared to the much larger area here compiled. The diagram of foliation presented here may reflect the effects of both the earlier folding along northwest trends and the later folding along northeast trends.

In the Harcuvar Mountains, foliation similarly tends to be gently dipping, and poles to the foliation form girdles perpendicular to northeast-trending axes (fig. 28*A*, *E*, *B*, *F*). The foliation diagrams from both the Late Cretaceous granite and the older rocks have similar patterns. In the Smith Peak and the Date Creek Ranch SW 7½-minute quadrangles (fig. 28*A*, *B*), the poles to foliation form a girdle whose axis trends N. 74° E. and plunges gently southwest. The trend of the Harcuvar antiform is about N. 75° E. at its eastern end. In the ECP and Alamo Dam SW 7½-minute quadrangles, the average axis of the girdle formed by the poles to foliation in the Cretaceous and older rocks is about N. 65 E. (fig. 28*E*, *F*), and the antiform trends N. 60° E.

Foliation and bedding in Phanerozoic metasedimentary rocks were compiled separately to see if the pattern differed from that in older or younger rocks. The metasedimentary rocks form slices in the older rocks. Data from the large slice south of Battleship Peak (Marshak and Vander Meulen, 1989) are not compiled on our diagrams, but we compare those data with our data from other slices. The pattern formed by poles to foliation in the metasedimentary rocks (fig. 23*A*, *E*) resembles that in the older layered gneiss. Detailed study in the Battleship Peak area where the metasedimentary slice is as much as 1,200 m thick (Marshak and others, 1987) produces a similar result; the poles to foliation in the basement rocks and the metasedimentary cover have the same distribution pattern (Marshak and Vander Meulen, 1989).

Few foliation planes in the eastern Buckskin Mountains lack northeast-trending stretched mineral lineation. They have various attitudes, although most dip gently to moderately like the mylonitic foliation (fig. 23*B*). In the central and western Buckskin Mountains, the poles to foliation lacking northeast-trending lineation form moderately developed girdles with northwest-trending axes and horizontal to gently northwest plunge (fig. 23*F*, *I*). We tried to detect the pattern of the older foliation by plotting the poles to all the foliation planes that contain the older northwest-trending lineation. We combined data from the Buckskin Mountains and the Harcuvar Mountains in order to have enough points to make a contour diagram. The pattern we obtained is not distinctly different from others; it resembles that from the metasedimentary rocks in the eastern Buckskin Mountains (fig. 23*A*).

In the Little Buckskin Mountains, the direction of the mylonitic lineation (fig. 27*B*) has two statistical highs about 22° apart. This could be caused by an irregularity in the path of ductile flow of the rock during formation of the lineation or a fold younger than the lineation. The distribution of the foliation does not show similar highs, but any irregularity formed during formation of the lineation or late deformation of the lineation would have been around a steeply plunging axis and would not have shown well on the gently dipping mylonitic foliation.

Minor Folds

Tight and isoclinal minor folds (figs. 29, 30) are widespread in the mylonitic layered gneiss throughout the northern Harcuvar complex. Axial planes of these folds are parallel with mylonitic foliation (fig. 2*6E*, *K*, *Q*). Axes may have diverse trends in folds seen in one large outcrop or nearby outcrops, but they tend to have a weak to moderate statistical northeast trend (fig. 26*F*, *L*, *R*).

These folds are more numerous in the eastern Buckskin Mountains than in the central and western Buckskin Mountains. In the eastern Buckskin Mountains, poles to axial planes form a poorly developed girdle around an axis trending N. 37° E. and plunging 7 southwest (fig. 26*E*). The plunge of this girdle is similar to that of the mean value of the mylonitic lineation in the pre-Tertiary rocks of the eastern Buckskin Mountains. Axes of these folds are generally gently plunging and have varied strikes (fig. 26*F*). However, the statistical mean of their strike is N. 62° E. plunging 5° southwest. These are the B1 folds of Shackelford (1976, 1989) in the Rawhide Mountains, which form the northern part of the eastern Buckskin Mountains as used in this report. The distribution of the fold axes found by Shackelford in that part of the eastern Buckskin Mountains area differs from our compilation for the entire eastern Buckskin Mountains in that no concentration

Figure 29. Hinge of northeast-trending fold formed by mylonitic granite gneiss. Alamo Dam 7½-minute quadrangle. Sec. 24, T. 10 N., R. 13 W., 550 meters from south line and 750 meters from north line. Hammer is 32 centimeters long.

of axial trends is apparent. The folds in the Rawhide Mountains tend to plunge southerly more steeply than in the entire area of the eastern Buckskin Mountains because the foliation in the mylonitic gneiss, to which the axial planes of the B1 folds are parallel, has southwesterly dips. No such folds were found in the mylonitic foliation in the Oligocene(?) and Miocene Swansea Plutonic Suite, but some were found in mylonite derived from Proterozoic granitic rock in the eastern Buckskin Mountains.

In the central Buckskin Mountains, axial planes have gentle dips parallel to that of the foliation (fig. 25*K*), and the axes are scattered but have some concentration in a northeasterly direction (fig. 25*L*). In the western Buckskin Mountains, these folds similarly have axial planes parallel with foliation (fig. 25*Q*), but the axes have a better developed northeast trend (fig. 25*R*) than in the central Buckskin Mountains. In the Battleship Peak area of the western Buckskin Mountains, folds of this type occur in the cover rocks and were designated class B folds by Marshak and Vander Meulen (1989). The basement rocks in the area of their study are plutonic and lack the layering that shows this type of fold elsewhere in the Buckskin Mountains. Class A folds are rootless isoclinal folds with thick hinges, and they grade to class B folds. A compilation of the axial planes and axes of the two types (called F1 and F2 in fig. 8 of Marshak and Vander Meulen, 1989) shows that their axial planes are parallel to the foliation, and their axes are distributed around the compass but have concentrations in east and northeast directions and gentle plunges to the west and southwest down the foliation planes. This pattern of folding is identical to that in the layered gneisses (fig. 26*Q*,*R*).

Tight and isoclinal folds in the eastern Harcuvar Mountains form a pattern similar to that of the foliation and lineation. Poles to the axial planes form a girdle with a horizontal, northeast-trending axis. The fold axes trend northeast and are subhorizontal, but a few have other strikes and are also horizontal (fig. 28*I*).

Older Foliation

Perhaps the oldest structures in the lower-plate rocks in the region are foliation planes that strike north to northeast and dip steeply. Only a few outcrops of layered gneiss in the area of this report have that attitude. In the Harcuvar Mountains (Reynolds and Spencer, 1993; Drewes and others, 1990) and in the Harquahala

Figure 30. Minor tight folds in mylonitic biotite-hornblende gneiss. Reid Valley 7½-minute quadrangle. In wash, sec. 29, T. 10 N., R. 13 W., 850 meters from south line and 210 meters east of quadrangle boundary. Hammer head is 18 centimeters long.

Mountains (DeWitt and others, 1988), foliation of that trend is attributed to Early Proterozoic deformation and metamorphism because such trends are typical of the Proterozoic rocks in the Colorado Plateau transition zone to the northeast, although variations from this attitude are present (Anderson and others, 1955; Bryant, 1992a; Karlstrom and Bowring, 1993).

In the western Harcuvar Mountains, four deformational events of Cretaceous age based on structural overprinting relations are found (Reynolds and Spencer, 1993). Two of them formed new foliation and northwest-trending lineation. Evidence for the older one is confined to the westernmost part of the Harcuvar Mountains. The younger one is younger than the granite of Tank Pass and is probably the one that formed the northwest-trending lineation in the Buckskin Mountains and eastern Harcuvar Mountains.

In the eastern Harcuvar Mountains, foliation planes lacking prominent northeast-trending mineral lineation have a distribution statistically similar to that of the mylonitic foliation. (Compare fig. 28*J* with 28*A*, *B*, *E*, *F*.) The lack of difference in the patterns of foliation containing the northwest-trending lineation and the foliations containing the Miocene northeast-trending mylonitic lineation suggests that the gently to moderately dipping foliation may have formed in part or entirely during one or more deformations during the Cretaceous. Some or all of such foliation may have formed during Cretaceous thrusting in which Paleozoic and Mesozoic sedimentary and volcanic rocks were overidden by thrust sheets of Proterozoic rock. Two of the deformations in the western Harcuvar Mountains were associated with south-to-southwest vergent thrusting, and they are correlated with the southwest movement on the Hercules thrust system in the Granite Wash Mountains and southward movement on the Harquahala thrust in the Harquahala Mountains (Reynolds and Spencer, 1993). In order to get the Phanerozoic rocks in the upper plate of the Rawhide detachment in the Buckskin Mountains down to depths sufficient for regional greenschist facies metamorphism, thrust sheets of Proterozoic basement rock must have overidden them during Cretaceous deformation in the Maria fold and thrust belt (fig. 1). Slices of metamorphosed Paleozoic and possibly Mesozoic rock exposed in the northern Harcuvar complex in the Buckskin Mountains may represent the remains of slices initially formed during thrusting. The Miocene extensional deformation could not have caused those rocks to be buried, but it exhumed the rocks buried during the Cretaceous orogeny.

Summary of Structural and Metamorphic Events

Layered gneisses of the northern Harcuvar complex are intruded by Early Proterozoic granitic rocks and consequently are of Early Proterozoic age or older. Because no Archean rocks have yet been found in the region, the gneisses are considered to be of Early Proterozoic age. They were deformed and perhaps migmatized in the Early Proterozoic. The protoliths of the nongranitic layers in the gneisses have igneous compositions ranging from basalt to rhyolite, but locally some layers were derived from shale. Probably the rocks were metamorphosed to at least amphibolite facies at that time because upper-plate Proterozoic rocks in the Poachie Range and east of the Harcuvar Mountains were metamorphosed at that grade. Granitic magmas intruded the lower-plate rocks during the Middle Proterozoic.

We do not know whether Middle Proterozoic diabase intruded the rocks of the Harcuvar complex. Sheets, dikes, and small intrusions of diabase are widespread in the Proterozoic rocks of the transition zone and in the upper-plate rocks of the Basin and Range province to the north. If diabase intruded during the Middle Proterozoic, it would have been converted to amphibolite during Cretaceous metamorphism and would be difficult to distinguish in the field from older mafic metaigneous rocks.

In Late Jurassic time, diorite, trondhjemite, and, possibly, granite intruded rocks in the eastern Buckskin Mountains. The only Jurassic plutons we recognize in the northern Harcuvar complex are in that area; elsewhere, there may be small, unrecognized bodies of this age.

In Early Cretaceous time about 110 m.y. ago, the rocks were migmatized and metamorphosed under amphibolite facies conditions. They were thrust south or southwest over Paleozoic and Mesozoic sedimentary and volcanic rocks. Probably much of the older structure in the Proterozoic rocks was obliterated by the formation of gently dipping foliation associated with thrusting and regional metamorphism and migmatization in Early and Late Cretaceous time. Some of the sedimentary rocks were caught up as lenses in the fault zones and were metamorphosed under amphibolite facies conditions. In Late Cretaceous time, large and small plutons and many sills of granite and pegmatite intruded the Proterozoic basement rocks and the slices of metasedimentary rock. Uplift and cooling in latest Cretaceous and early Tertiary time followed.

In early Miocene and possibly late Oligocene, diorite, gabbro, granodiorite, and granite of the Swansea Plutonic Suite intruded the Proterozoic basement rocks before or during extension. The more felsic rocks of the suite carry numerous xenoliths of Middle Proterozoic granitic rock derived from deeper levels in the crust. Temperatures and pressures were suitable for ductile flow of the felsic rocks. The intrusive mass now forms a semiconcordant northeast-southwest-trending body parallel to the direction of regional extension. Some northwest-trending gabbro dikes were emplaced at about the same time. Extension by ductile flow formed foliation and lineation in many of the Miocene plutonic rocks. The ductile flow brought rocks out from 15–20-km depth beneath the transition zone and up into a brittle environment in which the detachment fault zone now bounding the Buckskin and Harcuvar core complexes formed. Cooling ages of the lower-plate rocks are younger than the stratigraphic ages of many of the rocks in the upper plate. Extension continued to at least 13 m.y. ago, and movement on the detachment fault in the eastern

Buckskin Mountains continued until at least that time. Weak regional extension continued in the upper plate northeast of the Buckskin Mountains until at least 9 m.y. ago, as indicated by tilting of basalts of that age.

Acknowledgments

Steve Reynolds and Jon Spencer encouraged me to start mapping in the Buckskin Mountains and furnished much valuable advice and good times in the field. This research was supported by the Geologic Framework, National Geologic Mapping, Pacific-Arizona Crustal Experiment (PACE), and COGEOMAP programs of the U.S. Geological Survey. Early in this work, L. David Nealey helped me get started in studying the geochemistry of the plutonic rocks in the Buckskin Mountains. We appreciate technical reviews of this report by Jon Spencer and John C. Reed, Jr.

References Cited

Anderson, C.A., Scholz, E.A., and Strobell, J.D., Jr., 1955, Geology and ore deposits of the Bagdad area, Yavapai County, Arizona: U.S. Geological Survey Professional Paper 278, 103 p.

Anderson, J.L., 1983, Proterozoic anorogenic granite plutons in North America, *in* Medaris, L.G., Jr., Byers, C.W., Mickelson, D.M., and Shanks, W.C., eds., Proterozoic geology—Selected papers from an international Proterozoic symposium: Geological Society of America Memoir 161, p. 133–154.

Bachl, C.A., Miller, C.F., Miller, J.S., and Faulds, J.E., 2001, Construction of a pluton—Evidence from an exposed cross section of the Searchlight pluton, Eldorado Mountains, Nevada: Geological Society of America Bulletin, v. 113, p. 1213–1228.

Baedecker, P.A., and McKown, D.M., 1987, Instrumental neutron activation of geochemical materials, *in* Baedecker, P.A., ed. Methods for geochemical analysis: U.S. Geological Survey Bulletin 1770, p. H1–H14.

Bancroft, Howland, 1911, Reconnaissance of the ore deposits in northern Yuma County, Arizona: U.S. Geological Survey Bulletin 451, 130 p.

Barth, A.P., Wooden, J.L., and Jacobson, C.E., and Probst, Kelley, 2004, U-Pb geochronology and geochemistry of the McCoy Mountains Formation, southeastern California—A Cretaceous retroarc foreland basin: Geological Society of America Bulletin, v. 116, no. 1–2. p. 142–153.

Brady, R.J., 2002, Very high slip rates on continental extensional faults—New evidence from (U-Th)/He thermochronometry of the Buckskin Mountains, Arizona: Earth and Planetary Science Letters, v. 197, p. 95–104.

Bryant, Bruce, 1992a, Geologic map of the Poachie Range, Mohave and Yavapai Counties, Arizona: U.S. Geological Survey Miscellaneous Investigations Map I-2198, scale 1:24,000.

Bryant, Bruce, 1992b, Preliminary geologic map of the Alamo Lake 30 x 60-minute quadrangle, west-central Arizona: U.S. Geological Survey Open-File Report 92–428, 23 p., 2 pls.

Bryant, Bruce, 1995, Geologic map, cross sections, isotopic dates, and mineral deposits of the Alamo Lake 30 x 60-minute quadrangle, west-central Arizona: U.S. Geological Survey Miscellaneous Investigations Series Map I–2489, scale 1:100,000.

Bryant, Bruce, Naeser, C.W., and Fryxell, J.F., 1991, Implications of low-temperature cooling history across the Colorado Plateau-Basin and Range boundary, west-central Arizona: Journal of Geophysical Research, v. 96, no. B7, p. 12375–12388.

Bryant, Bruce, and Wooden, J.L., 1989, Lower-plate rocks of the Buckskin Mountains, Arizona—A progress report, *in* Spencer, J.E., and Reynolds, S.J., eds., Geology and mineral resources of the Buckskin and Rawhide Mountains, west-central Arizona: Arizona Geological Survey Bulletin 198, p. 47–50.

Bryant, Bruce, Wooden, J.L., and Nealey L.D., 1993, The Swansea Plutonic Suite—Synextensional magmatism in the Buckskin and Rawhide Mountains, west-central Arizona: Geological Society of America Abstracts with Programs, v. 25, no. 5, p. 15.

Bryant, Bruce, Wooden, J.L., Gehrels, G.E., and Spencer, J.E., 1996, Plutonic and metamorphic history, northern part of the Harcuvar metamorphic complex, Buckskin and eastern Harcuvar Mountains, west-central Arizona: Geological Society of America Abstracts with Programs, v. 28, no. 5, p. 51.

Bryant, Bruce, Wooden, J.L., and Nealey, L.D., 2001, Geology, Geochemistry, and Pb-isotopic composition of Proterozoic rocks, Poachie region, west-central Arizona—A study of the east boundary of the Proterozoic Mojave crustal province: U.S. Geological Survey Professional Paper 1639, 54 p.

Carl, B.S., and Glanzer, A.F., 2002, Extent and significance of the Idependence dike swarm, eastern California, *in* Glanzer, A.F., Walker, J.D., and Bartley, J.M., eds., Geologic evolution of the Mojave Desert and the southwestern Basin and Range: Geological Society of America Memoir 195, p. 117–130.

Carter, T.J., Kohn, B.P., Foster, D.A., and Gleadow, A.J.W., 2004, How the Harcuvar Mountains metamorphic core complex became cool—Evidence from apatite (U-Th)/He thermochronometry: Geology, v. 32, no. 11, p. 985–988.

Clayton, R.W., and Okaya, D.A., 1991, Subsurface geometry of the Buckskin-Bullard detachment fault system beneath the Basin and Range–Colorado Plateau transition zone, imaged by CALCRUST seismic reflection profiles in west-central Arizona [abs]: Geological Society of America Abstracts with Programs, v. 23, no. 7, p. A132.

DeWitt, Ed, 1989, Geochemistry and tectonic polarity of Early Proterozoic (1700–1750 Ma) plutonic rocks, north central Arizona, *in* Jenny, J.P., and Reynolds, S.J., eds., Geologic evolution of Arizona: Arizona Geological Society Digest 17, p. 149–163.

DeWitt, Ed, and Reynolds, S.J., 1990, Late Cretaceous plutonism and cooling in the Maria fold and thrust belt, west-central Arizona [abs]: Geological Society of America Abstracts with Programs, v. 22, p. 18.

DeWitt, Ed, Richards, S.M., Hassemer, J.R., and Hanna, W.F., 1988, Mineral resources of the Harquahala Mountains wilderness study area, La Paz and Maricopa Counties, Arizona: U.S. Geological Survey Bulletin 1701–C, 27 p.

Drewes, Harald, DeWitt, Ed, Hill, R.H., Hanna, W.F., Knepper, D.H., Jr., Tuftin, S.E., Reynolds, S.J., Spencer, J.E., and Azam, Sarwar, 1990, Mineral resources of the Harcuvar wilderness study area, La Paz County, Arizona: U.S. Geological Survey Bulletin 1701–F, 29 p.

Falkner, C.M., Miller, C.F., Wooden, J.L., and Heizler, M.T., 1995, Petrogenesis and tectonic significance of the calc-alkaline, bimodal Aztec Wash pluton, Eldorado Mountains, Colorado River extensional corridor: Journal of Geophysical Research v. 100, no. 7, p. 10453–10476.

Faulds, J.E., Hillemeyer, F.L., and Smith, E.I., 1988, Geometry and kinematics of a Miocene "accommodation zone" in the central and southern Eldorado Mountains, Arizona and Nevada, *in* Weide, D.L. and Faber, M.L., eds., This extended land, geological journeys in the southern Basin and Range: Field trip guidebook, Geological Society of America Cordilleran section meeting, Las Vegas, Nevada, p. 293–310.

Foster, D.A., Gleadow, A.J.W., Reynolds, S.J., and Fitzgerald, P.G., 1993, Denudation of metamorphic core complexes and the reconstruction of the transition zone, west-central Arizona—Constraints from apatite fission track thermochronology: Journal of Geophysical Research, v. 98, no. B2, p. 2167–2185.

Fridrich, C.J., DeWitt, Ed, Bryant, Bruce, Richard, Steve, and Smith, R.P., 1998, Geologic map of the Collegiate Peaks wilderness area and the Grizzly Peak caldera, Sawatch Range, central Colorado: U.S. Geological Survey Map I–2565, scale 1:50,000, 29. p.

Gleason, J.D., Spencer, J.E., and Richard, S.M., 1999, Geochemistry of mafic dikes and sills from the lower McCoy Mountains Formation, La Paz County, western Arizona: Arizona Geological Suvey Open-File Report 99–1, 24 p.

Hanson, G.N., 1980, Rare-earth elements in petrogenetic studies of igneous systems: Annual Review of Earth and Planetary Sciences, v. 8, p. 371–406.

Howard, K.A., Nielson, J.E., Wilshire, H.G., Nakata, J.K., Goodge, J.W., Reneau, S.L., John, B.E., and Hansen, V.L., 2000, Geologic map of the Mohave Mountains area, Mohave County, western Arizona: U.S. Geological Survey Miscellaneous Investigations Series I–2308, 2 sheets, text, scale 1:48,000.

Isachsen, C.E., Gehrels, G.E., Riggs, N.R., Spencer, J.E., Ferguson, C.A., Skotnicki, S.J., and Richard, S.M, 1999, U-Pb geochronologic data from zircons from eleven granitic rocks in central and western Arizona: Arizona Geological Survey Open-File Report 99–5, 27 p.

Karlstrom, K.E., and Bowring, S.A., 1993, Proterozoic orogenic history of Arizona in Van Schmus W.R., and Bickford, M.E., eds., Trancontinental Proterozoic provinces, *in* Reed, J.C., Jr., Bickford, M.E., Houston, R.S., Link, P.K., Rankin, D.W., Sims, P.K., and Van Schmus, W.R., eds., Precambrian-Conterminous U.S.—The geology of North America, v. C–2: Geological Society of America, p. 188-211.

King, Bi-Shia, and Lindsay, J., 1990, Determination of 12 selected trace elements in geologic materials by energy dispersive X-ray fluorescence spectrometry, *in* Arbogast, B.F., ed., Quality assurance manual for the Branch of Geochemistry, U.S. Geological Survey: U.S. Geological Survey Open-File Report 90–668, p. 161–165.

Knapp, James H., and Walker, J.D., 1989, Mesozoic to Tertiary magmatism in the Mesquite and Moon Mountains areas, western Arizona—Implications for tectonic development [abs]: Geological Society of America abstracts with Programs, v. 21, no. 5, p. 103.

Laubach, S.E., Reynolds, S.J., and Spencer, J.E., 1987, Mesozoic stratigraphy of the Granite Wash Mountains, west-central Arizona, *in* Dickinson, W.R., and Klute, M.A., eds., Mesozoic rocks of southern Arizona and adjacent areas: Arizona Geological Society Digest v. 18, p. 91–100.

Lawton, T.F., and McMillan, N.J., 1999, Arc abandonment as a cause of passive continental rifting—Comparison of the Jurassic Mexican Borderland and the Cenozoic Rio Grande rift: Geology, v. 27, no. 9, p. 779–782.

Le Maitre, R.W., 1976, The chemical variability of some common igneous rocks: Journal of Petrology, v. 17, no. 4, p. 589–637.

Lichte, F.E., Meier, A.L., and Crock, J.C., 1987, Determination of the rare-earth elements in geological materials by inductively coupled plasma mass spectrometry: Analytical Chemistry, v. 59. no. 8, p. 1150–1157.

Lister, G.S., and Baldwin, S.L., 1993, Plutonism and the origin of metamorphic core complexes: Geology, v. 21, p. 607–610.

Lucchitta, Ivo, and Suneson, N.H., 1994a, Geologic map of the Signal quadrangle, Mohave County, Arizona: U.S. Geological Survey Geologic Quadrangle Map GQ–1709, scale 1:24,000.

Lucchitta, Ivo, and Suneson, N.H., 1994b Geologic map of the Centennial Wash Quadrangle, Mohave and La Paz Counties, Arizona: U.S. Geological Survey Geologic Quadrangle Map GQ–1718, scale 1:24,000.

Marshak, Stephen, and Vander Meulen, Marc, 1989, Geology of the Battleship Peak area, southern Buckskin Mountains, Arizona—Structural style below the Buckskin detachment fault, *in* Spencer, J.E., and Reynolds, S.J., Geology and mineral resources of the Buckskin and Rawhide Mountains, west-central Arizona: Arizona Geological Survey Bulletin 198, p. 51–66.

Marshak, Stephen, Vander Meulen, Marc, and Bhagat, Snehal, 1987, Geology of the Battleship Peak area, Buckskin Mountains, La Paz County, Arizona: Arizona Bureau of Geology and Mineral Technology Miscellaneous Map MM–87–B, scale 1:8,000.

McCarthy, Jill, Larkin, Steven P., Fuis, Gary S., Simpson, Robert W., and Howard, Keith A., 1991, Anatomy of a metamorphic core complex—Seismic refraction/wide-angle reflection profiling in southeastern California and western Arizona: Journal of Geophysical Research, v. 97, no. B7, p. 12259–12291.

McCarthy, Jill, and Parsons, Tom, 1994, Insights into Cenozoic evolution of the Basin and Range–Colorado Plateau transition from coincident seismic refraction and reflection data: Geological Society of America Bulletin, v. 106, p. 747–759.

McKown, D.M., and Knight, R.J., 1990, Determination of uranium and thorium in geologic materials by delayed neutron counting, *in* Arbogast, B.F., ed., Quality assurance manual for the Branch of Geochemistry, U.S. Geological Survey: U.S. Geological Survey Open-File Report 90–668, p. 146–150.

Nelson, S.T., Davidson, J.P., and Sullivan, K.R., 1992, New age determinations of central Colorado Plateau laccoliths, Utah—Recognizing disturbed K-Ar systematics and re-evaluating tectonomagmatic relationships: Geological Society of America Bulletin, v. 104, n. 12, p. 1547–1560.

Osborne, G.M., 1981, The structural geology of the Squaw Peak area of the Buckskin Mountains, Yuma County, Arizona: Los Angeles, University of Southern California, unpublished Master's thesis, 164 p.

Papp, C.S.E., Aruscave, P.J., and Brandt, E.L., 1990, Determination of ferrous oxide in geologic materials by potentiometric titration, *in* Arbogast, B.F., ed., Quality assurance manual for the Branch of Geochemistry, U.S. Geological Survey: U.S. Geological Survey Open-File Report 90–668, p. 139–145.

Pribble, S.T., 1990, Determination of fluoride in silicates by ion-selective electrode following $LiBO_4$ fusion and HNO_3 dissolution, *in* Arbogast, P.F., ed., Quality assurance manual for the Branch of Geochemistry, U.S. Geological Survey: U.S. Geological Survey Open-File Report 90–688, p. 123–126.

Rehrig, W.A., 1982, Metamorphic core complexes of the southwestern United States—An updated analysis, *in* Frost, E.G., and Master, D.L., eds., Mesozoic-Cenozoic tectonic evolution of the Colorado River region, California, Arizona, and Nevada (Anderson-Hamilton volume): San Diego, Calif., Cordilleran Publications, p. 551–559.

Rehrig, W.A., and Reynolds, S.J., 1980, Geologic and geochronologic reconnaissance of a northwest-trending zone of metamorphic core complexes in southern and western Arizona, *in* Crittenden, M.D., Jr., Coney, P.J., and Davis, G.H., eds., Cordilleran metamorphic core complexes: Geological Society of America Memoir 153, p. 131–157.

Reynolds, S.J., and Spencer, J.E., 1984, Geologic map of the Aguila Ridge–Bullard Peak area, eastern Harcuvar Mountains, west-central Arizona: Arizona Bureau of Mines and Mineral Technology Open-File Report 84–4, 2 p., scale 1:24,000.

Reynolds, S.J., and Spencer, J.E., 1985, Evidence for large-scale transport on the Bullard detachment fault, west-central Arizona: Geology v. 13, p. 353–356.

Reynolds, S.J., and Spencer, J.E., 1989. Pre-Tertiary rocks and structures in the upper plate of the Buckskin detachment fault, west-central Arizona, *in* Spencer, J.E., and Reynolds S.J., eds., Geology and mineral resources of the Buckskin and Rawhide Mountains, west-central Arizona: Arizona Geological Survey Bulletin, no. 198, p. 67–102.

Reynolds. S.J., and Spencer, J.E., 1993, Geologic map of the western Harcuvar Mountains, La Paz County, west-central Arizona: Arizona Geological Survey Open-File Report 93–8, 9 p., scale 1:24,000.

Reynolds, S.J., Spencer, J.E., and DeWitt, Ed, 1987, Stratigraphy and U-Th-Pb geochronology of Triassic and Jurassic rocks in west-central Arizona, *in* Dickinson, W.R., and Klute, M.A., eds., Mesozoic rocks of southern Arizona and adjacent areas: Arizona Geological Digest, v. 18, p. 65–85.

Reynolds, S.J., Spencer, J.E., Richard, Stephen M., and Laubach, Stephen E., 1986, Mesozoic structures in west-central Arizona, *in* Beatty, Barbara, and Wilkinson, P.A.K., eds., Frontiers in geology and ore deposits of Arizona and the southwest: Arizona Geological Society Digest v. 16, p. 35–51.

Richard, S.M., Fryxell, J.E., and Sutter, J.F., 1990, Tertiary structure and thermal history of the Harquahala and Buckskin Mountains, west-central Arizona—Implications for denudation by a major detachment fault system: Journal of Geophysical Research, v. 95, no. B12, p. 19973–19987.

Shackelford, T.J., 1976, Structural geology of the Rawhide Mountains, Mohave County, Arizona: Los Angeles, University of Southern California, unpublished Ph.D. thesis, 176 p.

Shackelford, T.J., 1989, Structural geology of the Rawhide Mountains, Mohave County, Arizona, *in* Spencer, J.E., and Reynolds, S.J., eds., Geology and mineral resources of the Buckskin and Rawhide Mountains, west-central Arizona: Arizona Geological Survey Bulletin 198, p. 15–46.

Shafiqullah, M., Damon, P.E., Lynch, D.J., Reynolds, S.J., Rehrig, W.A., and Raymond, R.H., 1980, K-Ar geochronology and geologic history of southwestern Arizona and adjacent areas, *in* Jenny, J.P., and Stone, Claudia, eds., Studies in western Arizona: Arizona Geological Society Digest v. 12, p. 201–260.

Spencer, J.E., and Reynolds, S.J., 1989a, Introduction to the geology and mineral resources of the Buckskin Mountains, *in* Spencer, J.E., and Reynolds, S.J., eds., Geology and mineral resources of the Buckskin and Rawhide Mountains, west-central Arizona: Arizona Geological Survey Bulletin 198, p. 1–10.

Spencer, J.E., and Reynolds, S.J., 1989b, Tertiary structure, stratigraphy, and tectonics of the Buckskin Mountains, *in* Spencer, J.E., and Reynolds, S.J., eds., Geology and mineral resources of the Buckskin and Rawhide Mountains, west-central Arizona: Arizona Geological Survey Bulletin 198, p. 103–167.

Spencer, J.E., and Reynolds, S.J., 1990a, Relationship between Mesozoic and Cenozoic tectonic features in west central Arizona and adjacent southeastern California: Journal of Geophysical Research, v. 95, no. B1, p. 539–555.

Spencer, J.E., and Reynolds, S.J., 1990b, Geology and mineral resources of the Bouse Hills, La Paz County, west-central Arizona: Arizona Geological Survey Open-File Report 90–9, 21 p., scale 1:24,000.

Spencer, J.E., and Reynolds, S.J., 1991, Tectonics of mid-Tertiary extension along a transect through west-central Arizona: Tectonics, v. 10, no. 6, p. 1204–1221.

Spencer, J.E., Reynolds, S.J., and Lehman, N.E., 1986, Geologic map of the Planet-Mineral Hill area, northwestern Buckskin Mountains, west-central Arizona: Arizona Bureau of Mines and Mineral Technology Open-File Report 86–9, 12 p., scale 1:24,000.

Spencer, J.E., Reynolds, S.J., and Lehman, N.E., 1989a, Appendix A, Map-unit descriptions and cross sections for plate 2 (Geologic map of the Planet–Mineral Hill area, northwestern Buckskin Mountains, west-central Arizona), *in* Spencer, J.E., and Reynolds, S.J., eds., Geology and mineral resources of the Buckskin and Rawhide Mountains, west-central Arizona: Arizona Geological Survey Bulletin 198, p. 263–269.

Spencer, J.E., Reynolds, S.J., and Lehman, N.E., 1989b, Geologic map of the Planet–Mineral Hill area, northwestern Buckskin Mountains, west-central Arizona *in* Spencer, J.E. and Reynolds, S.J. eds., Geology and mineral resources of the Buckskin and Rawhide Mountains, west-central Arizona: Arizona Geological Survey Bulletin 198, plate 2, scale 1:24,000.

Spencer, J.E., Richard, S.M., Gehrels, George, Gleason, J.D., and Dickinson, W.R., 2005, Geochronologic and geochemical evidence for extension of the Bisbee trough to the lower part of the McCoy Mountains Formation in southwestern Arizona: Geological Society of America Abstracts with Programs, v. 37, no. 7, p. 482.

Spencer, J.E., Richard, S.M., Reynolds, S.J., Miller, R.J., Shafiqullah, M., Gilbert, W.G., and Grubensky, M.J., 1996, Spatial and temporal relationships between mid-Tertiary magmatism and extension in southwestern Arizona: Journal of Geophysical Research, v. 100, no. B7, p. 10321–10351.

Spencer, J.E., Shafiqullah, M., Miller, R.J., and Pickthorn, L.G., 1989, K-Ar geochronology of Miocene extension, volcanism, and potassium metasomatism in the Buckskin and Rawhide Mountains, *in* Spencer, J.E., and Reynolds, S.J., eds., Geology and mineral resources of the Buckskin and Rawhide Mountains, west-central Arizona: Arizona Geological Survey Bulletin 198, p. 184–189.

Spencer, J.E., and Welty, J.W., 1989, Geology of mineral deposits in the Buckskin and Rawhide Mountains, *in* Spencer, J.E. and Reynolds, S.J., eds., Geology and mineral resources of the Buckskin and Rawhide Mountains, west-central Arizona: Arizona Geological Survey Bulletin 198, p. 223–254.

Streckeisen, A.L., 1973, Plutonic-rock classification and nomenclature recommended by the IUGS subcommission on the systematics of igneous rocks: Geotimes, v. 10, p. 26–31.

Taggart, J.E., Jr., Bartel, A.J., and Siems, D.F., 1990, High precision major element analsis of rocks and minerals by wavelength dispersive X-ray fluorescence spectroscopy, *in* Arbogast, B.F., ed., Quality assurance manual for the Branch of Geochemistry, U.S. Geological Survey: U.S. Geological Survey Open-File Report 90–558, p. 166–172.

Wilson, E.D., 1960, Geologic map of Yuma County, Arizona: University of Arizona and Arizona Bureau of Mines, scale 1:375,000.

Wilson, E.D., and Moore, R.T., 1959, Geologic map of Mohave County, Arizona: University of Arizona and Arizona Bureau of Mines, scale 1:375,000.

Wooden, J.L., and DeWitt, Ed, 1991, Pb isotopic evidence for the boundary between the Early Proterozoic Mojave and Central Arizona crustal provinces in western Arizona in Karlstrom, K.E., ed., Proterozoic geology and ore deposits of Arizona: Arizona Geological Society Digest 19, p. 27–50.

Wooden, J.L., and Miller, D.M., 1990, Chronologic and isotopic framework for Early Proterozoic crustal evolution in the eastern Mojave desert region: Journal of Geophysical Research, v. 95, no. B12, p. 20133–20146.

Woodward, R.J., 1981, The structural geology of the Swansea area, east-central Buckskin Mountains, Yuma County, Arizona: Los Angeles, University of Southern California, unpublished Master's thesis, 106 p.

Wright, J.E., Anderson, J.L., and Davis, G.A., 1986, Timing of plutonism, mylonitization, and decompression in a metamorphic core complex, Whipple Mountains, CA: Geological Society of America Abstracts with Programs, v. 18, no. 2, p. 201.

Appendix. Location and Description of Analyzed Samples

1. Mylonitic medium- to coarse-grained granitic rock containing sills of garnet-bearing leucogranite and pegmatite in Proterozoic granodiorite to granite gneiss unit. 930 m N., 59°E. from spot elevation 3,110. SE1¼ sec. 1, T. 9 N., R. 13 W., 34°08'52"N., 113°33'40"W., Alamo Dam 7½-minute quadrangle, La Paz County. Outcrop in wash 80 m north of right-angle turn. Anhedral quartz to 1.5 mm in diameter. The largest grains are between pulled-apart fragments of plagioclase crystals. Plagioclase (An_{30}) in porphyroclasts as much as 4 mm long, biotite as much as 1 mm long, and potassic feldspar in a matrix with a grain size of 0.05–0.3 mm. Accessory sphene, allanite, apatite, and zircon. Secondary chlorite from biotite and carbonate. Major-oxide and trace-element concentrations, see table 4. Field no. B–268A.

2. Well-foliated porphyritic biotite granite containing potassic feldspar crystals as much as 2 cm long from Proterozoic granodiorite to granite gneiss unit. 820 m S. 26° W. from spot elevation 2,177, NW corner sec. 15, T. 8 N., R. 15 W., 34°02'38"N., 113°47'53"W., Butler Pass 7½-minute quadrangle, La Paz County. Quartz as much as 2 mm in diameter in aggregates of anhedral and strained grains, subhedral plagioclase (An_{20}) as much as 2 mm long, anhedral potassic feldspar as much as 2 cm long containing inclusions of plagioclase, myrmekite, and biotite, synkinematic biotite as much as 3 mm long, accessory apatite, sphene, epidote, and zircon. A well-recrystallized porphyritic granite. Major-oxide and trace-element concentrations, see table 4. Field no. B–587.

3. Medium- to fine-grained biotite granite gneiss from Proterozoic granodiorite to granite gneiss unit. Outcrop 60 m west of 2,404-ft knob on ridge in north-central sec. 2, T. 8 N., R. 15 W., 34°04'09"N., 113°47'14"W., Butler Pass 7½-minute quadrangle, La Paz County. Anhedral strained quartz as much as 0.5 mm in diameter, anhedral plagioclase (An_{20}) as much as 1.2 mm long, anhedral potassic feldspar as much as 1.6 mm long, synkinematic biotite as much as 2 mm long, accessory sphene, opaque mineral, allanite, epidote, and apatite, and secondary chlorite from biotite and epidote. A completely recrystallized plutonic rock showing few of the cataclastic features typically associated with Tertiary mylonitization. Major-oxide and trace-element concentration, see table 4. Field no. B–587.

4. Well-foliated fine-grained phase of granite gneiss from Proterozoic granodiorite to granite gneiss unit. Outcrop on 2,383-ft knob on ridge in north part of sec. 5, T. 8 N., R. 14 W., 34°04'10"N., 113°44'36"W., Butler Well 7½-minute quadrangle, La Paz County. Anhedral quartz, plagioclase (An_{20}), potassic feldspar with a grain size of about 0.8 mm, synkinematic biotite as much as 1 mm long, accessory sphene, epidote, and apatite. A completely recrystallized plutonic rock. Major-oxide and trace-element concentrations, see table 4. Field no. B–665.

5. Biotite granite gneiss from Proterozoic granodiorite to granite gneiss unit. Has flattened feldspar grains to 5 mm long. Local northeast-trending lineation. Cut by pegmatite stringers 2–30 cm thick. From outcrop on ridge at 2,140-ft altitude, 34°04'42"N., 113°43'04"W., Butler Well 7½-minute quadrangle, La Paz County. Anhedral quartz as much as 1 mm in diameter. strongly strained and broken into subindividual grains, anhedral plagioclase (An_{20}) as much as 2 cm in diameter, anhedral microcline as much as 2 mm in diameter, synkinematic biotite as much as 1 mm long, accessory sphene, allanite, epidote, opaque mineral, and zircon and secondary chlorite from biotite. A completely recrystallized plutonic rock showing minor cataclastic effects. Major-oxide and trace-element concentrations, see table 4. Field no B–653.

6. Mylonitic porphyritic granite from Proterozoic granodiorite to granite gneiss unit in slab slumped from outcrop 1,085 m N., 41°W. from spot elevation 2,461 25 m down wash from Field no. 565. Sec. 31 T. 10 N., R. 12 W., 34°09'59"N., 113°32'50"W., Alamo Dam 7½-minute quadrangle, La Paz County. Anhedral quartz as ductilely deformed grains as much as 4 mm long and as lenticular aggregates as much as 6 mm long, plagioclase (An_{26}) as much as 0.7 mm in diameter, anhedral potassic feldspar as much as 1.5 mm in diameter and a lenticular mass 1 cm long, possibly a metaphenocryst, and synkinematic to postkinematic biotite as much as 0.3 mm long, in a matrix of recrystallized quartz, plagioclase, and potassic feldspar having a grain size of 0.05–0.3 mm. Accessory sphene, opaque mineral, allanite, apatite, and zircon and secondary chlorite from biotite. U-Pb age determination, see figure 13. Major-oxide and trace-element concentrations, see table 4. Field no. B–565A.

7. Mylonitic granite from Proterozoic granodiorite to granite gneiss unit. Outcrop in wash 1,110 m N., 41°W. from spot elevation 2,461. Sec. 31, T. 10 N., R. 12 W., 34°09'59"N., 113°32'50"W., Alamo Dam 7½-minute quadrangle. Fine to medium grained and intruded by pegmatites and leucogranite. Anhedral quartz as ductilely deformed grains as much as 1.5 mm long and aggregates as much as 2 mm long. Anhedral, partly sausseritized plagioclase (An_{25}) as much as 1 mm in diameter. Anhedral potassic feldspar as much as 1 mm in diameter. Chlorite after synkinematic biotite. Accessory biotite, allanite, sphene, apatite, zircon, and opaque mineral. Secondary epidote and concentrated in a veinlet perpendicular foliation. Carbonate in thin films parallel foliation. U-Pb zircon age determination, see figure 13. Field no. B–565.

8. Mylonitic porphyritic granodiorite cut by aplite dikes of the youngest phases of the Swansea Plutonic Suite. Interpreted to be inclusion in Swansea Plutonic Suite. Content and size of potassic feldspar porphyroclasts vary. Spoil from cut along abandoned railroad to Swansea. 470 m N. 37° W. from Bench Mark 1608 on Lincoln Ranch road. North part sec. 16, T. 9 N., R. 15 W., 34°07'26"N., 113°49'29"W., Butler Pass 7½-minute quadrangle, La Paz County. Fractured and strained porphyroclasts of potassic feldspar as much as 1.2 cm long, subhedral plagioclase (An_{32}) porphyroclasts as much as 2 mm long, anhedral ductilely drawn-out quartz grains as much as 0.5 mm long interstitial to the feldspar porphyroclasts, anhedral to subhedral porphyroclasts of dark green hornblende as much as 0.7 mm long, biotite as bent porphyroclasts as much as 1 mm long and 0.1 mm and smaller recrystallized grains. Accessory sphene, allanite, apatite, epidote, and opaque mineral. Major-oxide and trace-element concentrations, see table 4. Field no. B–495–92.

9. Mylonitic porphyritic granodiorite or granite from 0.8-m-thick inclusion concordant with mylonitic foliation in Swansea Plutonic Suite from roadcut in Swansea road 550 meters N., 35° E. from township corner at 1,689-ft altitude. SW1¼ sec. 31, T. 10 N., R. 15 W., 34°09'46"N., 113°51'58"W., Swansea 7½-minute quadrangle, La Paz County. Quartz 0.05–0.2 mm in diameter forms aggregates of ductilely drawn-out grains and local mosaic-textured aggregates. Potassic feldspar in broken porphyroclasts as much as 1 cm long having some microcline twinning, partly altered plagioclase in broken porphyroclasts as much as 3 mm in diameter, biotite as much as 0.4 mm long and new biotite <0.2 mm, epidote contemporaneous with both the old and new biotite, and very fine grained quartz and feldspar mortar. Accessory sphene, allanite, epidote, and opaque mineral, and secondary chlorite from biotite. Neomineralization during mylonitization epidote, quartz, and biotite. U-Pb age determination, see figure 13. Major-oxide and trace-element concentrations, see table 4. Field no. B–562.

10. Mylonitic porphyritic granite cut by dikes of aplite, the youngest member of the Swansea Plutonic Suite. Strongly mylonitized and cut by fractures containing epidote. Outcrop on east side of wash 710 m N. 88° E. of top of hill 1452. At south margin of sec. 23, T. 10 N., R. 15 W., 34°10'52"N., 113°47'12"W., Swansea 7½-minute quadrangle, La Paz County. Ductilely elongated and strained mosaic-textured aggregates of quartz broken porphyroclasts of locally perthitic potassic feldspar as much as 2 cm long, having locally developed microcline twinning, porphyroclasts of sericitized plagioclase as much as 2 mm long, secondary chlorite from biotite, and epidote. Very fine grained quartz-feldspar mortar containing chlorite and epidote between porphyroclasts and in zones parallel with the mylonitic foliation. Accessory allanite, zircon, and opaque mineral. Major-oxide and trace-element concentrations, see table 4. Field no. B–1111.

11. Mylonitic biotite-hornblende gneiss from outcrop in wash. Cut by biotite trondhjemite and muscovite trondhjemite sills that are now disrupted into “fish” by ductile deformation. 280 m N. 79° W. from spot elevation 2,461 in SE part of sec. 31, T. 10 N., R. 12 W., 34°09'34"N., 113°32'31"W., Alamo Dam 7½-minute quadrangle, La Paz County. Anhedral plagioclase (An_{39}) as much as 1 mm in diameter and locally bent and broken subhedral blue-green hornblende as much as 3 mm long. Accessory minerals are apatite, zircon, sphene, epidote, and opaque mineral. Major-element and trace-element concentrations, see table 5. Field no. B–93–2C.

12. Mylonitized hornblende diorite or gabbro having feldspar porphyroclasts as much as 2 cm in diameter and variable feldspar content. Contains some layers of more felsic mylonite. Scattered porphyroclasts as much as 2 cm in diameter. Contains a 10-cm-thick pegmatite lens. Some fractures with epidote along them. Outcrop in wash 140 m south of spot elevation 2,461, NE corner sec. 6, T. 9 N., R. 12 W., 34°09'27"N., 113°32'22"W., Alamo Dam 7½-minute quadrangle, La Paz County. Anhedral rounded porphyroclasts of plagioclase (An_{28}) as much as 1 mm in diameter and dark green hornblende as much as 1 mm long in a matrix containing quartz, plagioclase, and hornblende having a grain size of 0.05–0.3 mm. Accessory allanite, apatite, sphene, and opaque mineral and secondary chlorite, epidote, and carbonate. A zone of microbreccia or ultramylonite concordant with the foliation cuts the rock and has a glassy or cryptocrystalline matrix and rounded grains of hornblende and plagioclase. U-Pb age determination, see figure 14. Major-oxide and trace-element concentrations, see table 5. Field no. B–566.

13. Well-foliated biotite trondhjemite gneiss cuts metadiorite. Outcrop in wash 280 m N. 79° W. from spot elevation 2,461 in SE part of sec. 31., T. 10 N., R. 12 W., 34°09'34"N., 113°32'31"W., Alamo Dam 7½-minute quadrangle. Anhedral plagioclase (An_{40}) as much as 1 mm in diameter, anhedral quartz 0.1-0.4 mm in grain size ranging from ductilely deformed to mosaic-textured aggregates between feldspar grains. Synkinematic biotite as much as 3 mm long. Accessory apatite, opaque mineral, and epidote. Major-oxide and trace element concentrations, see table 5. Field no. B–93–2A.

14. Well foliated muscovite trondhjemite gneiss cuts metadiorite. Outcrop in wash N. 79° W. from spot elevation 2,461, SE part sec. 31, T. 10 N., R. 12 W., 34°09'34"N., 113°32'31"W., Alamo Dam 7½-minute quadrangle, La Paz County. Anhedral plagioclase (An_{20}) generally about 0.5 but as much as 1 mm in diameter, quartz ductilely strung out to 2 mm long but mostly

0.2–0.5 mm in diameter. Synkinematic muscovite as much as 2 mm long, accessory potassic feldspar, biotite, allanite, epidote, and opaque see table 5. Field no. B–93–2B.

15. Streaky, well-foliated, granite layer in well-layered sequence of biotite-quartz-feldspar gneiss, biotite plagioclase porphyroclast gneiss, granite gneiss, and some pegmatite. Proterozoic and Cretaceous layered gneiss unit. Outcrop contains lenticular zones of less mylonitized rock having folds with NE-trending axes and variable axial plane. Mylonitic rock has NE-trending mineral lineation. About 60 percent of rock is mylonitic. Outcrop 50 m west of sharp bend in wash 520 m N., 45º W. from spot elevation 3,375, W. margin sec. 7, T. 8 N., R. 10 W., 34°02'57", N., 113°20'55" W., Smith Peak 7½-minute quadrangle, La Paz County. Mosaic-textured quartz plagiocase ($An_{\sim 20}$), and potassic feldspar 0.2–0.5 mm in diameter and a few porphyroclasts of potassic feldspar and plagioclase as much as 3 mm in diameter. Synkinematic to postkinematic biotite 0.05–0.25 mm long. Accessory sphene, apatite, zircon, allanite, myrmekite, and opaque mineral and secondary chlorite from biotite. U-Pb zircon age determination, see figure 15. Major-oxide and trace-element concentrations, see table 5. Field no. HA–118.

16. Fine- to medium-grained mylonitic biotite granite outcrop at sharp bend in one of channels in wash 910 m S. 49º W. from spot elevation 3,110. 34°08'16" N., 113°34'38" W., Alamo Dam 7½-minute quadrangle, La Paz County. Quartz in anhedral grains as much as 2 mm long, anhedral plagioclase (An_{20}) porphyroclasts as much as 2 mm long, anhedral, slightly perthitic potassic feldspar in a matrix of those minerals having a grain size of 0.1–0.3 mm. Synkinematic biotite as much as 0.5 mm long tends to be in aggregates. Accessory myrmekite, allanite, opaque mineral, sphene, zircon, and apatite. Secondary chlorite from biotite. Major-oxide and trace-element concentrations, see table 5. Field no. B–564.

17. Medium-grained hornblende gabbro of the Swansea Plutonic Suite weakly and locally foliated. Outcrop on west-facing slope of hill 750 m N. 38° E. of spot elevation 1,668. NE1/4 sec. 13, T. 9 N., R. 16 W., 34°07'22" N., 113°52'37" W., Powerline Well 7½-minute quadrangle, La Paz County. Euhedral to subhedral normally zoned plagioclase (An_{40}) as much as 3 mm long, and anhedral to subhedral brown to olive green, green, and light green partly altered hornblende as much as 3 mm long. Some new grains of light green actinolite. Accessory apatite and sphene and secondary chlorite from hornblende. Epidote and chlorite in a late fracture <0.1 mm wide. A few discontinuous shear zones contain chlorite and actinolite. Major-oxide and trace-element concentrations, see table 6. Field no. B–469.

18. Coarse-grained hornblende gabbro of the Swansea Plutonic Suite locally has some weakly developed foliation and some fractures containing epidote. Outcrop in wash 400 m S. 71° W. from spot elevation 1,236, south part sec. 10, T. 10 N., R. 14 W. 34°13'03" N., 113°42'19" W., Reid Valley 7½-minute quadrangle, La Paz County. Euhedral to subhedral plagioclase (An_{40}) as much as 5 mm long and brown, green, and light green, subhedral to anhedral, partly altered hornblende as much as 5 mm long interstitial to plagioclase grains. Accessory apatite and opaque mineral and secondary Mg-rich chlorite in fractures in feldspars. Cut by a shear zone with mortar along it. U-Pb zircon age determination, see figure 16. Major-oxide and trace-element concentrations, see table 6. Field no. B–563.

19. Quartz-bearing biotite-hornblende diorite of the Swansea Plutonic Suite from outcrop on road west of Swansea road north of Midway. 310 m S. 64° W. from spot elevation 1,629, NW¼ sec. 26, T. 9 N., R. 16 W., 34°05'47" N., 113°54'07" W., Powerline Well 7½-minute quadrangle, La Paz County. Euhedral to subhedral normally zoned plagioclase ($An_{40\text{-}28}$) as much as 3 mm long locally bent, broken, and sericitized, biotite as much as 1.5 mm long, locally bent, anhedral to subhedral dark green hornblende as much as 1 mm long, interstitial quartz 0.1–0.2 mm in diameter, accessory sphene, allanite, apatite, and opaque mineral, and secondary sericite and chlorite. An igneous texture with a weak local cataclastic overprint. Major-oxide and trace-element concentrations, see table 6. Field no. B–458A.

20. Mylonitic hornblende-bearing biotite granodiorite gneiss of the Swansea Plutonic Suite from cut along abandoned railroad to Swansea. 470 m N. 37° W. from Bench Mark 1608 on Lincoln Ranch road. N. central sec. 16, T. 9 N., R. 15 W., 34°07'26" N., 113°49'29" W., Butler Pass 7½-minute quadrangle, La Paz County. Quartz as ductilely elongate grains and aggregates as much as 2 mm long, bent and broken euhedral to anhedral rounded grains of plagioclase as much as 3 mm long, porphyroclasts of potassic feldspar as much as 3 mm long, and two generations of biotite. Older brown bent biotite as much as 0.8 mm long and very fine grained greenish-brown biotite that formed during mylonitization. Dark green hornblende in locally broken porphyroclasts as much as 1.3 mm long. Quartz-feldspar mortar between larger grains. Accessory sphene, allanite, apatite and opaque mineral and secondary epidote and chlorite. Major-oxide and trace-element concentrations, see table 6. Field no. B–495B.

21. Mylonitic porphyritic biotite granodiorite of the Swansea Plutonic Suite from roadcut on Swansea road 550 m N. 35º E. from township corner at 1,689-ft altitude. SW¼ sec. 31, R. 10 N., R. 15 W., 34°09'46" N., 113°51'58" W., Swansea 7½-minute quadrangle, La Paz County. Ductilely deformed quartz as strung out aggregates as

much as 2 mm long having a strained mosaic texture and average grain size of 0.05 mm, anhedral to subhedral plagioclase (An_{25}), as much as 2 mm long, having local oscillatory zoning, anhedral to subhedral potassic feldspar in porphyroclasts as much as 0.4 mm long, locally showing weakly developed microcline twinning, and a matrix of quartz, feldspar, and new biotite with a grain size of <0.05 mm except for epidote, which is as long as 0.15 mm. Accessory apatite, sphene, allanite, zircon, and opaque minerals. Major oxide and trace-element concentrations, see table 6. Field no. B–562–92.

22. Aplite sill 1 m thick concordant with mylonitic foliation in the Swansea Plutonic Suite. Latest phase of the suite. Cut in abandoned railroad grade to Swansea 470 m N. 37° W. from Bench Mark 1608 on Lincoln Ranch road. North-central sec. 16, T. 9 N., R. 15. W., 34°07'26" N., 113°49'29" W., Butler Pass 7½-minute quadrangle, La Paz County. Euhedral phenocrysts of plagioclase (An_{30}) as much as 3 mm long in a well-foliated, fine-grained matrix of 0.01–0.05 mm quartz, feldspar, and biotite and accessory sphene, allanite, epidote, and opaque mineral and secondary chlorite. Major oxide and trace-element concentrations, see table 6. Field no. B–495C.

23. Mylonitic potassic feldspar-bearing porphyritic granodiorite of the Swansea Plutonic Suite from dump of mine shaft at symbol 380 m N. 63° E. from spot elevation 1,572, north edge sec. 28, T. 9 N., R. 16 W. 34°05'58" N., 113°55'38" W., Powerline Well 7½-minute quadrangle, La Paz County. Subhedral plagioclase (An_{25}) as much as 1 mm long, having some oscillatory and normal zoning potassic feldspar as much as 1 mm in diameter and quartz in aggregates of recrystallized grains as much as 2 mm long in a matrix of quartz, feldspar, and biotite with a grain size of 0.3 mm. Mortar of quartz, feldspar and new biotite <0.15 mm. Accessory sphene, hornblende, allanite, and opaque mineral and secondary chlorite and epidote. Major-oxide and trace-element concentrations, see table 6. Field no. B–464.

24. Medium-grained, somewhat mylonitic monzogranite of the Swansea Plutonic Suite from top of 1,800-ft hill 440 m N. 5° W. from Bench Mark 1608 on Lincoln Ranch road. NW¼ sec. 16, T. 9 N., R. 15 W., 34°07'29" N., 113°49'42" W., Butler Pass 7½-minute quadrangle, La Paz County. Quartz in aggregates of ductilely deformed grains as much as 5 mm long, plagioclase (An_{29}) and perthitic potassic feldspar in porphyroclasts as much as 2 mm long, and bent and sheared brown biotite as much as 1 mm long in a very fine grained matrix of quartz, feldspar, and greenish-brown biotite. Accessory sphene, zircon, apatite, and opaque mineral. Major-oxide and trace-element concentrations, see table 6. Field no. B–496.

25. Mylonitized granite of the Swansea Plutonic Suite containing feldspar porphyroclasts as much as 5 mm long. Outcrop in wash 840 m N. 81° E. from spot elevation 1,261 on top of hill. NE¼ sec. 20, T. 10 N., R. 15 W. 34°11'45" N., 113°50'13" W., Swansea 7½-minute quadrangle, La Paz County. Quartz in matrix mostly 0.1–0.2 mm but some elongate ductilely deformed grains as much as 2 mm long. Plagioclase ($An_{\sim 20}$)as much as 3 mm long and potassic feldspar with poorly developed microcline twinning as porphyroclasts as much as 4 mm in diameter in a matrix of quartz, feldspar, and biotite with a grain size of as much as 0.5 mm. Biotite recrystallized during mylonitization has a grain size <0.15 mm. Accessory opaque mineral, apatite, zircon, sphene, and allanite. Secondary chlorite and epidote. U-Pb concordia diagram, see figure 16. Major-oxide and trace-element concentrations, see table 6. Field no. B–561.

26. Mylonitic medium-grained granite of the Swansea Plutonic Suite containing feldspar porphyroclasts as much as 5 mm long from crest of ridge 370 m S. 70° E. from spot elevation 2,008. West part sec. 22, T. 9 N., R. 16 W., 34°06'30" N., 113°55'13" W., Powerline Well 7½-minute quadrangle, La Paz County. Quartz in ductilely deformed grains as long as 0.3 mm, anhedral to subhedral, locally perthitic potassic feldspar in strained and broken porphyroclasts as much as 4 mm long, anhedral to subhedral plagioclase (An_{17}) in porphyroclasts 3 mm long in matrix of quartz-feldspar mortar containing synkinematic biotite typically 0.05 mm but longer in the strain shadow of porphyroclasts. Some biotite as much as 0.6 mm long is included in porphyroclasts or is bent. Accessory sphene, zircon, and opaque mineral and secondary chlorite from biotite. Major-oxide and trace-element concentrations, see table 6. Field no. B–463.

ISBN 978-1411320413